



**Effect of Biochar as Geobattery and Geoconductor on Microbial  
Fe(III) Reduction and Methanogenesis  
in a Paddy Soil**

**Dissertation**

vorgelegt von  
M.Sc. Zhen Yang  
aus Shaanxi, VR China

Tübingen  
2020



**Effect of Biochar as Geobattery and Geoconductor on Microbial  
Fe(III) Reduction and Methanogenesis  
in a Paddy Soil**

**Dissertation**

der Mathematisch-Naturwissenschaftliche Fakultät

der Eberhard-Karls-Universität Tübingen

Zur Erlangung des Grades eines

Doktors der Naturwissenschaften

(Dr.rer.nat)

Vorgelegt von

M.Sc.Zhen Yang

aus Shaanxi, VR China

Tübingen

2020



Gedruckt mit Genehmigung der Mathematisch-Naturwissenschaftlichen Fakultät der Eberhard Karls Universität Tübingen

Tag der mündlichen Qualifikation: 29.04.2020

Dekan: Prof. Dr. Wolfgang Rosentiel

Berichterstatter: Prof. Dr. Andreas Kappler

Berichterstatter: Prof. Dr. Ruben Kretzschmar

--世界上只有一种英雄主义，就是认识生活的真相后依然热爱它--

--罗曼·罗兰

--There is only one heroism in the world:  
to see the world as it is and to love it.--

By Roman Rolland

# Contents

<b>1 Summary</b> .....	1
<b>Zusammenfassung</b> .....	3
<b>2 Introduction</b> .....	5
<b>3 Aggregation-dependent electron transfer via redox-active biochar particles stimulate microbial Fe(III) reduction</b> .....	17
3.1 Abstract.....	19
3.2 Introduction.....	20
3.3 Materials and methods.....	21
3.4 Results and discussion.....	23
3.5 Environmental implication.....	34
3.6 References.....	35
Supporting Information.....	40
<b>4 Coupled function of biochar as geobattery and geoconductor alters soil microbial community composition and electron transfer pathways in a paddy soil</b> .....	60
4.1 Abstract.....	62
4.2 Introduction.....	63
4.3 Materials and methods.....	64
4.4 Results and discussion.....	67
4.5 Conclusion and environmental Implication.....	75
4.6 References.....	77
Supporting Information.....	82
<b>5 Discussion and Outlook</b> .....	92
<b>Curriculum vitae</b> .....	100
<b>Statement of personal contribution</b> .....	103
<b>Acknowledgements</b> .....	104

## Summary

### 1.1 Abstract

Biochar is the product of thermal degradation of organic matter in the absence of oxygen (pyrolysis), and is distinguished from charcoal by its use as a soil amendment. Biochar as a soil amendment is capable of improving soil fertility and mitigating climate change, which is related to soil microbial composition shifts. Biochar has been demonstrated to be a redox-active and conductive carbon matrix. Biochar has been used as an electron shuttle influencing dissimilatory Fe(III) reduction by mediating electron transfer via surface redox functional groups (i.e. its ability to take up and donate electrons via redox-active functional groups, thus functioning as geobattery) between microorganisms and Fe(III) minerals. Additionally, biochar as conductive material has been suggested to contribute to electron transfer from electron-donating microorganisms (e.g. *Geobacter* spp.) to electron-accepting microorganisms (e.g. *Methanosarcina*) via its conductive carbon matrix (functioning as geoconductor). This electron transfer mechanism is involved in a conductive-materials interspecies electron transfer (CIET) process contributing to methanogenesis, especially in anoxic environments such as paddy soils.

Electron shuttling mechanisms have been proved to stimulate electron transfer between Fe(III)-reducing bacteria and Fe(III) minerals. An increasing number of observations, however, have questioned the geobattery function of biochar stimulating microbial Fe(III) reduction because of an inhibition effect of biochar (at low concentration) on microbial Fe(III) reduction as it was observed recently. To this end, this thesis determined the rates and extent of microbial Fe(III) reduction by *Shewanella oneidensis* MR-1 in cell suspension experiments amended with different ratios of wood-derived biochar to ferrihydrite (g biochar/mol Fe) and different biochar particle sizes. Moreover, this thesis also has shown the extent of aggregation of cells, biochar and ferrihydrite at different biochar:Fh ratios and has investigated the fate of electrons from substrate oxidation flow to microbial Fe(III) reduction and could be stored in biochar based on thermodynamically calculations. This thesis has explicitly illustrated the contribution of biochar as geobattery and geoconductor to microbial Fe(III) reduction, which depends on the extent of aggregation of cells, biochar and Fe(III) minerals, and biochar particle sizes (Chapter 3).

When biochar was applied to paddy soil, biochar as soil amendment alters the soil microbial community and mitigates methane emissions. Biochar can participate in biogeochemical electron transfer processes due to its function as geobattery) and its function as geoconductor.



Each of these two mechanisms has been separately demonstrated to play a role in biogeochemical iron cycling and greenhouse gas formation. Yet, little is known about the coupling of both biochar electron transfer mechanisms, despite the fact that naturally occurring electron transfer through biochar is expected to rely on both geobattery and geoconductor mechanisms simultaneously. Here we conducted anoxic microcosm incubations to investigate how biochar influences electron transfer in a paddy soil and affects the indigenous soil microbial community. We found that the coupled function of biochar as geobattery and geoconductor simultaneously promoted the rates of microbial Fe(III) reduction and methanogenesis by 2.1- and 2.3-fold, respectively, with smaller biochar particles leading to higher rates of Fe(III) reduction and methanogenesis than larger particles. In contrast, the redox-active model compound anthraquinone-2,6-disulfonate (AQDS), which functions solely as geobattery, only stimulated iron reduction in our microcosms. While the biochar geobattery mechanism dominated microbial Fe(III) mineral reduction, the stimulation of methanogenesis was likely a result of the conductive-particles interspecies electron transfer caused by biochar functioning as geoconductor. Microbial community analysis supported this hypothesis by showing that the addition of biochar stimulated the syntrophic activity of acetate-oxidizing *Geobacteraceae* taxa and methane-producing *Methanosarcina* taxa and an obvious increase in copy numbers of 16S rRNA genes specific for *Geobacter* spp. and methyl-coenzyme M reductase subunit alpha (*mcrA*) gene. In summary, our results demonstrated that a coupled effect of biochar functioning both as geobattery and geoconductor affect soil microbial metabolisms by facilitating electron transfer either from cells to minerals or cells to cells, influencing methane emission in a paddy soil (Chapter 4).

Taken together, the results presented in this thesis revealed that coupled function of biochar as geobattery and geoconductor play an important role either in microbial Fe(III) reduction or methanogenesis. Extent of aggregation of cells-biochar and biochar-Fe(III) minerals influence the electron transfer mechanisms via biochar from microorganisms to microorganisms or from microorganisms to Fe(III) minerals. These new findings improve our understanding about the role of biochar in electron transfer and highlight the importance of biochar as soil amendment in dissimilarity Fe(III) reduction and methanogenesis.

## 1.2 Zusammenfassung

Biokohle ist das Produkt des thermischen Abbaus von organischer Substanz in Abwesenheit von Luftsauerstoff (Pyrolyse) und unterscheidet sich von Holzkohle durch die Verwendung als Bodenverbesserungsmittel. Biokohle als Bodenverbesserungsmittel ist in der Lage, die Bodenfruchtbarkeit zu verbessern und den Klimawandel abzuschwächen, was mit der Verschiebung des mikrobiellen Konsortiums des Bodens zusammenhängt. Biokohle ist nachweislich ein redox-aktives und kohlenstoffmatrix-leitendes Material. Während der letzten Jahrzehnte wurde Biokohle als Elektronenshuttle (sog. *Geobatterie*) eingesetzt, um Elektronentransferprozesse mittels funktioneller Oberflächen-Redoxgruppen zwischen Mikroorganismen und redoxaktiven Verbindungen während biogeochemischer Prozesse, insbesondere der Reduktion von Fe(III), zu stimulieren. Zusätzlich wurde vorgeschlagen, dass Biokohle als leitfähiges Material über seine leitfähige Kohlenstoffmatrix (als *Geoleiter*) zum Elektronentransfer von elektronenspendenden Mikroorganismen (z.B. *Geobacter* spp.) zu elektronenaufnehmenden Mikroorganismen (z.B. *Methanosarcina*) beiträgt. Dieser Elektronentransfer-Mechanismus ist an einem Leitmaterial-Elektronentransferprozess beteiligt, der die Methanogenese, insbesondere in anoxischen Umgebungen wie z.B. Reisfeldböden, fördert.

Es wurde nachgewiesen, dass Elektronen-Shuttle-Mechanismen den Elektronentransfer zwischen Fe(III)-reduzierenden Bakterien und schwerlöslichen Fe(III)-Mineralien stimulieren. Eine zunehmende Anzahl an Beobachtungen hat jedoch die Geobatteriefunktion von Biokohle, die die mikrobielle Fe(III)-Reduktion stimuliert, in Frage gestellt, da ein Hemmeffekt der Biokohle (bei niedriger Konzentration) auf die mikrobielle Fe(III)-Reduktion, wie er kürzlich beobachtet wurde, besteht. Zu diesem Zweck wurden in dieser Arbeit die Raten und das Ausmaß der mikrobiellen Fe(III)-Reduktion bestimmt, indem *Shewanella oneidensis* MR-1 Suspensionsexperimente durchgeführt wurden, die mit unterschiedlichen Verhältnissen an Biokohle aus Holz zu Ferrihydrit (g Biokohle/mol Fe) und Biokohle unterschiedlicher Partikelgröße ergänzt wurden. Darüber hinaus hat diese Arbeit auch das Ausmaß der Aggregation von Zelle, Biokohle und Ferrihydrit bei verschiedenen Biokohle:Fh-Verhältnissen, beschrieben und die Anzahl der Elektronen aus Substratoxidation und mikrobieller Fe(III) Reduktion, die thermodynamisch in Biokohle gespeichert werden, untersucht. Die vorliegende Arbeit hat darüber hinaus den Effekt einer Geobatterie und die Elektronentransfermechanismen von Biokohle hin zur mikrobiellen Fe(III)-Reduktion dargestellt und erläutert wie dieser Effekt vom Ausmaß der Aggregation zwischen Zellen, Biokohle und Fe(III)-Mineralien und nicht zuletzt den Partikelgrößen Biokohle abhängt (Kapitel 3).

Biokohle als Bodenverbesserungsmittel verändert die mikrobielle Gemeinschaft des Bodens und vermindert die Methanemissionen. Darüber hinaus kann Biokohle aufgrund ihrer Redoxaktivität (d.h. ihrer Fähigkeit, über redoxaktive funktionelle Gruppen Elektronen aufzunehmen und abzugeben, also als *Geobatterie* zu fungieren) und ihrer Leitfähigkeit (d.h. als elektrischer Leiter, eines sogenannten Geoleiter, zu fungieren) an biogeochemischen Elektronentransferprozessen teilnehmen. Jeder dieser beiden Mechanismen spielt nachweislich eine Rolle beim biogeochemischen Eisenkreislauf und bei der Treibhausgasbildung. Über die Kopplung der beiden Biokohle-Elektronentransfermechanismen ist jedoch wenig bekannt, obwohl man davon ausgeht, dass der natürlich vorkommende Elektronentransfer durch Biokohle gleichzeitig auf den Mechanismen der *Geobatterie* und des Geoleiters beruht. In der vorliegenden Arbeit haben wir anoxische Mikrokosmos-Inkubationen durchgeführt, um zu untersuchen, wie die Biokohle den Elektronentransfer in einem Reisfeld beeinflusst und wie sie sich auf die indigene mikrobielle Bodengemeinschaft auswirkt. Wir fanden heraus, dass die gekoppelte Funktion von Biokohle als Geobatterie und Geoleiter gleichzeitig die mikrobielle Eisen(III)-Reduktion und Methanogenese fördert, wobei kleinere Biokohlepartikel zu höheren Fe(III)-Reduktionsraten und Methanogenese führen als größere Partikel. Die redoxaktive Modellverbindung Anthrachinon-2,6-Disulfonat (AQDS), die ausschließlich als Geobatterie fungiert, stimulierte hingegen in unseren Mikrokosmen nur die Eisenreduktion. Während der Biokohle-Geobatterie-Mechanismus die mikrobielle Fe(III)-Mineralienreduktion dominierte, war die Stimulation der Methanogenese wahrscheinlich eine Folge des direkten Elektronentransfers zwischen den Spezies, der durch die Biokohle, die als Geoleiter fungiert, verursacht wurde. Die Analyse der mikrobiellen Gemeinschaften unterstützte diese Hypothese, indem sie zeigte, dass die Zugabe von Biokohle die synthetische Aktivität der Acetat-oxidierenden Geobacteraceae Taxa und der methanproduzierenden Methanosarcina Taxa stimulierte. Zusammenfassend zeigten unsere Ergebnisse einen gekoppelten Effekt von Biokohle, die sowohl als Geobatterie als auch als Geoleiter fungiert, den mikrobiellen Bodenstoffwechsel beeinflusst und zum Elektronentransfer zwischen Zellen und Mineralien oder Zellen und Zellen, die die Methanemission in einem Reisfeld beeinflussen, führt (Kapitel 4).

Zusammenfassend zeigten die in dieser Arbeit vorgestellten Ergebnisse, dass die gekoppelte Funktion von Biokohle als Geobatterie und Geoleiter, eine wichtige Rolle sowohl bei der mikrobiellen Fe(III)-Reduktion als auch der Methanogenese spielen. Das Ausmaß der Aggregation von Zellen-Biokohle und Biokohle-Fe(III)-Mineralien beeinflusst die Mechanismen des Elektronentransfers über Biokohle zwischen Mikroorganismen und Mikroorganismen oder

-Zusammenfassung-

Mikroorganismen und Fe(III)-Mineralien. Diese neuen Erkenntnisse erweitern unser Verständnis über Elektronentransfermechanismen von Biokohle und unterstreichen die Bedeutung von Biokohle als Bodenverbesserungsmittel und deren Effekt auf mikrobielle Fe(III) Reduktion und Methanogenese in anoxischen Böden.

## Introduction

### 1. Biochar in the environment and electron transfer pathways

#### 1.1 Origin of biochar and Environmental implication on greenhouse gas emission

Biochar, defined as 'charcoal for application to soil', has been used as soil amendment to improve the soil fertility originated in the Amazon basin at least 2500 years ago (Kookana et al., 2011). First of all, Terra Preta sites have been found mainly along the major rivers of the Amazon basin, containing more carbon as its darker color compared to the surrounding soil (Eden et al., 1984). Meanwhile, productivity of crops in terra preta is twice that of crops grown in nearby soil (DeLuca et al., 2015).

Char is made when organic matter smoulders in an oxygen-limited environment, rather than burn (Marris E, 2016). The particles of the char (or biochar) produced this way are able to gather up nutrients and water that otherwise might be washed out of the reach of roots (Lehmann et al., 2011; Zimmerman AR., 2010). Besides the ability of biochar to improve soil fertility, biochar also contributes to carbon sequestration (Ippolite et al., 2012). Evidence suggested that components of carbon in biochar are highly recalcitrant in soil, with reported residence times for wood biochar being in the range of 100s to 1,000s of year, *i.e.* approximately 10-1,000 times longer than residence times of most soil organic matter (Farrell et al., 2013; Jiang et al., 2016). Therefore, biochar applied to soil can serve as a long-term carbon sink. Sequestering biochar carbon in soil contributes greatly to reduce nutrient leaching and greenhouses gas emission (*i.e.* N<sub>2</sub>O) (Steiner et al., 2010) and mitigate soil-borne CH<sub>4</sub> emissions, especially from paddy soil (Jeffery et al., 2016), which is caused by shifting microbial community composition (Feng et al., 2012). Among various sources of atmospheric methane, rice paddy fields are considered one of the most important. It has been reported that the annual paddy CH<sub>4</sub> emission ranges from 25 to 54 Tg CH<sub>4</sub> (Sass, 1994), which is 4-9% of the total emission of 598 Tg CH<sub>4</sub> (IPCC 2001). In general, anaerobic decomposition of organic materials stems electrons which flow to methanogenesis in flooded rice paddy soil (Glissmann and Conrad, 2000), but paddy soil is rich in iron where N and C cycling is strongly associated with microbes involved in microbial Fe(III) reduction (Colombo et al., 2014). Microbial Fe(III) reduction provides an alternative electron-accepting process that diverts electron flow to Fe(III) reduction and out-performs methanogenesis (Frenzel et al, 1999; Bond and Lovley 2002; Hori et al., 2010;). Recently, it has been reported that electron flowing mechanisms via biochar involves biochar as either geobattery or geoconductor (Sun et al., 2017; Zhang et al., 2018; Prado et al., 2019). Such electron transfer mechanisms via biochar are able to influence electron-driven competition between methanogenesis and microbial Fe(III) reduction once

biochar is applied to water-logged environments (*i.e.* paddy soil). Owing to the current interests in climate change mitigation, and the irreversibility of biochar application to soil, an effective evaluation of biochar and its effects on methane emission and underlying electron transfer mechanisms have been studied and discussed in the later chapters.

### 1.2 Electron transfer pathways of biochar serving as geobattery and/or geoconductor

Biochar is generally made intentionally by biomass pyrolysis under limited oxygen conditions (Manyà 2012; Lehmann and Joseph, 2015). Biochar contains either electroactive carbon matrices (Sun et al., 2017; Prado et al., 2019) or surface redox-active functional group components (Klüpfel et al., 2014; Wu et al., 2017; Sun et al., 2018), which is greatly responsible for electron transfer. Due to the charging and discharging cycles of its surface redox-active functional groups, biochar has been suggested to serve as geobattery that can reversibly accept and donate electrons. Wood-derived biochar has an obvious higher electron accepting (EAC) and donating capacity (EDC), attributed to surface redox active functional groups, than grass-derived biochar by electrochemical analysis (Klüpfel et al., 2014). The highest EAC and EDC of wood-derived biochar is in the range of 400-700°C. Biochar pyrolysis at 700°C has a higher EAC than EDC (Fig. 1) which corresponds to a high content in quinone moieties observed at 700°C.

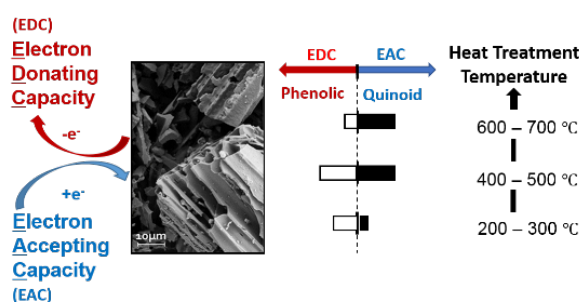


**Fig. 1.** Electron accepting capacities (EAC) and electron donating capacities (EDC) of biochar prepared at heat treatment temperature in the range of 200-700°C (Klüpfel et al., 2014).

In addition, a rapid direct electron transfer via pyrogenic carbon matrices provides a novel electron transfer pathway via electroactive carbon matrices of biochar (Sun et al., 2017 and 2018). Pyrogenic carbon (biochar) performs a direct electron transfer with more than three times faster than the charging and discharging cycles of surface functional groups. In addition, surface functional groups contribute to the total electron transfer of biochar to a lower extent by gradually increasing pyrolysis temperature from 300°C to 700°C even to 800°C. Large and increasingly condensed polyaromatic sheets become dominant at high pyrolysis temperature. Thus, electron transfer mechanisms via biochar include i) electron transfer by accepting and donating electrons via redox-active functional groups in biochar as geobattery (e.g. quinone/hydroquinone) at low HTTs range of 400-600°C, ii) (direct) transfer of electrons via

the polyaromatic carbon matrix in biochar as geoconductor at high HTT's range of 700-800°C, or iii) both pathways exhibited when biochar pyrolysis at 600-700°C (Fig. 2). Nevertheless, few studies clarify electron transfer mechanisms via carbon between surface redox-active functional groups and polyaromatic carbon matrices in biochar making at different pyrolysis temperatures.

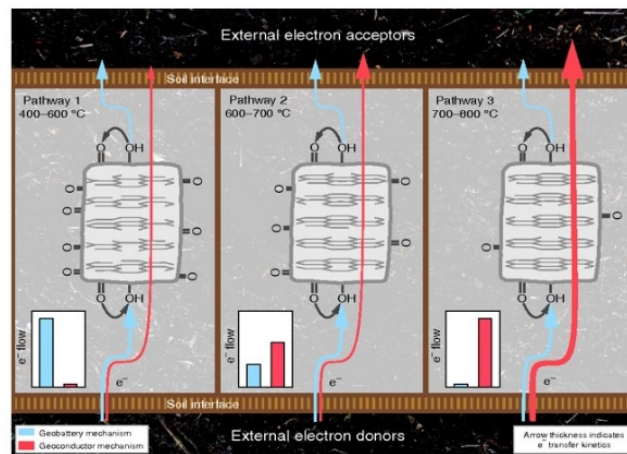


**Fig. 2.** Schematic diagram of the pyrogenic carbon internal pathway for electron flow. Blue arrows indicate the charge and discharge cycles of the geobattery mechanism; red arrows indicated the direct electron transfer through the geoconductor mechanism. Arrow thickness represents the magnitude of transfer kinetics. The dominating electron flow is illustrated in the inset chart of each pathway. The ordering carbon structures determining the pathway 1, 2 and 3 are based on the Raman spectroscopy of pyrogenic carbon matrices (Sun et al., 2017).

## 2. Microbial electron shuttling via biochar as geobattery during microbial Fe(III) mineral reduction

As one of the most abundant elements in the Earth's crust, iron can be found in the environment in numerous dissolved and solid forms and in predominantly two redox states, i.e. Fe(II) and Fe(III) (Konhauser et al, 2011). Microbial Fe(III) reduction generally participates in many biogeochemical processes such as release of phosphate and arsenic (Borch et al., 2009). However, microbial Fe(III) reduction is limited by the step of effective accessibility of Fe(III)-reducing bacteria to poorly soluble Fe(III) minerals. Due to biochar's capability of accepting and donating electrons by surface redox active functional groups, biochar is suggested to be able to act as electron acceptor (Yu et al., 2016) and electron donor (Saquing et al., 2016). This chemical property enables biochar to undergo a unique reaction process: the so-called electron shuttling process. That is, Fe(III)-reducers (e.g. *Shewanella* spp., and *Geobacter* spp.) donate electrons to native biochar, and then reduced biochar donates electrons to Fe(III)

minerals with charging and discharging cycles. This process of accepting (charging) and donating (discharging) electrons via biochar has been demonstrated to stimulate rate and extent of microbial Fe(III) reduction (Kappler et al., 2014; Xu et al., 2017, Fig. 3), coupled to enhancing anaerobic ammonium oxidation (Zhou et al., 2016) and accelerating reduction and transformation of some redox contaminants (i.e. Cr (VI), pentachlorophenol) (Yu et al., 2015; Yuan et al., 2017; Xu et al., 2019).

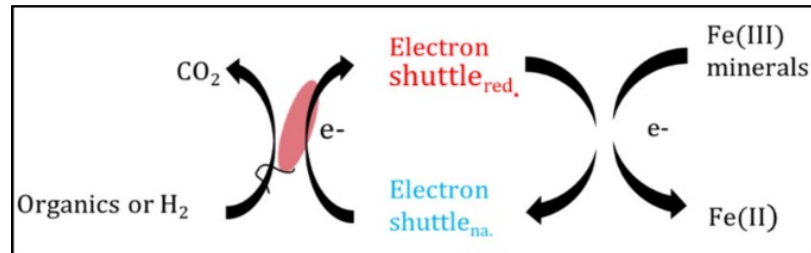


**Fig. 3.** Biochar can act as an electron shuttle between the Fe(III)-reducer (*Shewanella oneidensis* MR-1) and Fe(III) mineral (ferrihydrite). Native (non-reduced) biochar can be reduced by microorganisms (e.g. Fe(III)-reducing bacteria), followed by the reduction of the terminal electron acceptor by reduced biochar in the second, abiotic electron transfer step. The reduced biochar donates electrons to ferric iron and is re-oxidized.

Once biochar is added to soils, biochar will be gradually broken down to small particles in the nano- to micro-size range by physical and chemical weathering as well as microbial decomposition (Lehmann and Joseph, 2015; Nguyen et al., 2008). These small biochar particles are reactive and can easily be transported through different soil layers and even leach into groundwater (Zhang et al., 2010) resulting in aggregation with microbes (Goiyeia and Pessenda, 2000) and minerals (Ye et al., 2016). It has been shown that smaller powdered biochar particles caused higher rates of microbial Fe(III) reduction compared to larger granulated biochar (Zhou et al., 2017). Thus, some research questions regarding i) whether concentration or particle size of biochar influences electron shuttling and microbial Fe(III) reduction ii) how does aggregation of biochar and microbes with Fe(III) minerals influence electron shuttling and microbial Fe(III) reduction, and iii) which mechanism, i.e. electron transfer via redox-active functional groups or via carbon matrices in biochar, dominates the electron transfer during the stimulation of microbial Fe(III) reduction. These are discussed in chapter 3.

### **3. Interspecies electron transfer (IET) via biochar as geoconductor involving conductive-material interspecies electron transfer (CIET) between Fe(III)-reducing bacteria and methanogens**



In flooded rice paddy soil, Fe(III)-reducing bacteria can inhibit methanogenesis by outcompeting methanogens thermodynamically for common electron donors such as acetate and/or hydrogen. Microbial cells can act as solid electron donors and transfer electrons to the other cells via various extracellular electron transfer mechanisms. In the environment IET enables one of the major steps of the global carbon cycle, the microbial mineralization of organic matter to methane (McInemey et al., 2009). The process comprises four stages (Shrestha and Rotaru, 2014). In the first three stages, complex molecules derived from organic matter such as polysaccharides, proteins, and lipids are hydrolyzed and converted into small molecules such as H<sub>2</sub>, CO<sub>2</sub>, formate, acetate, propionate, and n-butyrate by complex microbial consortia. In the last stage, methanogens either decarboxylate acetate to produce methane or oxidize H<sub>2</sub> or formate to reduce CO<sub>2</sub> into methane. The utilization of acetate and H<sub>2</sub> (interspecies hydrogen transfer, IHT) or formate (interspecies formate transfer, IFT) by methanogens can be described as indirect IET (IIET) with microbial species involved in the third stage of microbial mineralization, which is the fermentation of small organic molecules to yield acetate, CO<sub>2</sub>, and H<sub>2</sub>. Other examples of IIET existing in nature or demonstrated under laboratory conditions rely on different electron shuttles including quinones (Smith et al., 2015), zero-valent sulfur and polysulfide, and cysteine. Contrary to IFT and IHT, none of these IIET mechanisms has been shown to be involved in electron uptake during microbial electrosynthesis.

Recent studies proposed that interspecies electron transfer (IET) can be performed directly between bacteria and methanogenic archaea, or with the aid of conductive materials, being potentially a more energy conserving approach, and thus improving the rate of methanogenesis (Stams et al., 2009; Rotaru et al., 2014). Clear evidence of conductive-material-mediated IET (CIET) was observed between *Geobacter* species, between *G. sulfurreducens* and *Thiobacillus denitrificans*, and between *G. sulfurreducens* and *Rhodospseudomonas palustris* (Roraru et al., 2014; Kato et al., 2012). Additionally, Chen's et al (2016) have demonstrated that biochar promotes electron transfer between *Geobacter sulfurreducens* and *Methanosarcina barkeri* in a manner similar to that previously reported for GAC stimulating methanogenesis and with accelerated rates of anaerobic metabolism.

The stimulation of methane production in anaerobic environment, especially anaerobic water treatment reactors amended with conductive materials such as magnetite, granular activated carbon (GAC), carbon nanotubes (CNT), and biochar among others (Liu et al., 2012; Kato et al., 2012; Roraru et al., 2014; Li et al., 2015; Cruz Viggi et al., 2014). In general, these materials are highly stable, with large surface area, high adsorption capacity, and high electrical conductivity. Such CIET between microbial cells with a conductive material serving as a cell to cell conduit for electrons facilitate electrons flow from electron-donating microorganisms to

electron-accepting microorganisms. When granular activated carbon is used, type IV pili comprising PilA pilin as well as *OmcS* become unnecessary for IET (Liu et al., 2012). These observations suggest that in environments riched in conductive materials species capable of CIET might be able to save energy by simplifying their biological EET networks (Shrestha and Rotaru, 2014). Because of the ubiquity of conductive minerals or materials in nature, CIET is probably a widespread phenomenon contributing to biogeochemical cycles.

Simultaneously increasing rates of both microbial Fe(III) reduction and methanogenesis was reported after the application of biochar to paddy soil microcosms. This was accompanied by shifting microbial community composition to *Geobacter* and *Methanosarcina* (Zhou et al., 2017). Yuan et al's study suggested to modulate methanogenesis through electron syntrophy between methanogens and *Geobacteraceae* (Yuan et al., 2018). Compared to wood-derived biochar, rice straw- and manure-derived biochar accelerate methanogenesis remarkably (Yuan et al., 2018). However, little is known about the contribution of electron transfer mechanisms via biochar either as geoconductor and geobattery behind the simultaneous improvement of Fe(II) and methane formation rates when biochar is applied to paddy soils. Apart from CIET, biochar as a redox mediator stimulating Fe(II) formation dependent on aggregation with cells and Fe(III) minerals should be considered, and different biochar particle size. These open questions are herein addressed and discussed in chapter 4.

#### **4. Objectives of this study**

Biochar as soil amendment can improve soil properties and contribute to carbon sequestration and also influence microbial iron reduction and greenhouses gas emission. Recently, it has been shown that biochar serving as a geobattery and geoconductor is responsible for mediating electron transfer during redox processes. Thus we expect that some mechanisms regarding electron shuttling and direct electron transfer via biochar influence the fate of electrons flowing. In addition, micro- and nano-sized biochar particles with high mobility can be transported to different soil layers and aggregate with microbes and Fe(III) minerals. However, it remains unclear how different particles and concentration of biochar influence electron shuttling; how aggregation of biochar, microbes and Fe(III) minerals influence electron transfer and microbial Fe(III) reduction; whether biochar influences electron transfer pathways between electron-donating and accepting microorganisms and thus influence methanogenesis in a paddy soil; and the underlying electron transfer mechanisms between biochar and soil microbial metabolic response.

#### **4.1 Study goals**

First this thesis reports the understanding of electron transfer between microorganisms and Fe(III) minerals via redox-active biochar. The objectives of this thesis shown in **Chapter 3** were

to clear how does concentration or particle size of biochar influence microbial Fe(III) reduction and how does aggregation of cells with biochar and ferrihydrite influence microbial Fe(III) reduction. To this end, analysis and experiments have been conducted i) to assess redox properties of biochar at different particle sizes; ii) to quantify effect of biochar particles on microbial Fe(III) mineral reduction; (iii) to quantify effect of biochar/Fh ratios on microbial Fe(III) reduction; (vi) to analyze aggregation of cells with different biochar/Fh ratios; and (v) to estimate contribution of electron transfer mechanisms via biochar to stimulation microbial Fe(III) reduction.

In addition, this thesis reports a coupled effect of biochar as geobattery and geoconductor on soil microbial metabolisms and electron transfer in a paddy soil. These objectives of this thesis shown in **Chapter 4** were to quantify impacts of biochar amendment on microbial Fe(III) reduction, methane emission, microbial community composition, abundance of functional genes and electron transfer pathways in a paddy soil. To this end, analysis and paddy soil microcosm experiments have been conducted i) to quantify effect of biochar with different particles and biochar/Fh ratio of 1.0 g/mmol Fe on microbial Fe(III) reduction and methanogenesis in a paddy soil; ii) to analyze soil microbial community composition and related functional genes; iii) to quantify consumption of acetate as the sole electron donor in the presence of biochar in a paddy soil; and (vi) to quantify contribution of biochar as geoconductor in conductive-materials interspecies electron transfer to methane emissions.

## References:

- Beesley, L., Moreno-Jiménez, E., Gomez-Eyles, J. L., Harris, E., Robinson, B., Sizmur, T., 2011. A review of biochars' potential role in the remediation, revegetation and restoration of contaminated soils. *Environmental pollution*, 159(12), 3269-3282.
- Bond, D. R., Lovley, D. R., 2002. Reduction of Fe (III) oxide by methanogens in the presence and absence of extracellular quinones. *Environmental Microbiology*, 4(2), 115-124.
- Borch, T., Kretzschmar, R., Kappler, A., Cappellen, P. V., Ginder-Vogel, M., Voegelin, A., Campbell, K., 2009. Biogeochemical redox processes and their impact on contaminant dynamics. *Environmental Science and Technology*, 44(1), 15-23.
- Chen, S., Rotaru, A. E., Shrestha, P. M., Malvankar, N. S., Liu, F., Fan, W., Lovley, D. R., 2014. Promoting interspecies electron transfer with biochar. *Scientific Reports*, 4, 5019.
- Colombo, C., Palumbo, G., He, J. Z., Pinton, R., Cesco, S., 2014. Review on iron availability in soil: interaction of Fe minerals, plants, and microbes. *Journal of Soils and Sediments*, 14(3), 538-548.
- Cruz Viggì, C., Rossetti, S., Fazi, S., Paiano, P., Majone, M., Aulenta, F., 2014. Magnetite particles triggering a faster and more robust syntrophic pathway of methanogenic propionate degradation. *Environmental Science and Technology*, 48(13), 7536-7543.
- DeLuca, T. H., Gundale, M. J., MacKenzie, M. D., Jones, D. L., 2015. Biochar effects on soil nutrient transformations. *Biochar for Environmental Management: Science, Technology and Implementation*, 2, 421-454.
- Marris, E. 2006. Black is the new green.
- Eden, M. J., Bray, W., Herrera, L., McEwan, C., 1984. Terra preta soils and their archaeological context in the Caquetá basin of southeast Colombia. *American Antiquity*, 49(1), 125-140.
- Farrell, M., Kuhn, T. K., Macdonald, L. M., Maddern, T. M., Murphy, D. V., Hall, P. A., Baldock, J. A., 2013. Microbial utilisation of biochar-derived carbon. *Science of the Total Environment*, 465, 288-297.

- Feng, Y., Xu, Y., Yu, Y., Xie, Z., Lin, X., 2012. Mechanisms of biochar decreasing methane emission from Chinese paddy soils. *Soil Biology and Biochemistry*, 46, 80-88.
- Frenzel, P., Bosse, U., Janssen, P. H., 1999. Rice roots and methanogenesis in a paddy soil: ferric iron as an alternative electron acceptor in the rooted soil. *Soil Biology and Biochemistry*, 31(3), 421-430.
- Glissmann, K., Conrad, R., 2000. Fermentation pattern of methanogenic degradation of rice straw in anoxic paddy soil. *FEMS Microbiology Ecology*, 31(2), 117-126.
- Hori, T., Müller, A., Igarashi, Y., Conrad, R., & Friedrich, M. W., 2010. Identification of iron-reducing microorganisms in anoxic rice paddy soil by 13 C-acetate probing. *The ISME Journal*, 4(2), 267.
- Ippolito, J. A., Laird, D. A., Busscher, W. J. (2012). Environmental benefits of biochar. *Journal of environmental quality*, 41(4), 967-972.
- Jeffery, S., Verheijen, F. G., Kammann, C., Abalos, D., 2016. Biochar effects on methane emissions from soils: a meta-analysis. *Soil Biology and Biochemistry*, 101, 251-258.
- Jiang, X., Haddix, M. L., Cotrufo, M. F. 2016. Interactions between biochar and soil organic carbon decomposition: Effects of nitrogen and low molecular weight carbon compound addition. *Soil Biology and Biochemistry*, 100, 92-101.
- Joseph, S., Husson, O., Graber, E. R., Van Zwieten, L., Taherymoosavi, S., Thomas, T., Munroe, P., 2015. The electrochemical properties of biochars and how they affect soil redox properties and processes. *Agronomy*, 5(3), 322-340.
- Kappler, A., Wuestner, M. L., Ruecker, A., Harter, J., Halama, M., Behrens, S., 2014. Biochar as an electron shuttle between bacteria and Fe (III) minerals. *Environmental Science and Technology Letters*, 1(8), 339-344.
- Kato, S., Hashimoto, K., Watanabe, K., 2012. Methanogenesis facilitated by electric syntrophy via (semi) conductive iron-oxide minerals. *Environmental Microbiology*, 14(7), 1646-1654.
- Klüpfel, L., Keiluweit, M., Kleber, M., Sander, M., 2014. Redox properties of plant biomass-derived black carbon (biochar). *Environmental science & technology*, 48(10), 5601-5611.
- Kookana, R. S., Sarmah, A. K., Van Zwieten, L., Krull, E., Singh, B., 2011. Biochar application to soil: agronomic and environmental benefits and unintended consequences. In *Advances in agronomy*, 112,103-143. Academic Press.
- Konhauser, K. O., Kappler, A., & Roden, E. E., 2011. Iron in microbial metabolisms. *Elements*, 7(2), 89-93.
- Lehmann, J., Rillig, M. C., Thies, J., Masiello, C. A., Hockaday, W. C., Crowley, D., 2011. Biochar effects on soil biota—a review. *Soil Biology and Biochemistry*, 43(9), 1812-1836.
- Lehmann, J., Joseph, S., 2015. Biochar for environmental management: an introduction. In *Biochar for environmental management* 33-46. Routledge.
- Li, H., Chang, J., Liu, P., Fu, L., Ding, D. and Lu, Y., 2015. Direct interspecies electron transfer accelerates syntrophic oxidation of butyrate in paddy soil enrichments. *Environmental Microbiology*, 17(5),1533-1547.
- Liu, F., Rotaru, A. E., Shrestha, P. M., Malvankar, N. S., Nevin, K. P., Lovley, D. R., 2012. Promoting direct interspecies electron transfer with activated carbon. *Energy and Environmental Science*, 5(10), 8982-8989.
- Lovley, D.R., 2017. Happy together: microbial communities that hook up to swap electrons. *The ISME Journal*, 11(2), 327.
- Manyà, J. J. (2012). Pyrolysis for biochar purposes: a review to establish current knowledge gaps and research needs. *Environmental Science and Technology*, 46(15), 7939-7954.
- McInerney, M.J., Sieber, J.R. and Gunsalus, R.P., 2009. Syntrophy in anaerobic global carbon cycles. *Current Opinion in Biotechnology*, 20(6), 623-632.
- Nguyen, B.T., Lehmann, J., Kinyangi, J., Smernik, R., Riha, S. J., Engelhard, M. H., 2008. Long-term black carbon dynamics in cultivated soil. *Biogeochemistry*. 89 (3): 295-308.
- Prado, A., Berenguer, R., Esteve-Núñez, A., 2019. Electroactive biochar outperforms highly conductive carbon materials for biodegrading pollutants by enhancing microbial extracellular electron transfer. *Carbon*, 146, 597-609.

- Rotaru, A.E., Shrestha, P.M., Liu, F., Markovaite, B., Chen, S., Nevin, K.P. Lovley, D.R., 2014. Direct interspecies electron transfer between *Geobacter metallireducens* and *Methanosarcina barkeri*. *Applied Environmental Microbiology*, 80(15), pp. 4599-4605.
- Rotaru, A.E., Shrestha, P.M., Liu, F., Shrestha, M., Shrestha, D., Embree, M., Zengler, K., Wardman, C., Nevin, K.P. and Lovley, D.R., 2014. A new model for electron flow during anaerobic digestion: direct interspecies electron transfer to *Methanosaeta* for the reduction of carbon dioxide to methane. *Energy Environmental Science*, 7(1), pp.408-415.
- Saquin, J. M., Yu, Y. H., Chiu, P. C., 2016. Wood-derived black carbon (biochar) as a microbial electron donor and acceptor. *Environmental Science Technology Letters*, 3(2), 62-66.
- Sass, R. L., 1994. Short summary chapter for methane. *Global Emission and Controls from Rice Fields and Other Agricultural and Industrial Sources*.
- Smith, J.A., Nevin, K.P. and Lovley, D.R., 2015. Syntrophic growth via quinone-mediated interspecies electron transfer. *Frontiers in Microbiology*, 6, p.121.
- Shrestha, P.M. and Rotaru, A.E., 2014. Plugging in or going wireless: strategies for interspecies electron transfer. *Frontiers in Microbiology*, 5, 237.
- Sieber, J.R., Le, H.M. McInerney, M.J., 2014. The importance of hydrogen and formate transfer for syntrophic fatty, aromatic and alicyclic metabolism. *Environmental Microbiology*, 16(1), pp.177-188.
- Stams, A.J. and Plugge, C.M., 2009. Electron transfer in syntrophic communities of anaerobic bacteria and archaea. *Nature Reviews Microbiology*, 7(8), p.568.
- Steiner, C., Das, K. C., Melear, N., Lakly, D., 2010. Reducing nitrogen loss during poultry litter composting using biochar. *Journal of Environmental Quality*, 39(4), 1236-1242.
- Summers, Z.M., Fogarty, H.E., Leang, C., Franks, A.E., Malvankar, N.S. Lovley, D.R., 2010. Direct exchange of electrons within aggregates of an evolved syntrophic coculture of anaerobic bacteria. *Science*, 330(6009), pp.1413-1415.
- Sun, T., Levin, B. D., Guzman, J. J., Enders, A., Muller, D. A., Angenent, L. T., Lehmann, J., 2017. Rapid electron transfer by the carbon matrix in natural pyrogenic carbon. *Nature Communications*, 8, 14873.
- Sun, T., Levin, B. D., Schmidt, M. P., Guzman, J. J., Enders, A., Martínez, C. E., Lehmann, J., 2018. Simultaneous quantification of electron transfer by carbon matrices and functional groups in pyrogenic carbon. *Environmental Science and Technology*, 52(15), 8538-8547.
- Thauer, R.K., Kaster, A.K., Seedorf, H., Buckel, W. and Hedderich, R., 2008. Methanogenic archaea: ecologically relevant differences in energy conservation. *Nature Reviews Microbiology*, 6(8), p.579.
- Wu, S., Fang, G., Wang, Y., Zheng, Y., Wang, C., Zhao, F., Zhou, D., 2017. Redox-active oxygen-containing functional groups in activated carbon facilitate microbial reduction of ferrihydrite. *Environmental Science and Technology*, 51(17), 9709-9717.
- Xu, S., Adhikari, D., Huang, R., Zhang, H., Tang, Y., Roden, E., Yang, Y., 2016. Biochar-facilitated microbial reduction of hematite. *Environmental Science and Technology*, 50(5), 2389-2395.
- Xu, X., Huang, H., Zhang, Y., Xu, Z., Cao, X., 2019. Biochar as both electron donor and electron shuttle for the reduction transformation of Cr (VI) during its sorption. *Environmental Pollution*, 244, 423-430.
- Ye, J., Zhang, R., Nielsen, S., Joseph, S.D., Huang, D. and Thomas, T., 2016. A combination of biochar–mineral complexes and compost improves soil bacterial processes, soil quality, and plant properties. *Frontier in Microbiology*. 7, 372.
- Yu, L., Wang, Y., Yuan, Y., Tang, J., Zhou, S., 2016. Biochar as electron acceptor for microbial extracellular respiration. *Geomicrobiology Journal*, 33(6), 530-536.
- Yu, L., Yuan, Y., Tang, J., Wang, Y., Zhou, S., 2015. Biochar as an electron shuttle for reductive dechlorination of pentachlorophenol by *Geobacter sulfurreducens*. *Scientific Reports*, 5, 16221.
- Yuan, Y., Bolan, N., PrévotEAU, A., Vithanage, M., Biswas, J. K., Ok, Y. S., Wang, H., 2017. Applications of biochar in redox-mediated reactions. *Bioresource Technology*, 246, 271-281.
- Yuan, H.Y., Ding, L.J., Zama, E.F., Liu, P.P., Hozzein, W.N., Zhu, Y.G., 2018. Biochar modulates methanogenesis through electron syntrophy of microorganisms with ethanol as a substrate. *Environmental Science and Technology* 52, 12198-12207.
- Zhang, Y., Xu, X., Cao, L., Ok, Y. S., Cao, X., 2018. Characterization and quantification of electron donating capacity and its structure dependence in biochar derived from three waste biomasses. *Chemosphere*, 211, 1073-1081.

-Introduction-

- Zhang, W., Niu J. Z., Morales, V.L., Chen, X.C., Hay, A. G., Lehmann, J.; Steenhuis, T. S., 2010. Transport and retention of biochar particles in agriculture soils contaminated by waste water and smelter dust. *Ecohydrology.*, 3, 497-508; [http:// doi:10.1002/eco.160](http://doi:10.1002/eco.160).
- Zhou, G. W., Yang, X. R., Li, H., Marshall, C. W., Zheng, B. X., Yan, Y., Zhu, Y. G., 2016. Electron shuttles enhance anaerobic ammonium oxidation coupled to iron (III) reduction. *Environmental Science and Technology*, 50(17), 9298-9307.
- Zhou, G. W., Yang, X. R., Marshall, C. W., Li, H.; Zheng, B.-X.; Yan, Y.; Su, J.-Q.; Zhu, Y. G., 2017. Biochar addition increases the rates of dissimilatory iron reduction and methanogenesis in ferrihydrite enrichments. *Frontiers in Microbiology*, 8, 589; [http:// doi: 10.3389/fmicbb.2017.00589](http://doi:10.3389/fmicbb.2017.00589).
- Zimmerman, A. R., 2010. Abiotic and microbial oxidation of laboratory-produced black carbon (biochar). *Environmental Science and Technology*, 44(4), 1295-1301.
- Tang, J., Zhuang, L., Ma, J., Tang, Z., Yu, Z. and Zhou, S., 2016. Secondary mineralization of ferrihydrite affects microbial methanogenesis in *Geobacter*-*Methanosarcina* cocultures. *Applied Environmental Microbiology*, 82(19), pp.5869-5877.
- Zhuang, L., Xu, J., Tang, J. and Zhou, S., 2015. Effect of ferrihydrite biomineralization on methanogenesis in an anaerobic incubation from paddy soil. *Journal of Geophysical Research: Biogeosciences*, 120(5), pp.876-886.

### Chapter 3 – Personal contribution

Experiments were conceptualized by myself and Prof. Andreas Kappler. The cell suspension experiments and data collection were carried out by myself. Markus Maisch performed Mössbauer spectroscopy and evaluated the data. Prof. Martin Obst performed CLSM spectroscopy and data analysis. Dr. Edison Subdiaga conducted electrochemical analysis of biochar and DAX-8 samples. The discussion and analysis of the obtained results were done by myself, Tianran Sun, Prof. Andreas Kappler, Prof. Ruben Kretschmar, Prof. Stefan Haderlein, and Edison Subdiaga. The manuscript was written by myself. All co-authors read and revised the manuscript.

# |3

## **Aggregation-dependent electron transfer via redox-active biochar particles stimulate microbial ferrihydrite reduction**

Yang, Z., Sun, T., Subdiaga, E., Obst, M., Haderlein, S.B., Maisch, M., Kretzschmar, R., Angenent, L.T. and Kappler, A.

*Published on Science of The Total Environment 2020, 703, 135515.*

Copyright 2020 Science direct.



**Aggregation-dependent electron transfer via redox-active biochar particles stimulate microbial ferrihydrite reduction**

Zhen Yang<sup>a</sup>, Tianran Sun<sup>b</sup>, Edison Subdiaga<sup>c</sup>, Martin Obst<sup>d</sup>, Stefan. B. Haderlein<sup>c</sup>, Markus Maisch<sup>a</sup>, Ruben Kretzschmar<sup>e</sup>, Largus T. Angenent<sup>b</sup>, Andreas Kappler<sup>a\*</sup>

<sup>a</sup>*Geomicrobiology, Center for Applied Geoscience, University of Tuebingen, Germany*<sup>b</sup>*Environmental Biotechnology, Center for Applied Geoscience, University of Tuebingen, Germany*

<sup>c</sup>*Environmental Mineralogy and Chemistry, Center for Applied Geoscience, University of Tuebingen, Germany*

<sup>d</sup>*Experimental Biogeochemistry, University of Bayreuth, Germany*

<sup>e</sup>*Soil Chemistry Group, Institute of Biogeochemistry and Pollutant Dynamics, CHN, ETH Zurich, Switzerland*

### 3.1 Abstract

Microbial Fe(III) reduction plays an important role for biogeochemical carbon and iron cycling in sediments and soils. Biochar is used as a soil amendment to increase fertility and lower N<sub>2</sub>O/CO<sub>2</sub> emissions. It is redox-active and can stimulate microbial Fe(III) mineral reduction. It is currently unknown, however, how the aggregation of cells and Fe(III) mineral with biochar particles influence microbial Fe(III) reduction. Therefore, we determined rates and extent of ferrihydrite (Fh) reduction in *S. oneidensis* MR-1 cell suspensions with different particles sizes of wood-derived Swiss biochar and KonTiki biochar at different biochar/Fh ratios. We found that at small biochar particle size and high biochar/Fh ratios, the biochar, MR-1 cells and Fh closely aggregated, therefore addition of biochar stimulated electron transfer and microbial Fh reduction. In contrast, large biochar particles and low biochar/Fh ratios inhibited the electron transfer and Fe(III) reduction due to the lack of effective aggregation. These results suggest that for stimulating Fh reduction, a certain biochar particle size and biochar/Fh ratio is necessary leading to a close aggregation of all phases. This aggregation favors electron transfer from cells to Fh via redox cycling of the electron donating and accepting functional groups of biochar and via direct electron transfer through conductive biochar carbon matrices. These findings improve our understanding of electron transfer between microorganisms and Fe(III) minerals via redox-active biochar and help to evaluate the impact of biochar on electron transfer processes in the environment.

**Keywords:** biochar, ferrihydrite, dissimilatory iron reduction, electron transfer, redox mediator, aggregations

### 3.2 Introduction

Iron is one of the most important redox-active elements in nature, participates in microbial respiration as electron acceptor, and plays an important role in biogeochemical processes in general (Lovley et al., 2004; Kappler et al., 2005; Weber et al., 2006; Konhauser et al., 2011). Microbial Fe(III) reduction leads to (trans)formation and dissolution of minerals and controls the retention and release of trace metals and nutrients associated with these minerals (Zachara et al., 2001; Borch et al., 2010; Weber et al., 2009). The main mechanisms of electron transfer from microorganisms to Fe(III) minerals include direct contact of cells to Fe(III) minerals and electron transfer via outer-membrane proteins (Myers and Myers, 2003; Newman, 2005). However, at neutral pH, microbial Fe(III) reduction is limited by the low solubility of Fe(III) minerals (Kappler et al., 2005; Weber et al., 2006). Therefore, microorganisms have developed other pathways to transfer electrons to Fe(III) minerals (Shi et al., 2016). This includes the release of chelating agents to solubilize Fe(III) minerals (Shi et al., 2012), conductive cell extensions (pili; called microbial nanowires) (Reguera et al., 2005 and Malvankar et al., 2014), and the use of redox-active electron shuttles such as cell-produced flavins or natural organic matter (NOM) (Borch et al., 2010; Lovley et al., 1996; Marsili et al., 2008; Bauer et al., 2009; Fuller et al., 2014; Glasser et al., 2017). Electron shuttles can accept electrons from Fe(III)-reducing bacteria followed by abiotic electron transfer from the reduced shuttles to Fe(III) minerals, chromate, chlorinated or nitroaromatic compounds (Lovley et al., 1996; Bauer et al., 2009; Gescher and Kappler, 2013; Roden et al., 2010).

Biochar, produced by artificial pyrolysis of biomass, was shown to have potential to serve as a soil amendment to increase soil fertility, for carbon sequestration, and to lower CO<sub>2</sub>/N<sub>2</sub>O emissions, probably caused by changes in microbial community composition (Cayuela et al., 2013; Harter et al., 2014; Deluca et al., 2009; Gul et al., 2016; Hagemann et al., 2017; Lehmann and Joseph, 2015). Recently biochar has also been shown to stimulate electron transfer from bacteria to Fe(III) minerals (Kappler et al., 2014, Klüpfer et al., 2014; Yu et al., 2015; Yuan et al., 2017). Biochar is capable of transferring electrons due to the redox-active surface quinone/hydroquinone groups and the conjugated  $\pi$ -electron system in the condensed polyaromatic carbon ring structures in the carbon matrices (Keiluweit et al., 2010). Biochar redox reactions can therefore occur through i) redox cycling (i.e. accepting and donating of electrons) via redox-active quinone/hydroquinone groups (Klüpfer et al., 2014), ii) storage and transfer of electrons via the electrical double-layer capacitance of carbon matrices (Sun et al., 2017; Deeke et al., 2012; Ji et al., 2014; Sudirjo et al., 2019), and iii) direct electron transfer through the electrical conductance of carbon matrices (Sun et al., 2017; Sun et al., 2018). After addition to soils, biochar will be gradually broken down to small particles in the  $\mu\text{m}$ - to mm-size range by physical and chemical weathering as well as microbial decomposition (Lehmann and Joseph, 2015; Nguyen et al., 2008). These small biochar particles can easily be transported

through different soil layers (Wang et al., 2013; Zhang et al., 2010) and aggregate with microbes (Goiyeia and Pessenda, 2000) and minerals (Ye et al., 2016). It has been shown that smaller powdered biochar particles caused higher rates of microbial Fe(III) reduction compared to larger granulated biochar (Zhou et al., 2017). However, it remained unclear whether and how aggregation of biochar and microbes with Fe(III) minerals influence the electron transfer across the respective solid interfaces, and which mechanism, i.e. electron transfer via redox-active functional groups or via carbon matrices in biochar, dominates the electron transfer during stimulation of microbial Fe(III) reduction.

Probing the dependency of microbial Fe(III) reduction on the aggregation with biochar helps to better understand the electron transfer fundamentals among the three phases and provide practical guidelines for the implementation of biochar particles in soil. The present study therefore investigated the dependency of the rate and extent of microbial ferrihydrite reduction on biochar-cell-ferrihydrite aggregation at different biochar particle size and biochar/ferrihydrite ratios. We used *Shewanella oneidensis* MR-1 as a model Fe(III)-reducing bacterium. *S. oneidensis* MR-1 is an important dissimilatory Fe(III)-reducing bacterium which is ubiquitous in freshwater, marine, soil and sedimentary environments. This strain has been used in various electron shuttling and Fe(III) minerals reduction studies, including experiments with ferrihydrite and biochar (Kappler et al., 2014). We employed light/fluorescence microscopy to analyze the aggregates as well as voltammetry and electron balance calculations to reveal the primary pathways for interfacial electron transfer. We hypothesized that aggregation influences the phase contact between biochar and minerals leading to either stimulation or inhibition of microbial Fh reduction.

### **3.3 Materials and methods**

#### *3.3.1. Preparation of Biochar Suspensions and Biochar Leachates*

Swiss biochar (s-biochar, Belmont-sur-Lausanne, VB, Switzerland) was produced from mixed wood waste materials and KonTiki biochar (k-biochar) from pine wood chips at 700°C. Different particle sizes of biochar were produced by milling (Pulverisette, zirconium oxide balls, Fritsch, Idar-Oberstein, Germany) leading to large-, medium- and small-sized biochars (properties shown in Table S1 and Fig. S3) corresponding to environmentally relevant particle sizes of 100s of nm to ca. 150 µm (Wang et al., 2013; Zhang et al., 2010; Song et al., 2019). The milling process results in increased specific surface area of biochar. Compared to initial biochar particles (200 and 102 m<sup>2</sup>/g for s-biochar and k-biochar, respectively), the biochar particles milled showed an increase in specific surface area (Table S1). Anoxic biochar suspensions were prepared as described in the SI.

## 2.2. Mediated Electrochemical Analysis

Degassed biochar powders with different particle sizes were suspended in 0.1 M anoxic phosphate buffer (pH 7; final concentration 1 g biochar/L). Electrochemical analysis of biochar suspensions was conducted as published (Xu et al., 2016; Kappler et al., 2014) recently and as described in the SI.

### 3.3.2. Fe(III) Mineral Reduction Experiments

Microbial Fe(III) reduction experiments were set up in triplicate in 16 mL glass tubes containing 7.2 mL of 30 mM bicarbonate buffer (pH 7), Fh (0.67, 1.0, 1.5, 5, 7.5 and 15 mM Fe as Fh) synthesized according to Amstaetter et al. 2012) as electron acceptor, sodium lactate (3 or 30 mM), and 500  $\mu$ L biochar suspension at different final concentrations of 1, 5, and 10 g/L, amended with  $2 \times 10^9$  *S. oneidensis* MR-1 cells/mL (cultivated as described in (Kappler et al. 2014). Anthraquinone-2,6-disulfonate (AQDS, 100  $\mu$ M) was used as a positive control for electron shuttling to evaluate the effect of biochar amendments on Fe(III) reduction. Abiotic control experiments contained biochar and Fh without MR-1 cells. An experiment using DAX-8 resin particles was done as control for non-conductive but similar-sized particles as the biochars. The effect of biochar leachates on microbial Fh reduction (Fig. S10) was determined using cell suspension experiments with bicarbonate buffer (30 mM), *S. oneidensis* MR-1 ( $2 \times 10^9$  cells/mL), Fh (15 mM), lactate (30 mM), and 0.5 mL of biochar leachates. Biochar toxicity was evaluated in a MR-1 Fe(III) reduction cell suspension experiment with bicarbonate buffer (30 mM), Fe(III)-citrate (5 mM), lactate (30 mM), and biochar (1, 5, and 10 g/L) (Fig. S11).

### 3.3.3 Analytical Methods

Surface functional groups of s-biochar and k-biochar with different particle sizes were analyzed by Fourier Transform Infrared Spectroscopy (FTIR, IR-Tracer-100, Shimadzu). TOC of freeze-dried biochar powder and DOC in biochar leachates were determined with a TOC analyzer (Analytik Jena, Germany). Biochar particle size was determined by laser diffraction (Malvern Mastersizer 2000). Total Fe(II) (soluble in 1M HCl) and Fe(tot) (soluble in 1M hydroxylamine hydrochloride, HAHCl) were determined using the ferrozine assay (Amstaetter et al., 2012; Stookey et al., 1970). The protein and polysaccharide contents of EPS were quantified using established protocols (Frólund et al., 1996; Zhang et al., 2013). Cell-mineral-biochar aggregates were visualized by bright field and fluorescence microscopy (Leica DM 5500B, Leica, Germany). *S. oneidensis* MR-1 cells were stained by DNA dye Syto 9 combined

with propidium iodide, excited at 488 nm). The three-dimensional aggregation of *S. oneidensis* MR-1, Fh and s-biochar was visualized by Confocal Laser-Scanning Microscopy (CLSM, Leica TCS SPE, Leica, Germany). The mineral identity and Fe(II)/Fe(III) content of minerals formed were determined by Mössbauer spectroscopy (Byrne et al., 2016). The zeta potentials of biochar particles (at pH 7, NaHCO<sub>3</sub> buffer) were determined by laser Doppler velocimetry (zetaser, Malvern Nano ZSP) and applying Smoluchowski's equation to convert electrophoretic mobility into zeta potential values.

#### 3.3.4 Statistical Analysis

Differences between treatments were analyzed by ANOVA using Tukey's test for mean values ( $p < .05$ ). All statistical analyses were carried out using SPSS Statistics 22.0.

### 3.4 Results and discussion

#### 3.4.1. Redox Properties of Biochars

To evaluate the redox properties of s-biochar and k-biochar, electron accepting capacity (EAC) and electron donating capacity (EDC) were quantified by mediated electrochemical analysis (Klöpffel et al., 2014) for large-sized particles (LP, main fraction  $>100 \mu\text{m}$ ), intermediate-sized particles (MP, small fraction  $0.1\text{-}0.5 \mu\text{m}$  and main fraction  $10\text{-}20 \mu\text{m}$ ), and small-sized particles (SP, small fraction  $0.1\text{-}0.3 \mu\text{m}$  and main fraction  $5\text{-}10 \mu\text{m}$ ) biochar (Fig. S1). The EAC values of all biochar particles were  $0.752 \pm 0.002$  to  $0.787 \pm 0.001 \text{ meq e}^-/\text{g}$  biochar for s-biochar and  $0.530 \pm 0.001$  to  $0.589 \pm 0.001 \text{ meq e}^-/\text{g}$  biochar for k-biochar, while the EDC values of all biochar particles were  $0.231 \pm 0.001$  to  $0.232 \pm 0.001 \text{ meq e}^-/\text{g}$  biochar for s-biochar and  $0.182 \pm 0.002$  to  $0.184 \pm 0.001 \text{ meq e}^-/\text{g}$  biochar for k-biochar (Fig. S1). We found that particle size had no influence on EAC and EDC indicating that the milling process applied to produce different particle sizes did not cause any redox property artifacts. EAC and EDC values determined for s-biochar and k-biochar are similar as determined electrochemically for another wood-derived biochar (Harter et al., 2014) Biochars produced at  $700^\circ\text{C}$ , as our biochars, typically are more oxidized (EAC>EDC). The highest range of EAC values were observed at production temperatures of  $500\text{-}700^\circ\text{C}$  (Klöpffel et al., 2014). EAC values of biochar correlate with its quinone content (Klöpffel et al., 2014) suggesting that our s-biochar has more quinone functional groups than the k-biochar. The EEC (sum of EAC and EDC), was calculated for s-biochar and k-biochar to be  $0.98\text{-}1.02$  and  $0.71\text{-}0.77 \text{ meq e}^-/\text{g}$  biochar for all particle sizes. These values are higher than EEC values of other wood-derived biochars ( $0.3\text{-}0.7 \text{ meq e}^-/\text{g}$ ) (Klöpffel et al., 2014) but comparable to values of activated carbon ( $1.34\text{-}1.42 \text{ meq e}^-/\text{g}$ ) (Wu et al., 2017). The EECs of biochars normalized to TOC ( $\text{meq e}^-/\text{mg}$

C) (Fig. S2) show that that the mixed wood-derived s-biochar has a higher EEC than the k-biochar. The surface functional groups of s-biochar and k-biochar were analyzed by FTIR. Ketones, aromatic carbon, and carboxyl groups were identified by C=C and C=O stretching bonds ( $1700\text{ cm}^{-1}$  and  $1600\text{ cm}^{-1}$ ) (Fig. S3). The absence of significant changes in the C=C and C=O stretching bonds between LP and SP of s-biochar and k-biochar indicates that the particle size (the milling process) had no obvious influence on the presence of functional groups in the biochar and confirms the observation that on a per weight basis, all particle sizes have similar EAC/EDC values.

### 3.4.2. Microbial Fh Reduction Rates and Extent

We conducted cell suspension experiments with Fh as electron acceptor, *S. oneidensis* MR-1 as Fe(III)-reducing bacterium and different particle sizes and concentrations of biochar (leading to different biochar:Fh ratios) to determine the rates and extent of microbial Fh reduction (Fig. 1; 16-hour long-term experiments are shown in Fig. S5). First Fh reduction experiments were performed with 10 g/L of s-biochar and 15 mM Fe as Fh (Fig. 1A). We found that all biochar particle sizes stimulated Fh reduction; the smaller the biochar particle size, the higher rates and extents of Fh reduction. AQDS has been shown to be an efficient electron shuttling model compound and was used here as exogenous electron shuttle for comparison to biochar (Rau et al., 2002; O'loughlin 2008; Jiang et al., 2008; Scott et al., 1998; Benner et al., 2002; Eusterhues et al., 2014). For small-particle s-biochar, the rate and extent of Fh reduction was even higher than with AQDS that significantly stimulated the rate and extent of microbial Fh reduction (ANOVA,  $p=.012$ ) in accordance with previous studies (Lovley et al., 1996; Byrne et al., 2016). Addition of DAX-8 resin particles with particle sizes similar as LP, MP and SP biochar showed no influence on microbial Fh reduction (Fig. S7). Additionally, we found no evidence that surface-attached microbial growth influenced microbial Fh reduction in the presence of DAX-8 suggesting that the positive biochar effect in our experiments is not due to a particle effect but is related to the redox activity of biochar.

In contrast to these first experiments with 10 g/L biochar and 15 mM Fh (biochar/Fh ratio of 0.67 g/mmol Fe), lower biochar concentrations of either 5 or 1 g/L, resulting in lower biochar/Fh ratios of 0.3 and 0.067 g/mmol Fe, inhibited microbial Fh reduction relative to experiments without biochar (Fig. 1B, 1C, 1D and Fig. S5). These results suggest an effect of the biochar:Fh ratio on microbial interactions with the biochar particles. To investigate whether a certain ratio of biochar to Fh is required to stimulate microbial Fh reduction, we performed experiments at high biochar/Fh ratios of 0.67, 1.0 and 1.5 g/mmol Fe, respectively, using either 5 or 1 g/L s-biochar (Fig. 2). We found that at a ratio of 0.67 with 5 g/L s-biochar (Fig. 2a, 16-hour experiments in Fig. S6), small-particle s-biochar stimulated electron transfer, medium-sized particles had no significant effect (ANOVA,  $p=.62$ ) while large-particle s-biochar

significantly slowed down (but did not completely prevent) Fe(III) reduction (ANOVA,  $p=.023$ ) compared to the setup without biochar. When increasing the biochar/Fh ratio to 1.0 g/mmol Fe (with 5 g/L s-biochar), large and medium-sized particles showed no significant effect (ANOVA,  $p=.13$ ) but small-sized particles stimulated (ANOVA,  $p = .003$ ) Fe(II) formation (Fig. 2B). For setups with 1 g/L of s-biochar and a biochar/Fh ratio of 0.67 g/mmol Fe, all biochar particle sizes showed an inhibitory effect on Fh reduction (Fig. 2C). When the biochar/Fh ratio was increased to 1.0 g/mmol Fe with 1 g/L biochar, small-particle s-biochar stimulated Fh reduction, medium-sized s-biochar showed no effect, and large-particle s-biochar inhibited Fe(II) formation (Fig. 2D). At a biochar/Fh ratio of 1.5 g/mmol Fe (with 1 g/L biochar), all biochar particle sizes stimulated microbial Fh reduction (Fig. 2E).

We also determined for k-biochar whether a certain biochar/Fh ratio is required to stimulate microbial Fh reduction (Fig. S8 and S9). When using setups with a k-biochar/Fh ratio of 0.67 g/mmol Fe (with 10 g/L k-biochar) or a ratio of 1.0 g/mmol Fe (with 1 g/L k-biochar), all k-biochar particles (LP, MP, and SP) slowed down Fe(II) formation compared to setups without shuttle. In contrast, at ratios of 2.0 g/mmol Fe (with 10 g/L k-biochar), 2.5 g/mmol Fe (with 5 g/L k-biochar) and 3.3 g/mmol Fe (with 1 g/L k-biochar) all three particles sizes of k-biochar stimulated microbial Fh reduction.

In summary these experiments have shown that smaller particle sizes and high biochar:Fh ratios stimulated microbial Fh reduction, while large particles and lower biochar:Fh ratio inhibited reduction relative to controls without biochar suggesting that a certain biochar/Fh ratio was necessary for stimulating Fh reduction (Fig. 2, bottom). For the biochars used in this study, the biochar/Fh ratio played a more important role than particle size for stimulation of microbial Fh reduction. At a certain ratio of biochar/Fh, the s-biochar (due to its higher electron accepting and donating capacity) showed higher rates and extent of microbial Fh reduction than k-biochar.

In a control experiment with 15 mM Fh and MR-1 cells we determined whether biochar leachate, i.e. redox-active molecules mobilized from the biochar particles during incubation in our experiment, had any effects on microbial Fh reduction (Fig. S10). We found that leachates from our biochar (ca. 4.5 mg C/L) did not have any apparent influence on rates and extents of microbial Fh reduction. Our result is in contrast to a previous study (Song et al., 2019) that showed stimulation of microbial Fh mineral reduction by straw-derived biochar leachates (TOC content up to 26.5 mg C/L), but is in agreement with Wu et al. (2017) who showed that the leachate from activated carbon could not enhance Fh reduction. These differences may be rationalized by the low DOC content of our leachate (ca. 4.5 mg C/L) that is lower than the threshold concentration (ca. 5-10 mg C/L) required for electron shuttling (Jiang et al., 2008). Finally, a Fe(III) reduction experiment with Fe(III) citrate (5 mM) and MR-1 cells with and without biochar particles showed that there is no toxic effect of the biochar used in our experiments on the MR-1 cells (Fig. S11).



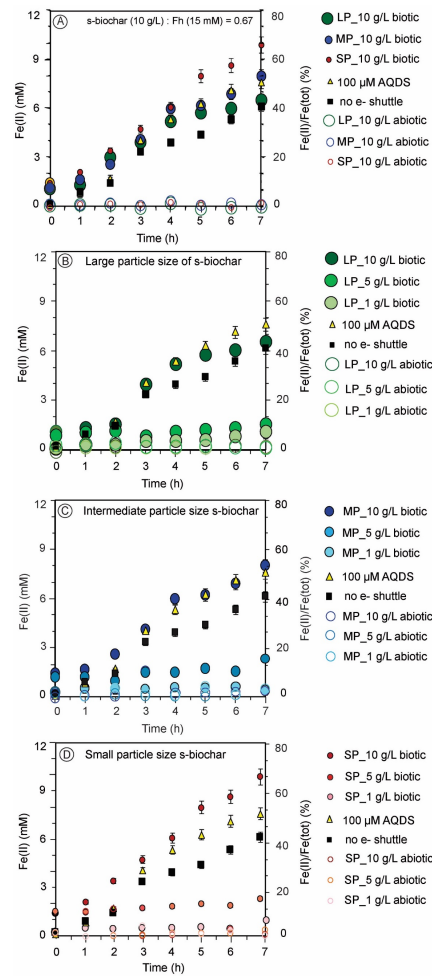


**Fig. 1.** Microbial ferrihydrite (Fh, 15 mM) reduction by *S. oneidensis* MR-1 in the presence of (A) large, intermediate and small particle size (LP, MP, SP) of Swiss biochar (s-biochar, 10 g/L), (B) 1, 5 and 10 g/L of large particle size s-biochar, (C) 1, 5 and 10 g/L of intermediate particle size s-biochar, and (D) 1, 5 and 10 g/L of small particle size s-biochar. Error bars represent standard deviations of triplicate experimental setups. The results for 16-h incubations are shown in Fig. S5.

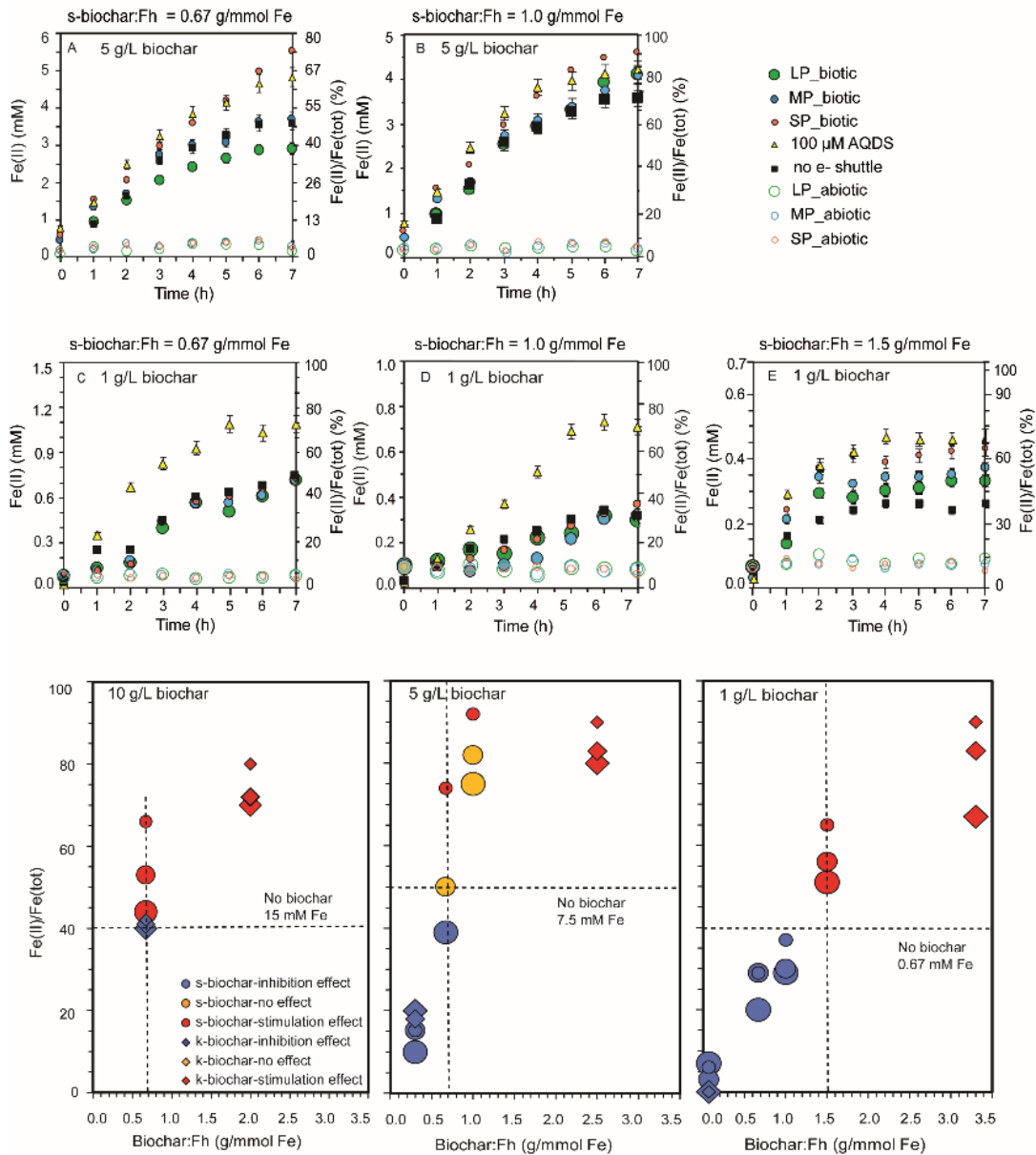


**Fig. 2.** Top: Microbial ferrihydrite (Fh) reduction by *S. oneidensis* MR-1 at different Swiss biochar (s-biochar) particle sizes and biochar:Fh ratios (g biochar per mmol Fe). (A) Ratio 0.67 with 7.5 mM Fh and 5 g/L biochar; (B) Ratio 1.0 with 5 mM Fh and 5 g/L s-biochar; (C) Ratio 0.67 with 1.5 mM Fh and 1 g/L s-biochar; (D) Ratio 1.0 with 1 mM Fh and 1 g/L s-biochar; (E) Ratio 1.5 with 0.67 mM Fh and 1 g/L s-biochar. Error bars represent standard deviations of triplicate experimental setups. The results for 16-h incubations are shown in Fig. S6. Bottom: Influence of biochar (s-biochar and KonTiki biochar, k-biochar) particle size (indicated by the size of the symbols) and biochar:Fh ratios (g biochar per mmol Fe) on microbial Fh reduction. Blue symbols and red symbols show experiments in which inhibition (blue) and stimulation (red) of microbial Fh reduction were observed, while yellow symbols show experiments where biochar addition had no effect on rates of Fe(III) reduction compared to setups without biochar addition.

### 3.4.3. Aggregation of *S. oneidensis* MR-1 Cells with Biochar and Fh

In the absence of dissolved electron shuttles (neither from biochar leachate nor from the MR-1 cells since they are not producing shuttles in non-growing cell suspensions), electron transfer from the MR-1 cells to Fh depends on the ability of electrons to be transferred either from cells directly to the Fh particles or from cells via redox-active biochar particles to the Fh. Therefore, we monitored aggregates of s-biochar with Fh and MR-1 cells by fluorescence microscopy at different s-biochar/Fh ratios. In setups of small-particle s-biochar with Fh (ratio of 0.67 g/mmol) where stimulation of Fh reduction was observed, the s-biochar particles were associated with the Fh (Fig. 3A) and the cells were attached to both Fh and biochar (Fig. 3B). Overlay images of bright-field and fluorescence images (Fig. 3C) indicated a close association of cells with s-biochar and Fh obviously facilitating electron transfer and therefore stimulating Fh reduction. In contrast, in images with 5 g/L large-particle s-biochar (ratio of 0.3 g/mmol Fe), the s-biochar particles were less associated with Fh (Fig. 3D) and the MR-1 cells were mainly attached to the s-biochar but not to Fh (Fig. 3E). Consequently, these setups showed inhibition of Fh reduction compared to setups without biochar, probably due to limited electron transfer from the cells to the Fh based on the greatly diminished contact with the Fh (Fig. 4F). When keeping the same s-biochar concentration of 5 g/L but with small-particle s-biochar and decreasing the Fh to 5 mM yielding a ratio of 1.0 g/mmol Fe, s-biochar particles showed an intimate association with Fh (Fig. 3G) and MR-1 cells were also associated with both s-biochar and Fh (Fig. 3H and 3I), suggesting again a close association of cells, Fh and s-biochar thus leading again to stimulation of Fh reduction. While dissolved electron shuttles can also contribute to a stimulation of electron transfer by diffusion, in the case of biochar particles diffusion probably plays a minor role as the biochar rather may act as a solid-state bridge between cells and Fh to accelerate electron transfer (Fig. 3A-C, and Fig. 3G-I). Additionally, these results suggest that MR-1 cell adhesion to biochar that is associated with Fh is necessary for stimulating electron transfer in the presence of biochar as an electron shuttle between MR-1 cells and Fh. Interestingly, a cell suspension experiment conducted with higher cell numbers ( $5 \times 10^9$  cells/mL) at the same s-biochar/Fh ratio of 0.3 g/mmol Fe showed no apparent increase in rates and extent of Fh reduction (Fig. S13), suggesting that there were still not enough cells that had access to Fh - either directly or indirectly via redox-active s-biochar particles.

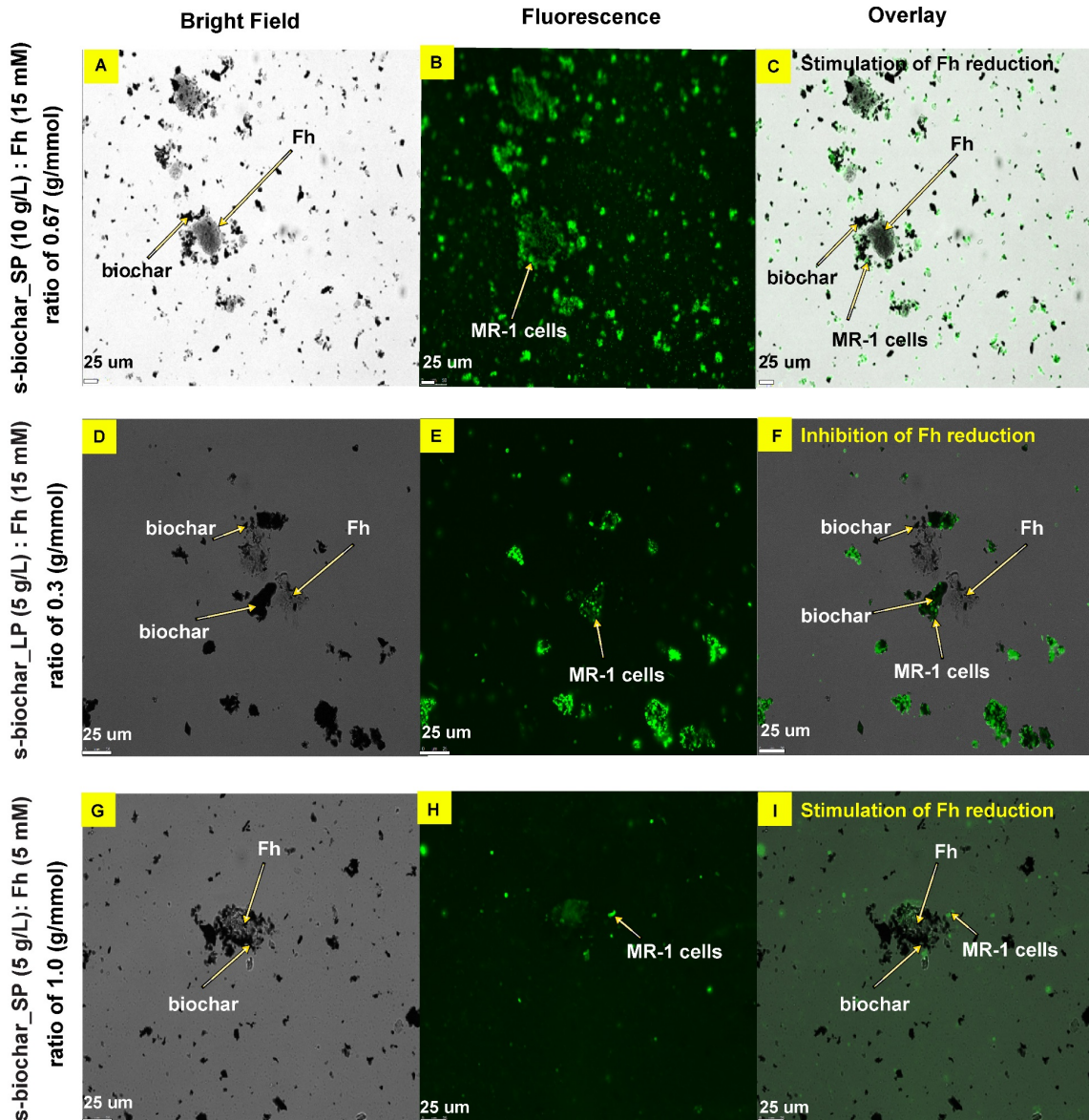


**Fig. 3.** Aggregation of Swiss biochar (s-biochar) with ferrihydrite (Fh) and *S. oneidensis* MR-1 cells (stained by DNA dye Syto 9 combined with propidium iodide) analyzed by fluorescence microscopy. Experiments with s-biochar:Fh ratios (g/mmol) of 0.67 (A-C), 0.3 (D-F) and 1.0 (G-I). The gray parts represent Fh, the black parts represent s-biochar particles and MR-1 cells are shown in green. (A) 10 g/L small particle size (SP) s-biochar associated with 15 mM Fh (bright field, no fluorescence), (B) MR-1 cells attached to particles (fluorescence), and (C) overlay of A and B showing the aggregation of MR-1 cells with s-biochar and Fh (which showed a stimulation of microbial Fh reduction). (D) 5 g/L large particle size (LP) s-biochar and 15 mM Fh, (E) MR-1 cells and particles, and (F) overlay of D and E showing aggregation of MR-1 cells with s-biochar and Fh (which showed an inhibition of microbial Fh reduction). (G) 5 g/L SP s-biochar associated with 5 mM Fh, (H) MR-1 cells attached to particles and (I) overlay of G and H showing the aggregation of MR-1 cells with s-biochar and Fh where a stimulation of microbial Fh reduction was observed again. Please note that the fluorescence images shown are representative images chosen among ca. 100 images. Due to overlay of cells, minerals and s-biochar particles they cannot be used for quantification of certain aggregates/associations.

Influence of cell-biochar-ferrihydrite aggregation (depending on Biochar particle size and Biochar:Fh ratio) on electron transfer mechanisms and the fate of electrons from lactate oxidation. To evaluate the electron transfer mechanisms and the fate of electrons released from lactate oxidation in the presence of different biochar:Fh ratios, we calculated the percentage of electrons recovered as Fe(II), electrons theoretically accepted by functional groups of biochar and remaining electrons in biochar carbon matrices or in cells (Table S2, Fig. 4). This allows to evaluate the contributions of different electron transfer pathways, i.e. electron transfer via redox cycling of functional groups of biochar as well as conductance and capacitance of the biochar carbon matrices, based on the extent of aggregation of cells, biochar and Fh (Fig. 5).

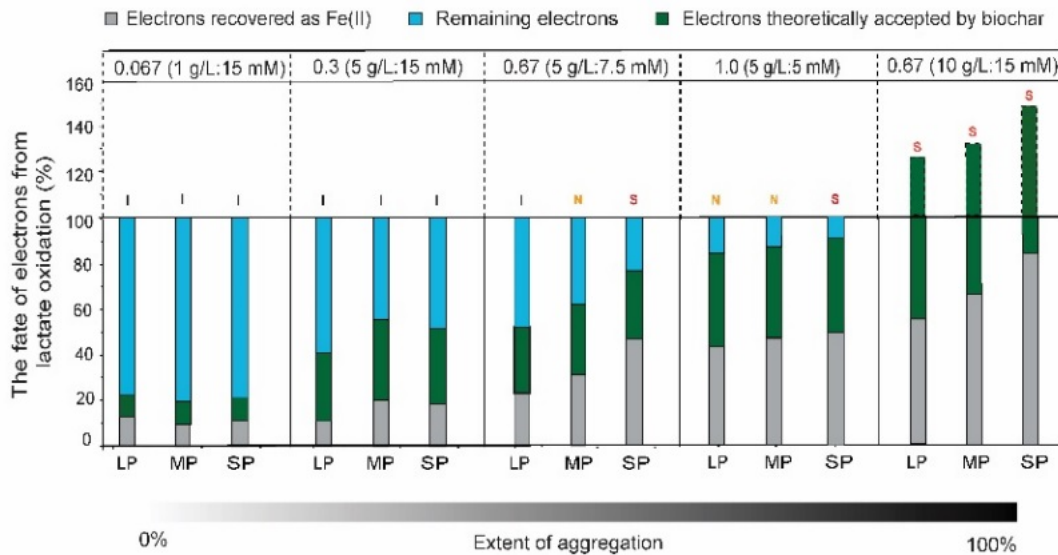


**Fig. 4.** The fate of electrons released from lactate oxidation in the presence of large (LP), medium (MP) and small particles (SP) of Swiss biochar (s-biochar) at biochar:Fh ratios (g biochar/mmol Fe) of 0.067, 0.3, 0.67 and 1.0. Electrons released from oxidation of lactate to acetate are recovered as either i) Fe(II) stemming from microbial Fe(III) reduction ((quantified as Fe(II) in our experiments), ii) electrons theoretically accepted by s-biochar (quantified from EAC of biochar measured) or iii) remaining electrons calculated as the difference between electrons released from lactate oxidation and electrons accepted by s-biochar and recovered as Fe(II), which includes electrons stored by the carbon matrices capacitance and electrons stored in cells (e.g. as lactate). 'I' (black), 'N' (orange), and 'S' (red) symbols on the top of bars indicate whether inhibition, no change or stimulation of microbial Fe(III) reduction occurred compared to setups without biochar amendment.

In the presence of biochar and Fh (biochar:Fh ratio of 0.067 g/mmol Fe), for all particle sizes, 10-11% of the electrons that were released from lactate oxidation by *S.oneidensis* MR-1 to acetate and CO<sub>2</sub> (4 electrons per lactate) were recovered as Fe(II) and up to 8-9% of the

released electrons could have been (theoretically) accepted by the redox-active functional groups of the biochar. Up to 80% of the remaining electrons were probably stored within the biochar due to its electrical double-layer capacitance (Sun et al., 2018) or in the cells (Fig. 4 and 5). In experiment with a biochar to Fh ratio of 0.067, biochar was poorly associated with Fh (i.e. the extent of aggregation of biochar with Fh is close to 0%; see Fig. S14a). The electrons donated from MR-1 cells were therefore stored in the  $\pi$ -electron system of carbon matrices instead of being released to Fh. These stored electrons were surrounded and charge balanced most likely by protons which were co-products with electrons in the MR-1 metabolism (Pinchuk et al., 2011). This microbial electron-proton system could have constituted an electrical double-layer in biochar and was responsible for capacitive electron storage. A similar electron storage mechanism has been found in capacitive microbial fuel cells (Deeke et al., 2012). Due to the insufficient association of biochar and Fh (Fig. 5), the 10-11% of Fe(II) formed probably stem from cells that were directly attached to Fh and reduced the Fh.

When increasing the biochar:Fh ratio to 0.3 g/mmol Fe with 5 g/L of biochar, more electrons were recovered as Fe(II) (13-22%) and more electrons can be accepted by redox-active functional groups of the biochar (34-36%). The fraction of remaining electrons, probably stored by the capacitance of the carbon matrices, decreased to 42-53%. When further increasing the biochar/Fh ratio to 0.67 g/mmol Fe, although a similar percentage of electrons can be accepted by the functional groups of biochar as in the 0.3 ratio setup, more electrons were recovered as Fe(II) (26-48%) and consequently less electrons (19-39%) were stored in the biochar and/or cells. These results suggest that at higher biochar/Fh ratios, as a result of the increased aggregation of biochar with Fh, electrons were directly transferred from the cells to the Fh by the conductive biochar carbon matrices, promoting Fe(II) formation, (Fig. S14b); the biochar conductivity was similar as it was described for a 700°C pyrolyzed sawdust biochar which contributed to electron transfer during persulfate oxidation (He et al., 2019). At the same biochar/Fh ratio of 0.67 g/mmol Fe with small-sized particles or at an even higher biochar/Fh ratio of 1.0 g/mmol Fe with all particle sizes, only a small fraction of electrons (8-19%) was stored in biochar and cells (Fig. 4) suggesting an efficient transfer of electrons from the cells to the Fh via the conductive biochar and via reduced functional groups of biochar. Generally, small-sized particles showed higher rates of Fe(II) formation and higher percentages of electrons recovered as Fe(II) than medium- and large-sized biochar particles probably because smaller biochar particles show a higher extent of aggregation with Fh (see e.g. Fig. S14c) facilitating direct electron transfer to Fh.

In setups with a biochar/Fh ratio of 0.67 g/mmol and 10 g/L biochar, for the three particle sizes (SP, MP, LP) up to 56-85% of electrons were recovered as Fe(II) and 65-67% could have been theoretically accepted by the functional groups of biochar, respectively (Fig. 4, Fig. S14d),

leading in all cases to a stimulation of Fe(II) formation compared to the biochar-free setups. Due to the intimate contact of the biochar with the Fh, in these cases probably no electrons were stored in the carbon matrices, i.e. most electrons were transferred from biochar to Fh (Fig. 4). It is obvious from these experiments that the stimulation of Fh reduction by biochar required a certain biochar/Fh ratio to facilitate direct electron transfer from bacteria via biochar to Fh (Fig. 5).

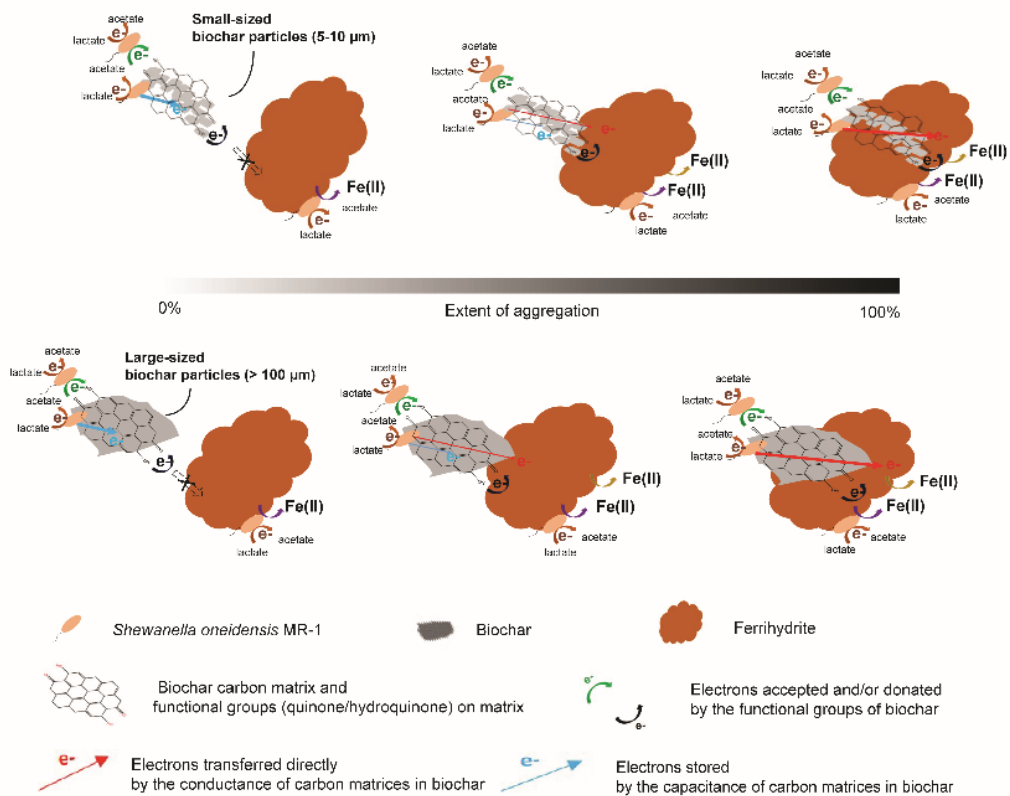


**Fig. 5.** Electron transfer pathways between *S. oneidensis* MR-1 cells and ferrihydrite (Fh) in the presence of small-sized (2-10 μm) and large-sized biochar particles (>100 μm) depending on the extent of aggregation of biochar and Fh. When Fh as electron acceptor is not close to the biochar (i.e. the extent of aggregation of biochar to Fh is close to 0%), electrons released from microbial lactate oxidation can be accepted by functional groups (quinones) of biochar or can be stored in biochar by the capacitance of carbon matrices. In this case, Fh reduction is only possible by cells directly associated with the Fh. With increasing extent of aggregation of biochar with Fh, the electrons start to be transferred to Fh by both electron donation of the hydroquinone groups and direct electron transfer by the carbon matrices, so that more and more Fe(II) will be produced.

### 3.3.4. Potential Factors Influencing the Aggregation of Cells, Biochar and Fh.

To better understand the aggregation of cells with biochar and Fh, we determined the zeta potential of the SP, MP and LP s-biochar. SP-sized s-biochar showed a more negative potential ( $-26.5 \pm 0.3$  mV) than MP-sized ( $-22.8 \pm 0.1$  mV) and LP-sized biochar ( $-15.2 \pm 0.2$  mV) (Fig. S14). These results are in agreement with previous studies (Eusterhues et al., 2014) on oak-derived biochar pyrolyzed at  $650^{\circ}\text{C}$  (particles of 0.25-2 mm) with a zeta potential close to -10 mV. The zeta potentials of the s-biochar particles were more negative than those of the MR-1 cells ( $-7.65 \pm 0.3$  mV; similar as other values of -6.4 mV) (Wu et al., 2017), suggesting that in particular the SP-sized s-biochar, that showed the most negative value, is expected to attach to a larger extent to the positively charged Fh with +18 mV (Li et al. 2015) than the cells (Fig. 3A, 3D and 3G). Consequently, a fast electron transfer from cells via biochar can happen when cells are attached to biochar.

We also observed that MR-1 cells were attached more to the negatively-charged biochar particles than to the Fh particles (Fig. 3F), suggesting that bacteria can bind efficiently to the biochar surface using hydrophobic interactions thus overcoming the repulsion by the negative surface charges (Suliman et al., 2017). Alternatively, the interactions of the negatively charged cells and the negatively charged biochar maybe supported by bridging cations. Additionally, with increasing Fh concentrations, the mineral particles can aggregate forming large mineral assemblages with a lower weight-based surface area (Viliacis-Garcia et al., 2015; Bompoti et al., 2017; Hiemstra and Van Riemsdijk, 2009) and less binding sites for biochar and cells. A recent study observed an inhibition of Fh reduction by *S. oneidensis* MR-1 by graphene material (Liu et al., 2018) and explained this by a limited accessibility of the Fh by the microorganisms. Our and their findings together indicate that on the one hand certain ratios of solid electron shuttle to Fh (in our case biochar/Fh) and a close aggregation of the biochar, MR-1 cells, and Fh is required to stimulate microbial Fh reduction and on the other hand high amounts of graphene-based materials or biochar present can inhibit electron transfer. Three-dimensional analysis of the same samples using CLSM confirmed the observations from fluorescence microscopy regarding cell-mineral-biochar aggregations and also revealed the secretion of extracellular polymeric substances (EPS) (Fig. S16). EPS can help microorganisms to attach to minerals and facilitate electron transfer between cells and the solid surface (Harris et al., 2010) owing to its redox properties (Cao et al., 2011; Li et al., 2016). Therefore, we investigated whether biochar influenced EPS secretion from MR-1 by quantification of the protein and polysaccharide contents after addition of different concentrations of s-biochar and 15 mM Fh (Fig. S17). We observed that low concentrations (1 and 5 g/L) of SP s-biochar decreased the protein but increased the polysaccharide content in EPS compared to setups without electron shuttle, while higher concentrations (10 g/L) of SP



s-biochar and AQDS (100  $\mu\text{M}$ ) behaved similar as setups without electron shuttle and showed a slight increase in protein contents compared to low concentration biochar amendments. Based on these observations, it is conceivable that biochar addition influenced the concentrations of redox-active compounds within the EPS and that these differences influence electron transport from the outer membrane of MR-1 cells via EPS to biochar particles. EPS was indeed shown to store redox-active flavins and cytochromes, enabling EPS-bound cells to transport electrons extracellularly to electron acceptors via extracellular electron transfer (EET), i.e. electron hopping across the EPS (Xiao et al., 2017). Additionally, a previous study (Caccavo et al., 1999) suggested the contribution of surface proteins to the adhesion of the dissimilatory Fe(III)-reducing bacterium *S. alga* BrY to poorly crystalline ferric hydroxide. The presence of lower and higher concentrations of potentially redox-active proteins in the EPS may offer additional explanations how low biochar concentrations (1 and 5 g/L) can inhibit and high concentrations (10 g/L) can stimulate electron transfer between *S. oneidensis* MR-1 and Fh.

### 3.5 Environmental Implications

Compared to previous studies that showed how biochar concentrations influence microbial ferrihydrite reduction, our present study revealed that stimulation or inhibition of microbial Fe(III) reduction depends on the aggregation of bacteria and biochar with the Fh influenced by biochar particle size and biochar/Fh ratio. These findings allow better evaluating the impact of biochar on electron transfer processes in soils or sediments. Biochar addition was shown to mobilize arsenic in paddy soils due to enhanced dissimilatory Fe(III) reduction (Wang et al., 2017), which is possibly attributed to the presence of high biochar/Fe(III) minerals with close aggregation of biochar, cells and minerals. In agricultural soils, biochar favored microbial Fe(III) reduction and thus lowered greenhouse gas emission (i.e.  $\text{N}_2\text{O}$  and  $\text{CH}_4$ ) (Wang et al., 2017). Microbial Fe(III) mineral reduction and methanogenesis compete for the same electron donors, in particular in anoxic environments such as paddy soils or wetlands (Achnich et al., 1995; Chidthaisong and Conrad, 2000; Teh et al, 2008). Based on our study, it is evident that it has also to be determined how much biochar of which particle size needs to be added to paddy soil to favor or inhibit microbial Fe(III) reduction therefore controlling methane emission.

Biochar addition to soils could alter the identity of secondary iron minerals formed during Fe(III) reduction and due to differences in mineral solubility, particle size and surface area, this could impact the fate of toxic metals as well as nutrients (Borch et al., 2010). Such effects on environmental processes are expected not only to happen after addition of biochar, but also in environments that have significant concentrations of pyrogenic carbon, such as soils (Schmidt et al., 2000; Lehmann et al., 2009), sediments (Beesley et al., 2001), and aqueous marine and

terrestrial habitats (Bird et al., 2015; Jung et al., 2016). The  $\mu\text{m}$ - and  $\text{nm}$ -particles of biochar as we have investigated here in the present study represent very reactive fractions participating in Earth's carbon cycling and various biogeochemical processes due to their reactivity and high mobility functioning as a carrier and thus facilitating the transport of contaminants and phosphorus transport alkaline soils (Chen et al., 2017; Chen et al., 2018; Wang et al., 2013). Aggregation of biochar and cells with Fe(III) mineral impacts electron transfer via biochar, which may further influence the environmental association, transport, retention and fate of contaminants, organic matter and metals.

### Acknowledgements

We gratefully acknowledge support by China Scholarship Council Foundation (No. 201606510018) and we also thank Ellen Röhm for particle size and TOC/DOC analysis and help with *S. oneidensis* cultivation. We also thank Annette Flicker for FTIR analysis.

### Supplementary data

It contains data on redox properties and functional groups of biochars, detailed experimental procedures and calculations, and information on three-dimensional aggregates and secondary mineral analysis.

### 3.6 References

- Achtnich, C., Bak, F., Conrad, R., 1995. Competition for electron-donors among nitrate reducers, ferric iron reducers, sulfate reducers, and methanogens in anoxic paddy soil. *Biol. Fertil. Soil.*, 19, (1), 65-72; [http:// doi:10.1007/BF00336349](http://doi:10.1007/BF00336349).
- Amstaetter, K., Borch, T., Kappler, A., 2012. Influence of humic acid imposed changes of ferrihydrite aggregation on microbial Fe(III) reduction. *Geochim. Cosmochim. Acta.*, 85, 326-341; [http:// doi:10.1016/j.gca.2012.02.003](http://doi:10.1016/j.gca.2012.02.003).
- Bauer, I., Kappler, A., 2009. Rates and extent of reduction of Fe(III) compounds and  $\text{O}_2$  by humic substances. *Environ. Sci. & Technol.*, 43 (13), 4902-4908; <http://doi: 10.1021/es900179s>.
- Beesley, L., Moreno-Jiménez, E., Gomez-Eyles, J.L., Harris, E., Robinson, B., Sizmur, T., 2001. A review of biochars' potential role in the remediation, revegetation and restoration of contaminated soils. *Environ. Pollut.*, 159 (12), 3269-3282.
- Benner, S., Hansel, C., Wielinga, B., M Barber, T., Fendorf, S., 2002. Reductive dissolution and biomineralization of iron hydroxide under dynamic flow conditions. *Environ. Sci. & Technol.*, 36 (8), 1705-1711; <http:// doi:10.1021/es0156441>.
- Bird, M.I., Wynn, J.G., Saiz, G., Wurster, C.M, McBeath, A., 2015. The pyrogenic carbon cycle. *Annu. Rev. Earth Planet. Sci.*, 43, 273-298.
- Bompoti, N., Chrysochoou, M., Machesky, M., 2017. Surface structure of ferrihydrite: Insights from modeling surface charge. *Chemi. Geol*, 464, 34-45
- Borch, T., Kretzschmar, R., Kappler, A., Van Cappellen, P., Ginder-Vogel, M., Voegelin, A., Campbell, K., 2010. Biogeochemical redox processes and their impact on contaminant dynamics. *Environ. Sci. & Technol.*, 44 (1), 15-23; <http:// doi: 10.1021/es9026248>.

- Byrne, J. M., Van der Laan, G., Figueroa, A. I., Qafoku, O., Wang, C., Pearce, C. I., Jackson, M., Feinberg, J., Rosso, K. M., Kappler, A., 2016. Size dependent microbial oxidation and reduction of magnetite nano- and micro-particles. *Sci. Rep.*, 6, 30969; [http:// doi:10.1038/srep30969](http://doi:10.1038/srep30969).
- Caccavo, F., 1999. Protein-mediated adhesion of the dissimilatory Fe (III)-reducing bacterium *Shewanella alga* BrY to hydrous ferric oxide. *App. Environ. Microbiol.*, 65 (11), 5017-5022.
- Cao, B., Ahmed, B., Kennedy, D. W., Wang, Z.; Shi, L., Marshall, M. J., Fredrickson, J. K., Isern, N. G., Majors, P. D., Beyenal, H., 2011. Contribution of extracellular polymeric substances from *Shewanella* sp. *HRCR-1* biofilms to U(VI) immobilization. *Environ. Sci. & Technol.*, 45 (13), 5483-5490; [http:// doi:10.1021/es200096j](http://doi:10.1021/es200096j).
- Cayuela, M. L., Sánchez-Monedero, M., Roig, A., Hanley, K., Enders, A., Lehmann, J., 2013. Biochar and denitrification in soils: When, how much and why does biochar reduce N<sub>2</sub>O emissions? *Sci. Rep.*, 3, 1723; [http:// doi: 10.1038/srep017312](http://doi:10.1038/srep017312).
- Chen, M., Wang, D.J., Yang, F., Xu, N., Cao, X.D., 2017. Transport and retention of biochar nanoparticles in a paddy soil under environmentally-relevant solution chemistry conditions. *Environ. Pollut.*, 230, 540-549.
- Chen, M., Alim, N., Zhang, Y., Xu, N., Cao, X., 2018. Contrasting effects of biochar nanoparticles on the retention and transport of phosphorus in acidic and alkaline soils. *Environ. Pollut.*, 239, 562-570; [http:// doi: 10.1016/j.envpol.2018.04.050](http://doi:10.1016/j.envpol.2018.04.050)
- Chidthaisong, A., Conrad, R., 2000. Turnover of glucose and acetate coupled to reduction of nitrate, ferric iron and sulfate and to methanogenesis in anoxic rice field soil. *Fems. Microbiol. Ecol.* 31 (1), 73-86.
- Deluca, T., Gundale, M. J., Mackenzie, M. D., Jones, D., 2009. Biochar effects on soil nutrient transformations. Earthscan Publications Ltd,.
- Deeke, A., Sleutels, T. H., Hamelers, H. V., Buisman, C. J., 2012. Capacitive bioanodes enable renewable energy storage in microbial fuel cells. *Environ. Sci. Technol.* 46(6), 3554-3560.
- Eusterhues, K., Hädrich, A., Neidhardt, J., Küsel, K., Keller, T., D. Jandt, K., Totsche, K., 2014. Reduction of ferrihydrite with adsorbed and coprecipitated organic matter: Microbial reduction by *Geobacter bremensis* vs. abiotic reduction by Na-dithionite. *Biogeosci.*, 11 (4), 11; [http:// doi:10.5194/bgd-11-6039-2014](http://doi:10.5194/bgd-11-6039-2014).
- Fuller, S. J., McMillan, D. G. G., Renz, M. B., Schmidt, M., Burke, I. T., Stewart, D. I., 2014. Extracellular electron transport-mediated Fe(III) reduction by a community of alkaliphilic bacteria that use flavins as electron shuttles. *Appl. Environ. Microbiol.*, 80 (1), 128-137; [http:// doi: 10.1128/AEM.02282-13](http://doi:10.1128/AEM.02282-13).
- Frølund, B., Palmgren, R., Keiding, K., Nielsen, P. H., 1996. Extraction of extracellular polymers from activated sludge using a cation exchange resin. *Water Res.*, 30 (8), 1749-1758; [http:// doi:10.1016/0043-1354\(95\)00323-1](http://doi:10.1016/0043-1354(95)00323-1).
- Jiang, J., Kappler, A., 2008. Kinetics of microbial and chemical reduction of humic substances: implications for electron shuttling. *Environ. Sci. & Technol.*, 42 (10), 3563-3569; [http:// doi:10.1021/es7023803](http://doi:10.1021/es7023803).
- Ji, H., Zhao, X., Qiao, Z., Jung, J., Zhu, Y., Lu, Y., Ruoff, R. S., 2014. Capacitance of carbon-based electrical double-layer capacitors. *Nat. Commun.* 5, 3317.
- Jung, K.W., Kim, K., Jeong, T.U, Ahn, K.H., 2016. Influence of pyrolysis temperature on characteristics and phosphate adsorption capability of biochar derived from waste-marine macroalgae (*Undaria pinnatifida* roots). *Bioresour. Technol.*, 200, 1024-1028.
- Harris, H.W., El-Naggar, M.Y., Bretschger, O., Ward, M.J., Romine, M.F., Obraztsova, A.Y, Nealson, K.H., 2010. Electrokinesis is a microbial behavior that requires extracellular electron transport. *Natl. Acad. Sci. U.S.A.* 107 (1), 326-331.
- Harter, J., Krause, H. M., Schuettler, S., Ruser, R., Fromme, M., Scholten, T., Kappler, A., Behrens, S., 2014. Linking N<sub>2</sub>O emissions from biochar-amended soil to the structure and function of the N-cycling microbial community. *Isme. J.*, 8 (3), 660-674; [http:// doi: 10.1038/ismej2013.160.28](http://doi:10.1038/ismej2013.160.28)
- Hagemann, N., Kammann, C. I., Schmidt, H.-P., Kappler, A., Behrens, S., 2017. Nitrate capture and slow release in biochar amended compost and soil. *PLoS One.*, 12 (2), 171-214; [http:// doi:10.1371/journal.pone.0171214](http://doi:10.1371/journal.pone.0171214).

- He, J., Xiao, Y., Tang, J., Chen, H., Sun, H., 2019. Persulfate activation with sawdust biochar in aqueous solution by enhanced electron donor-transfer effect. *Sci. Total Environ.*, 690, 768-777.
- Hiemstra, T., Van Riemsdijk, W.H., 2009. A surface structural model for ferrihydrite I: Sites related to primary charge, molar mass, and mass density. *Geochim. Cosmochim. Acta.*, 73 (15), 4423-4436.
- Glasser, R. N., Saunders, H. S., Newman, K. D., 2017. The colorful world of extracellular electron shuttles. *Annu. Rev. Microbiol.*, 71, 731-751; DOI: 10.1146/annurev.micro-090816-093919.
- Gescher, J., Kappler, A., 2013. *Microbial Metal Respiration: From Geochemistry to Potential Applications*. Springer Heidelberg Press: New York, Dordrecht, London,.
- Gouveia, S.E.M., Pessenda, L.C.R., 2000. Datation parte <sup>14</sup>C de charbons inclus dans le sol por l'etude du role de la remontee biologique de matiere et du colluvionnement dans la formation de latosols de l'etat de Sao Paulo, Bresil, *C.R. Acad.Sci.*, 330, 133-138.
- Gul, S., Whalen, J., 2016. Biochemical cycling of nitrogen and phosphorus in biochar-amended soils. *Soil Biol. Biochem.*, 103, 1-15; [http:// doi:10.1016/j.soilbio.2016.08.001](http://doi:10.1016/j.soilbio.2016.08.001)
- Kappler, A., Straub, K. L., 2005. Geomicrobiological cycling of iron. *Rev. Mineral. Geochem.*; 59, 85-108; [http:// doi: 10.2138/rmg](http://doi:10.2138/rmg).
- Kappler, A., Wuestner, M. L., Ruecker, A., Harter, J., Halama, M., Behrens, S., 2014. Biochar as an electron shuttle between bacteria and Fe(III) minerals. *Environ. Sci. & Technol. Lett.*, 1 (8), 339-344; [http:// doi: 10.1021/ez5002209.005.59.5](http://doi:10.1021/ez5002209.005.59.5).
- Keiluweit, M., Nico, P. S., Johnson, M. G., Kleber, M., 2010. Dynamic molecular structure of plant biomass-derived black carbon (biochar). *Environ. Sci. Technol.*, 44, 1247-1253
- Konhauser, K., Kappler, A., Roden, E. E., 2011. Iron in microbial metabolisms. *Elements.*, 7 (2), 89-93; [http:// doi:10.2113/gselments.7.2.8.9](http://doi:10.2113/gselments.7.2.8.9).
- Kluepfel, L., Keiluweit, M., Kleber, M., Sander, M., 2014. Redox properties of plant biomass-derived black carbon (biochar). *Environ. Sci. & Technol.*, 48 (10), 5601-5611; [http:// doi: 10.1021/es500906d](http://doi:10.1021/es500906d).
- Lehmann, J., Joseph, S., 2015. *Biochar for Environment Management Science and Technology*. London .Sterling, VA.
- Lehmann, J., Czimczik, C., Laird, D., Sohi, S., 2009. Stability of biochar in soil. *Biochar for environmental management: science and technology*, Eds. Earthscan in the UK and USA, ,183-206.
- Li, F., Geng, D, Cao, Q., 2015. Adsorption of As (V) on aluminum-, iron-, and manganese-(oxyhydr) oxides: equilibrium and kinetics. *Desalin. Water Treat.*, 56 (7), 1829-1838.
- Li, S. W., Sheng, G. P., Cheng, Y.-Y.; Yu, H. Q., 2016. Redox properties of extracellular polymeric substances (EPS) from electroactive bacteria. *Sci. Rep.*, 6, 39098; [http:// doi: 10.1038/srep39098](http://doi:10.1038/srep39098).
- Liu, G., Yu, H., Wang, N., Jin, R., Wang, J., Zhou, J., 2018. Microbial reduction of ferrihydrite in the presence of reduced graphene oxide materials: Alteration of Fe(III) reduction rate, biomineralization product and settling behavior. *Chemi. Geol.*, 476, 272-279; [http:// doi:10.1016/j.chemgeo.2017.11.023](http://doi:10.1016/j.chemgeo.2017.11.023).
- Lovley, D. R., Coates, J. D., BluntHarris, E. L., Phillips, E. J. P., Woodward, J. C., 1996. Humic substances as electron acceptors for microbial respiration. *Nature.*, 382 (6590), 445-448; [http:// doi: 10.1038/382445a0](http://doi:10.1038/382445a0).
- Lovley, D. R., Holmes, D. E., Nevin, K. P., 2004. Dissimilatory Fe(III) and Mn(IV) reduction. *Adv. Microb. Physiol.*, 49, 219-286; [http:// doi: 10.1016/S006S-2911\(04\)49005-5](http://doi:10.1016/S006S-2911(04)49005-5).
- Marsili, E., Baron, B. D., Shikhare, D. I., Coursolle, D., Gralnick, A. J., Bond, R. D., 2008. *Shewanella* secretes flavins that mediate extracellular electron transfer. *Proc. Natl. Acad. Sci. U S A.*; 105 (10), 3968-3973; [http:// doi: 10.1073/pnas.0710525105](http://doi:10.1073/pnas.0710525105).
- Malvankar, N. S., Lovley, D. R., 2014. Microbial nanowires for bioenergy applications. *Curr. Opin. Biotechnol.* 27, 88-95; [http:// doi: 10.1016/j.copbio.2013.12.003](http://doi:10.1016/j.copbio.2013.12.003).
- Myers, C., Myers, J., 2003. Cell surface exposure of the outer membrane cytochromes of *Shewanella oneidensis* MR-1. *Lett. Appl. Microbiol.*, 37 (3), 254-8; [http:// doi: 10.1046/j.1472-765X.2003.01389.x](http://doi:10.1046/j.1472-765X.2003.01389.x).
- Newman, K. D., 2005. Direct and indirect mechanisms of microbial iron reduction. *Geochim. Cosmochim. Acta.*, 4 (1), 5520-5525.
- Nguyen, B.T., Lehmann, J., Kinyangi, J., Smernik, R., Riha, S. J., and Engelhard, M. H., 2008. Long-term black carbon dynamics in cultivated soil. *Biogeochemistry.* 89 (3): 295-308.

- O'Loughlin, E. J.; 2008. Effects of electron transfer mediators on the biodegradation of lepidocrocite ( $\gamma$ -FeOOH) by *Shewanella putrefaciens* CN32. *Environ. Sci. Technol.*, 42 (18), 6876–6882 [http://doi: 10.1021/es800686d](http://doi:10.1021/es800686d).
- Pinchuk, G. E., Geydebekht, O. V., Hill, E. A., Reed, J. L., Konopka, A. E., Beliaev, A. S., Fredrickson, J. K. (2011). Pyruvate and lactate metabolism by *Shewanella oneidensis* MR-1 under fermentation, oxygen limitation, and fumarate respiration conditions. *Appl. Environ. Microbiol.*, 77(23), 8234-8240.
- Rau, J., Knackmuss, H.-J., Stolz, A., 2002. Effects of different quinoid redox mediators on the anaerobic reduction of azo dyes by bacteria. *Environ. Sci. Technol.*, 36 (7), 1497–1504; [http://doi: 10.1021/es010227](http://doi:10.1021/es010227).
- Reguera, G., McCarthy, D. K., Mehta, T., Nicoll, S. J., Tuominen, M., Lovley, R. D., 2005. Extracellular electron transfer via microbial nanowires. *Nature.*, 435 (7045), 1098-10101; [http://doi: 10.1038/nature03661](http://doi:10.1038/nature03661).
- Roden, E. E., Kappler, A., Bauer, I., Jiang, J., Paul, A.; Stoesser, R.; Konishi, H.; Xu, H., 2010. Extracellular electron transfer through microbial reduction of solid-phase humic substances. *Nature Geo.*, 3, 417-421; [http://doi: 10.1038/ngeo870.21](http://doi:10.1038/ngeo870.21).
- Scott, D. T., McKnight, D. M., Blunt-Harris, E. L., Kolesar, S. E., Lovley, D. R., 1998. Quinone moieties act as electron acceptors in the reduction of humic substances by humics-reducing microorganisms. *Environ. Sci. Technol.*, 32 (19), 2984-2989; [http://doi: 10.1021/es982014z](http://doi:10.1021/es982014z).
- Schmidt, M.W, Noack, A.G., 2000. Black carbon in soils and sediments: analysis, distribution, implications, and current challenges. *Global Biogeochemical. Cy.*, 14 (3), 777-793.
- Shi, L., Dong, H., Reguera, G., Beyenal, H., Lu, A., Liu, J., Yu, H.-Q., K. Fredrickson, J., 2016. Extracellular electron transfer mechanisms between microorganisms and minerals. *Nat. Rev. Microbiol.*, 14 (10), 651-662; [http://doi: 10.1038/nrmicro.2016.93](http://doi:10.1038/nrmicro.2016.93).
- Shi, L., Rosso, K. M., Zachara, J. M., Fredrickson, J. K., 2012. Mtr extracellular electron-transfer pathways in Fe(III)-reducing or Fe(II)-oxidizing bacteria: a genomic perspective. *Biochem. Soc. Trans.* 40 (6), 1261-1267; [http://doi: 10.1042/BST20120098](http://doi:10.1042/BST20120098).
- Sudirjo, E, Strik, D., Buisman, C. J., 2019. Marine sediment mixed with activated carbon allows electricity production and storage from internal and external energy sources: a new rechargeable bio-battery with bi-directional electron transfer properties. *Front. Microbiol.* 10, 934.
- Sun, T.R., Levin, B.D.A., Guzman, J.J.L., Enders, A., Muller, D.A., Angenent, L.T., Lehmann, J. 2017. Rapid electron transfer by the carbon matrix in natural pyrogenic carbon. *Nat. Commun.*, 8, 14873.
- Sun, T., Levin, B. D. A., Schmidt, M. P., Guzman, J. J. L., Enders, A., Martínez, C. E., Muller, D. A., Angenent, L. T., Lehmann, J., 2018. Simultaneous quantification of electron transfer by carbon matrices and functional groups in pyrogenic carbon. *Environ. Sci. Technol.*, 52 (15), 8538-8547; [http://doi: 10.1021/acs.est.8bb02340](http://doi:10.1021/acs.est.8bb02340).
- Suliman, W., Harsh, J. B., Fortuna, A. M., Garcia-Pérez, M., Abu-Lail, N. I., 2017. Quantitative effects of biochar oxidation and pyrolysis temperature on the transport of pathogenic and nonpathogenic *Escherichia coli* in biochar-amended sand columns. *Environ. Sci. Technol.*, 51 (9), 5071-5081.
- Song, B., Chen, M., Zhao, L., Qiu, H., Cao X., 2019. Physicochemical properties and colloidal stability of micro- and nano particle biochar derived from a variety of feedstock sources. *Sci. Tot. Environ.*, 15, 661: 685-695. [http://doi: 10.1016/j.scitotenv.2019.01.193](http://doi:10.1016/j.scitotenv.2019.01.193).
- Stookey, L. L., 1970. Ferrozine---a new spectrophotometric reagent for iron. *Anal. Chem.*, 42 (7), 779-781; [http://doi: 10.1021/ac60289a016](http://doi:10.1021/ac60289a016).
- Teh, Y. A., Dubinsky, E. A., Silver, W. L., Carlson, C. M., 2008. Suppression of methanogenesis by dissimilatory Fe(III)-reducing bacteria in tropical rain forest soils: implications for ecosystem methane flux. *Glob. Change Biol.*, 14 (2), 413-422; <http://doi:10.1111/j.1365-2486.2007.01487x>.
- Villacís-García, M., Ugalde-Arzate, M., Vaca, K., Escobar, M., Martínez-Villegas, M., 2015. Laboratory synthesis of goethite and ferrihydrite of controlled particle sizes. *Bol. Soc. Geol. Mex.*, 67 (3), 433-446.
- Wang, D.J., Zhang W., Hao, X. Z., Zhou D.M., 2013. Transport of biochar in saturated granular media: effects of pyrolysis temperature and particle size. *Environ. Sci. Technol.*, 47, (2), 821-828. 41; <http://doi:org.10.1021.es303794d>.

- Wang, N., Xue, X.M., Juhasz, A.L., Chang, Z.Z., Li, H.B., 2017. Biochar increases arsenic release from an anaerobic paddy soil due to enhanced microbial reduction of iron and arsenic. *Environ. Pollut.*, 220, 514-522.
- Wang, N., Chang, Z.Z., Xue, X.M., Yu, J.G., Shi, X.X., Ma, L.Q., Li, H.B., 2017. Biochar decreases nitrogen oxide and enhances methane emissions via altering microbial community composition of anaerobic paddy soil. *Sci. Total Environ.*, 581, 689-696.
- Weber, K., Achenbach, A. L., Coates, D. J., 2006, Microbes pumping iron: anaerobic microbial iron oxidation and reduction. *Nat. Rev. Microbiol.* 4 (10), 752-764; Biochar decreases nitrogen oxide and enhances methane emissions via altering microbial community composition of anaerobic paddy soil [http:// doi:10.1038/nrmicro1490](http://doi:10.1038/nrmicro1490).
- Weber, F.-A., Voegelin, A., Kretzschmar, R., 2009. Multi-metal contaminant dynamics in temporarily flooded soil under sulfate limitation. *Geochim. Cosmochim. Acta.*, 73 (19), 5513-5527, [http:// doi: 10.1016/j.gca.2009.06.011](http://doi:10.1016/j.gca.2009.06.011).
- Wu, S., Fang, G., Wang, Y., Zheng, Y., Wang, C., Zhao, F., Jaisi, D. P., Zhou, D. M., 2017. Redox-active oxygen-containing functional groups in activated carbon facilitate microbial reduction of ferrihydrite. *Environ. Sci. Technol*, 51 (17), 9709-9717; [http:// doi: 10.1021/acs.est.7bb01854](http://doi:10.1021/acs.est.7bb01854).
- Wu, J.W, Ng, I.S., 2017. Biofabrication of gold nanoparticles by *Shewanella* species. *Bioresour. Bioprocess.*, 4 (1), 50.
- Xu, S., Adhikari, D., Huang, R., Zhang, H., Tang, Y., Roden, E., Yang, Y., 2016. Biochar-facilitated microbial reduction of hematite. *Environ. Sci. Technol.*, 50 (5), 2389-2395; [http:// doi:10.1021/acs.est.5b05517](http://doi:10.1021/acs.est.5b05517).
- Xiao, Y., Zhang, E., Zhang, J. D., Dai, Y.F., Yang, Z.H., Christensen, H. E. M., Ulstrup, J., Zhao, F., 2017. Extracellular polymeric substances are transient media for microbial extracellular electron transfer. *Sci. Adv.*, 3 (7), 77-82; [http:// doi: 10.1126/sciadv.1700623](http://doi:10.1126/sciadv.1700623).
- Ye, J., Zhang, R., Nielsen, S., Joseph, S.D., Huang, D. and Thomas, T., 2016. A combination of biochar–mineral complexes and compost improves soil bacterial processes, soil quality, and plant properties. *Front. Microbiol.* 7, 372.
- Yu, L., Yuan, Y., Tang, J., Wang, Y., Zhou, S., 2015. Biochar as an electron shuttle for reductive dechlorination of pentachlorophenol by *Geobacter sulfurreducens*. *Sci. Rep.*, 5, 16221; [http:// doi: 10.1038/srep16221](http://doi:10.1038/srep16221).
- Yuan, Y., Bolan, N., PrévotEAU, A., Vithanage, M., Biswas, J. K., Ok, Y. S., Wang, H., 2017. Applications of biochar in redox-mediated reactions. *Bioresour. Technol.*, 246, 271-281; [http:// doi: 10.1016/j.biortech.2017.06.154](http://doi:10.1016/j.biortech.2017.06.154).
- Zachara, J. M., Fredrickson, J. K., Smith, S. C., Gassman, P. L., 2001. Solubilization of Fe(III) oxide-bound trace metals by a dissimilatory Fe(III) reducing bacterium. *Geochim. Cosmochim. Acta.*, 65 (1), 75-93; [http:// doi: 10.1016/S0016-7037\(00\)00500-7](http://doi:10.1016/S0016-7037(00)00500-7).
- Zhang, W., Niu J. Z., Morales, V.L., Chen, X.C., Hay, A. G., Lehmann, J.; Steenhuis, T. S, 2010. Transport and retention of biochar particles in agriculture soils contaminated by waste water and smelter dust. *Ecohydrol.*, 3, 497-508; [http:// doi:10.1002/eco.160](http://doi:10.1002/eco.160).
- Zhou, G. W., Yang, X. R., Marshall, C. W., Li, H.; Zheng, B.-X.; Yan, Y.; Su, J.-Q.; Zhu, Y.-G., 2017. Biochar addition increases the rates of dissimilatory iron reduction and methanogenesis in ferrihydrite enrichments. *Front. Microbiol.*, 8, 589; [http:// doi: 10.3389/fmicbb.2017.00589](http://doi:10.3389/fmicbb.2017.00589).
- Zhang, H. L., Fang, W., Wang, Y. P., Sheng, G. P., Zeng, R. J., Li, W.-W., Yu, H.-Q., 2013. Phosphorus removal in an enhanced biological phosphorus removal process: roles of extracellular. *Environ. Sci. & Technol.*, 47, (20), 11482-11489. 41; [http:// doi.org.10.1021.es303794d](http://doi.org.10.1021.es303794d).

## SUPPORTING INFORMATION

-----

### **Aggregation-dependent electron transfer via redox-active biochar particles stimulate microbial ferrihydrite reduction**

Zhen Yang<sup>a</sup>, Tianran Sun<sup>b</sup>, Edison Subdiaga<sup>c</sup>, Martin Obst<sup>d</sup>, Stefan. B. Haderlein<sup>c</sup>, Markus Maisch<sup>a</sup>, Ruben Kretzschmar<sup>e</sup>, Largus T. Angenent<sup>b</sup>, Andreas Kappler<sup>a\*</sup>

<sup>a</sup>*Geomicrobiology, Center for Applied Geoscience, University of Tuebingen, Germany*<sup>b</sup>*Environmental Biotechnology, Center for Applied Geoscience, University of Tuebingen, Germany*

<sup>c</sup>*Environmental Mineralogy and Chemistry, Center for Applied Geoscience, University of Tuebingen, Germany*

<sup>d</sup>*Experimental Biogeochemistry, University of Bayreuth, Germany*

<sup>e</sup>*Soil Chemistry Group, Institute of Biogeochemistry and Pollutant Dynamics, CHN, ETH Zurich, Switzerland*

Number of figures in supporting information: 17

Number of tables in supporting information: 2

**Preparation of biochar suspensions and leachates.** Anoxic biochar suspensions were prepared by deoxygenating fine-powdered biochar overnight in the evacuated vacuum chamber of an anoxic glovebox (100% N<sub>2</sub>). Degassed biochar was suspended in anoxic doubly deionized (DDI) water (>18.2 MΩ·cm; Milli-Q, Millipore Corporation) in the glovebox to final concentrations of 1, 5, and 10 g/L. The suspensions were treated for 10 min with an ultrasonic probe (Sonics Vibra-cell VCX 500 with a microtip at 150 W) to disperse the biochar particles. These biochar suspensions were sterilized by autoclaving (120°C, 20 min). Aqueous biochar leachates were prepared by centrifuging anoxic biochar suspensions (1, 5, and 10 g/L) through centrifuge filters (0.22 μm, Costar-Spin-X Centrifuge-Tube) inside an anoxic glovebox, and sterilized by autoclaving (120°C, 20 min).

The electron accepting (EAC) and donating capacities (EDC) (meq e<sup>-</sup>/g) were quantified by using mediated electrochemical analysis either in reductive (mediated electrochemical reduction, MER); E<sub>H</sub> (pH 7) = -0.49 V, zwitterionic viologen 4,4'-bipyridinium-1,1'-bis(2-ethylsulfonate) (ZiV), vs. SHE) or oxidative (mediated electrochemical oxidation, MEO); E<sub>H</sub> (pH 7) = +0.61 V, 2,2'-Azino-bis(3-ethylbenzthiazoline-6-sulfonic acid) (ABTS), vs. SHE) mode. EAC and EDC were calculated by integration of electrical current signals after baseline correction and normalization to mass of biochar in the sample (meq e<sup>-</sup>/g,  $EAC = \frac{\int_{red} I dt}{F m_{biochar}}$  and  $EDC = \frac{\int_{ox} I dt}{F m_{biochar}}$ ). Electrons transferable per carbon mass (meq e<sup>-</sup>/mg C) were calculated based on the biochar concentrations and carbon content per gram biochar, respectively.

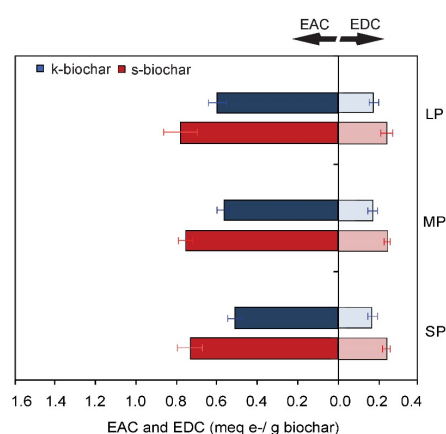


**Figure S1.** Electron accepting capacity (EAC, meq e<sup>-</sup>/g) and electron donating capacity (EDC, meq e<sup>-</sup>/g) of Swiss biochar (s-biochar, red bars) and KonTiki biochar (k-biochar, blue bars). Error bars represent standard deviations of triplicate setups. LP, MP and SP represent large intermediate and small-sized particles of biochar, respectively.



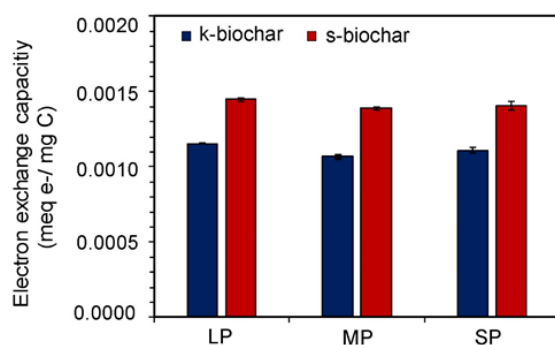


**Figure S2.** Electron exchange capacities of Swiss biochar (s-biochar) and KonTiki biochar (k-biochar) with small, intermediate and large-sized particles (LP, MP and SP) normalized to total carbon contents (TOC) (meq e-/mg C).

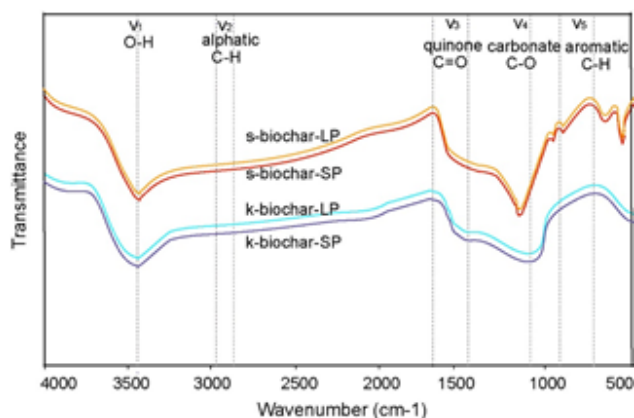


**Figure S3.** Fourier-transform infrared (FTIR) spectra of Swiss biochar (s-biochar) and KonTiki biochar (k-biochar) (large and small particle size, i.e. LP and SP). Dashed lines indicate the presence of the following functional groups: v<sub>1</sub>, hydroxyl (-OH, 3449 cm<sup>-1</sup>); v<sub>2</sub>, aliphatic (-CH, -CH<sub>2</sub>, or -CH<sub>3</sub>, 2920 and 2847 cm<sup>-1</sup>); v<sub>3</sub> quinone (-C=O-, 1630 cm<sup>-1</sup>); v<sub>4</sub>, carbonate (870 cm<sup>-1</sup>), v<sub>5</sub>, aromatic (-CH-), 670 cm<sup>-1</sup>).

**Particle size of biochar.** Both Swiss Biochar (s-biochar) and KonTiki (k-biochar) were ground by a ball mill. Biochar was ground at different speeds and for different milling times to prepare large particle size biochar (130 rpm for 60 min), intermediate particle size biochar (130 rpm for 60 min and 180 rpm for 60 min) and small particle size biochar (130 rpm for 60 min and at 180 rpm for 120 min), respectively.

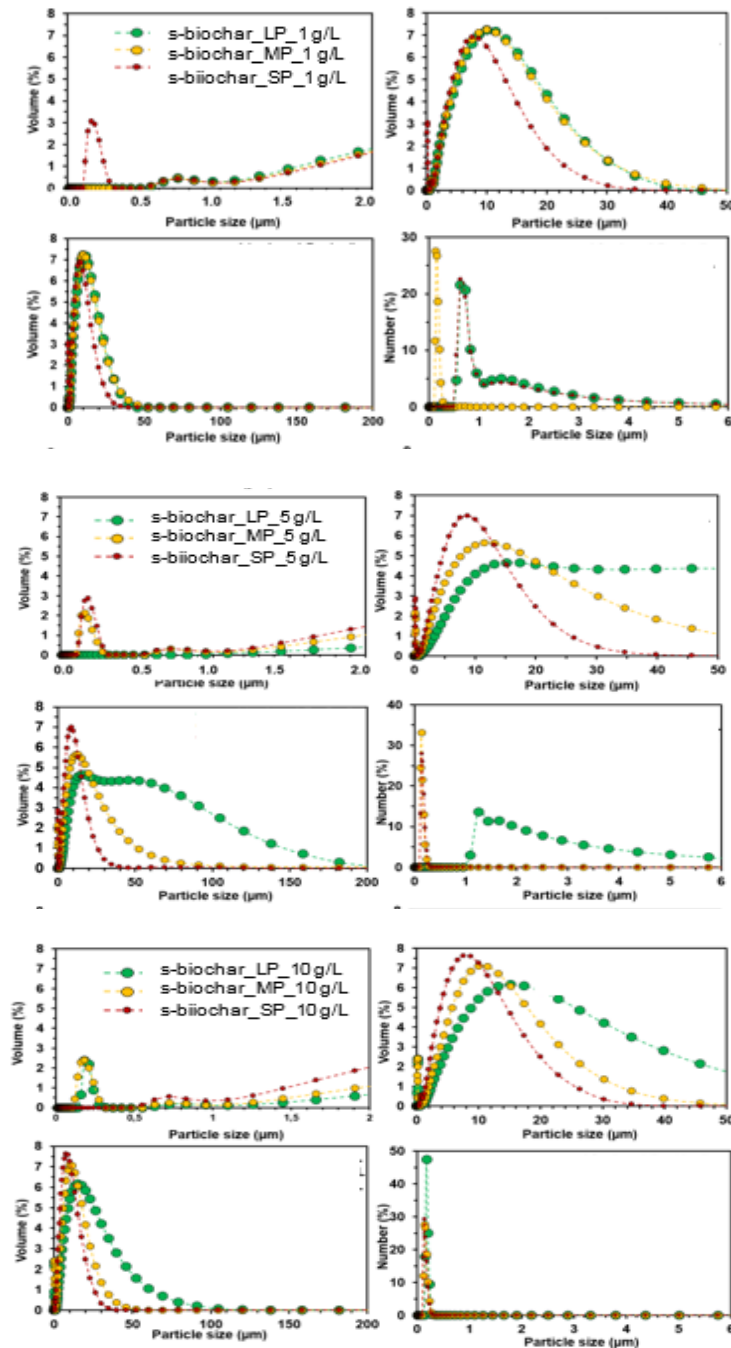


**Figure S4.** Particle size distribution of Swiss biochar (s-biochar) at different concentrations (1, 5 and 10 g/L) for the three different particle sizes (large-sized particles, LP; intermediate-size particles, MP and small-sized particles, SP).

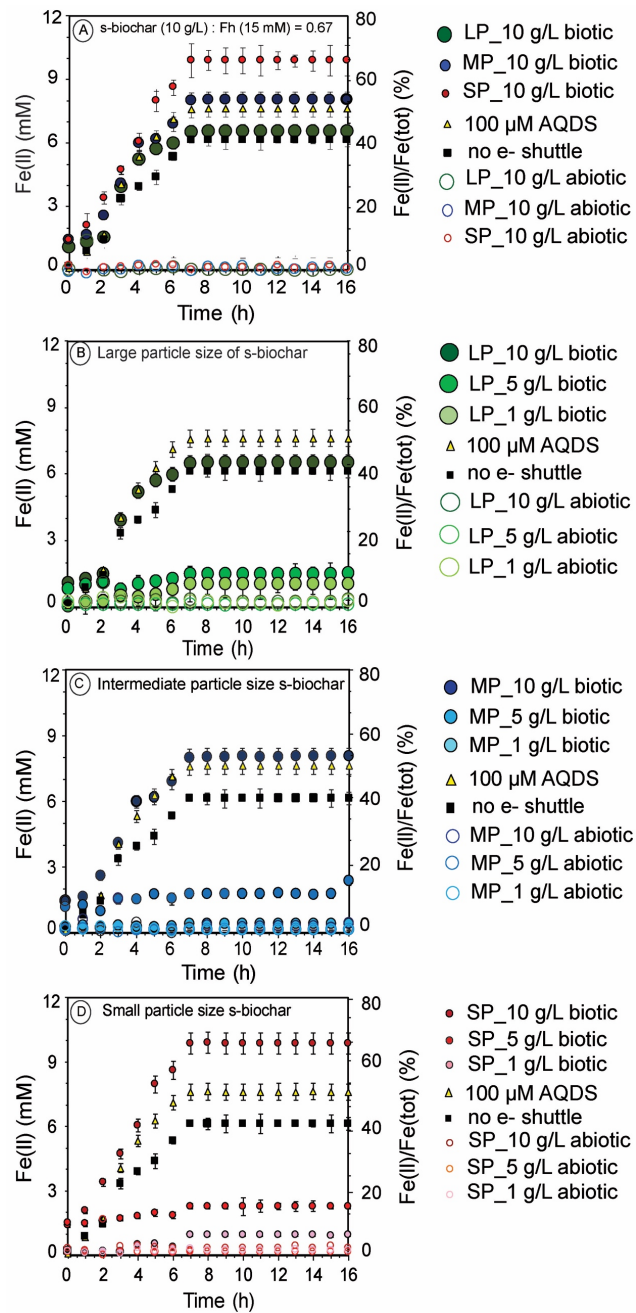


**Figure S5.** Rates and extent of microbial ferrihydrite (Fh, 15 mM) reduction over 16 hours incubation by *S. oneidensis* MR-1 in the presence of (A) large, intermediate and small-sized particles (LP, MP, SP) Swiss biochar (s-biochar) (10 g/L), (B) 1, 5 and 10 g/L of LP s-biochar, (C) 1, 5 and 10 g/L of MP s-biochar, and (D) 1, 5 and 10 g/L of SP s-biochar. Error bars represent standard deviations of triplicate experimental setups.

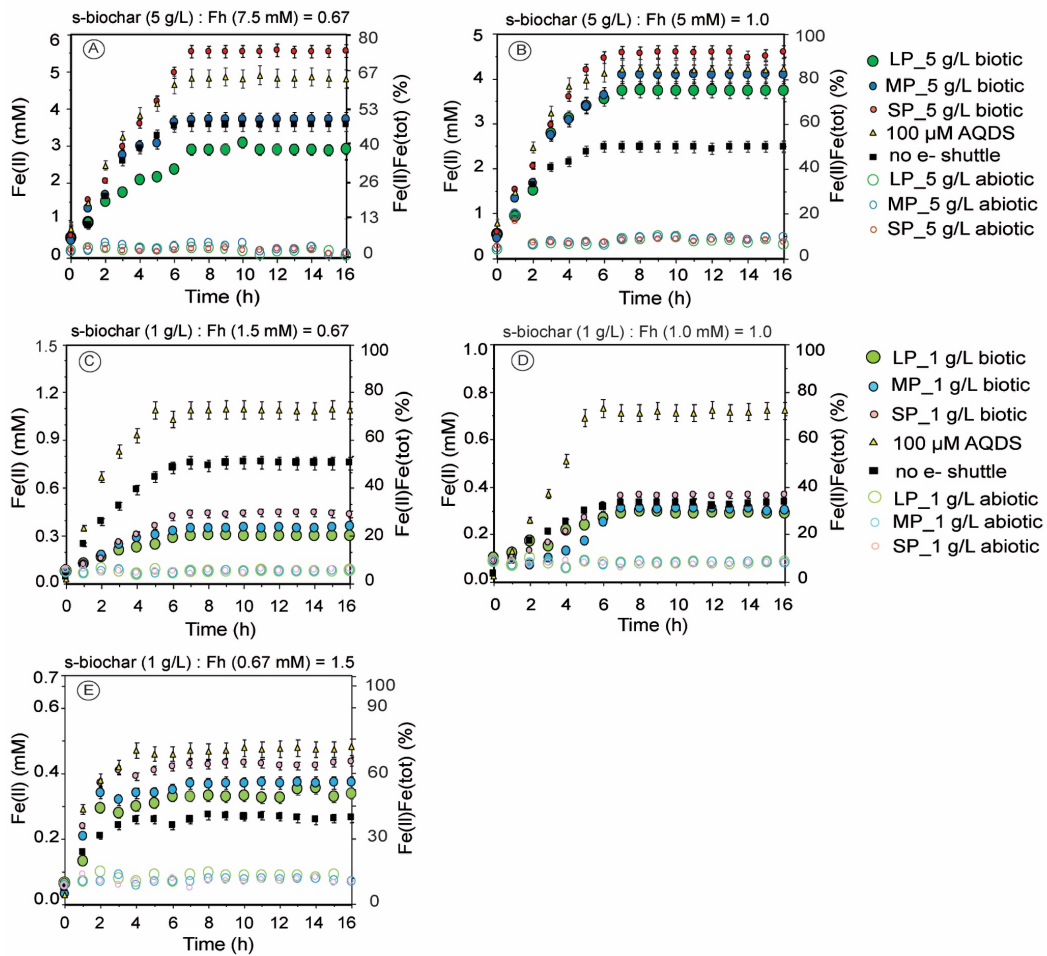


**Figure S6.** Rates and extent of microbial ferrihydrite (Fh) reduction by *S. oneidensis* MR-1 at different Swiss biochar (s-biochar) particle sizes and s-biochar:Fh ratios over a 16-h incubation. (A) Ratio 0.67 g s-biochar/mmol Fe with 7.5 mM Fh and 5 g/L of small-sized particles (SP), intermediate-sized particles (MP) and large-sized particles (LP) s-biochar; (B) Ratio 1.0 g s-biochar/mmol Fe with 5 mM Fh and 5 g/L of SP, MP and LP s-biochar; (C) Ratio 0.67 g s-biochar/mmol Fe with 1.5 mM Fh and 1 g/L of SP, MP and LP s-biochar; (D) Ratio 1.0 g s-biochar/mmol Fe with 1 mM Fh and 1 g/L of SP, MP and LP s-biochar; (E) Ratio 1.5 g s-biochar/mmol Fe with 0.67 mM Fh and 1 g/L of SP, MP and LP s-biochar. Error bars represent standard deviations of triplicate experimental setups.

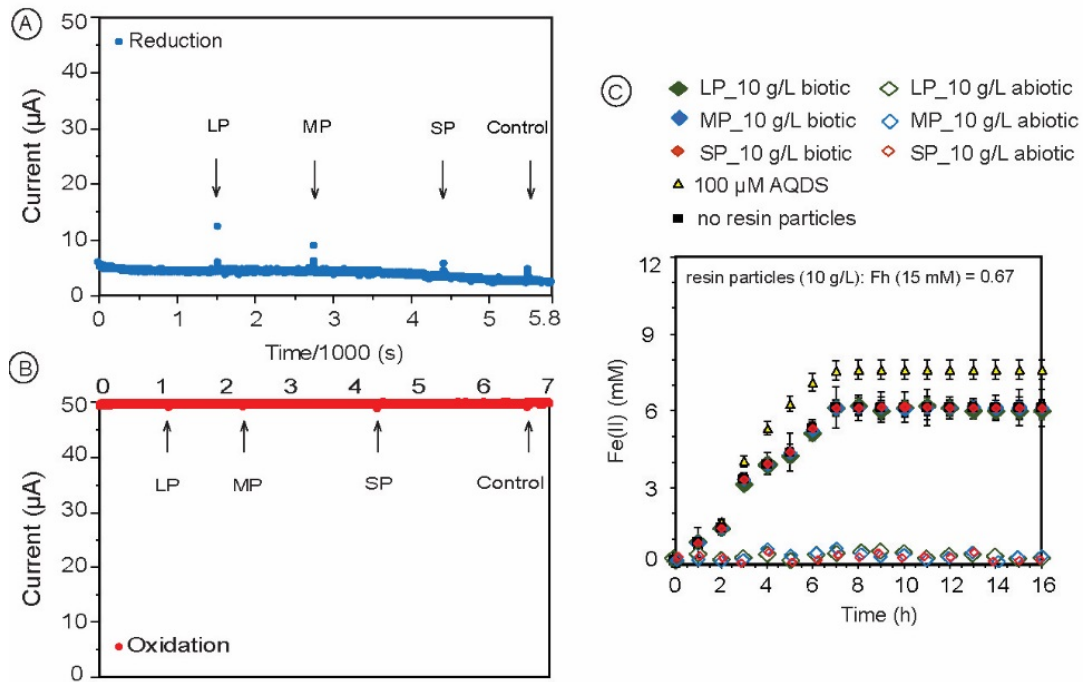


**Figure S7.** Redox characterization of DAX-8 resin particles (suspended in 0.1 M phosphate buffer), that have a similar particle-size as the biochar particles and evaluation of the effect of these particles on ferrihydrite (Fh) reduction in *S. oneidensis* MR-1 cell suspension experiments. LP, MP and SP represent large particles, intermediate particles and small particles of DAX-8 resin. (A) and (B) reduction and oxidation capacity of DAX-8 resin particles. Only minor current peaks (see arrows in A and B; maximum values of 12 µA) were detected in these samples suggesting that the DAX-8 resin particles with LP, MP and SP are not redox-active. Phosphate buffer (0.1 M) is used as control. (C) Microbial Fh (15 mM) reduction in the presence of different particle sizes of DAX-8 resin particles with 1, 5 and 10 g/L concentrations over a 16-h incubation.

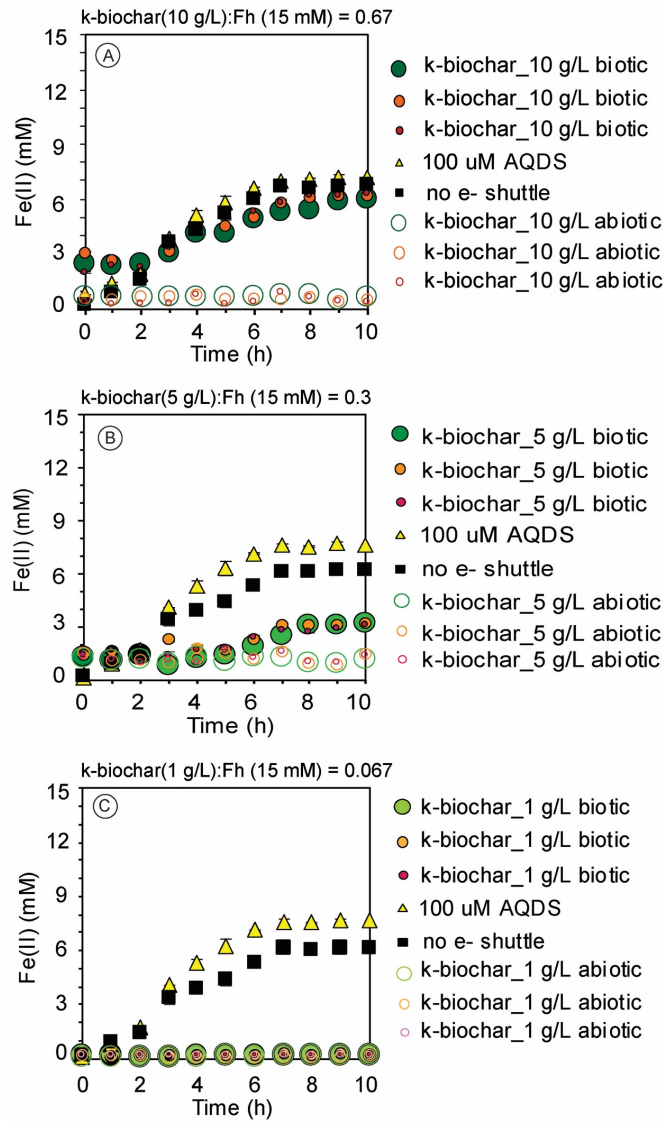


**Figure S8.** Microbial ferrihydrite (Fh) reduction by *S. oneidensis* MR-1 at different at different KonTiki biochar (k-biochar) particle sizes and k-biochar:Fh ratios. (A) Ratio 0.67 g k-biochar/mmol Fe with 15 mM Fh and 10 g/L of small-sized particles (SP), intermediate-sized particles (MP) and large-sized particles (LP) k-biochar; (B) Ratio 0.3 g k-biochar/mmol Fe with 15 mM Fh and 5 g/L of SP, MP and LP k-biochar; (C) Ratio 0.067 g k-biochar/mmol Fe with 15 mM Fh and 1 g/L of SP, MP and LP k-biochar; Error bars represent standard deviations of triplicate experimental setups. These results showed that all k-biochar particle sizes decrease or even inhibit electron transfer when reacting with 15 mM Fh compared to setups without biochar or with AQDS as electron shuttle.

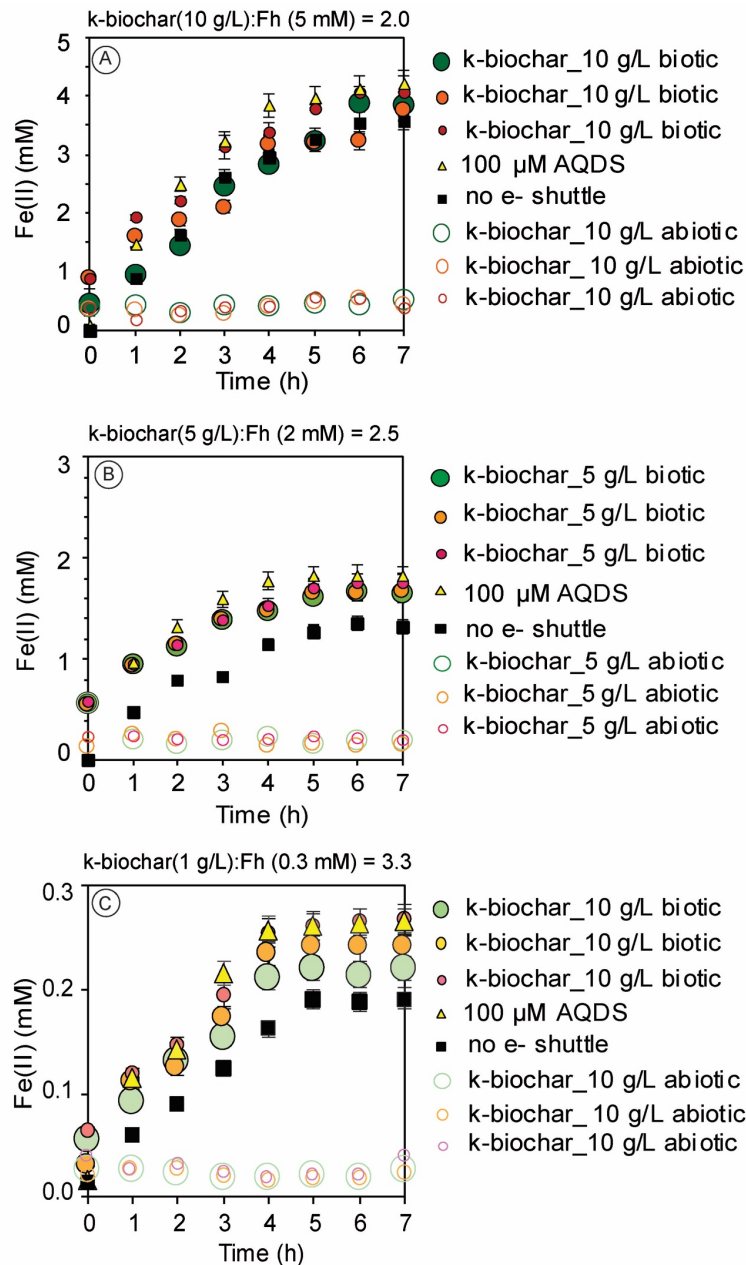


**Figure S9.** Microbial ferrihydrite (Fh) reduction by *S. oneidensis* MR-1 at different KonTiki biochar (k-biochar) particle sizes and k-biochar:Fh ratios. (A) Ratio 2.0 g /mmol Fe with 5 mM Fh and 10 g/L of small-sized particles (SP), intermediate-sized particles (MP) and large-sized particles (LP) k-biochar; (B) Ratio 2.5 g k-biochar/mmol Fe with 2.5 mM Fh and 5 g/L of SP, MP and LP k-biochar; (C) Ratio 3.3 g k-biochar/mmol Fe with 0.3 mM Fh and 1 g/L of SP, MP and LP k-biochar. Error bars represent standard deviations of triplicate experimental setups. These results showed a certain k-biochar:Fh ratio (g/mmol) is necessary to see no reduction or even inhibition of microbial Fh reduction.

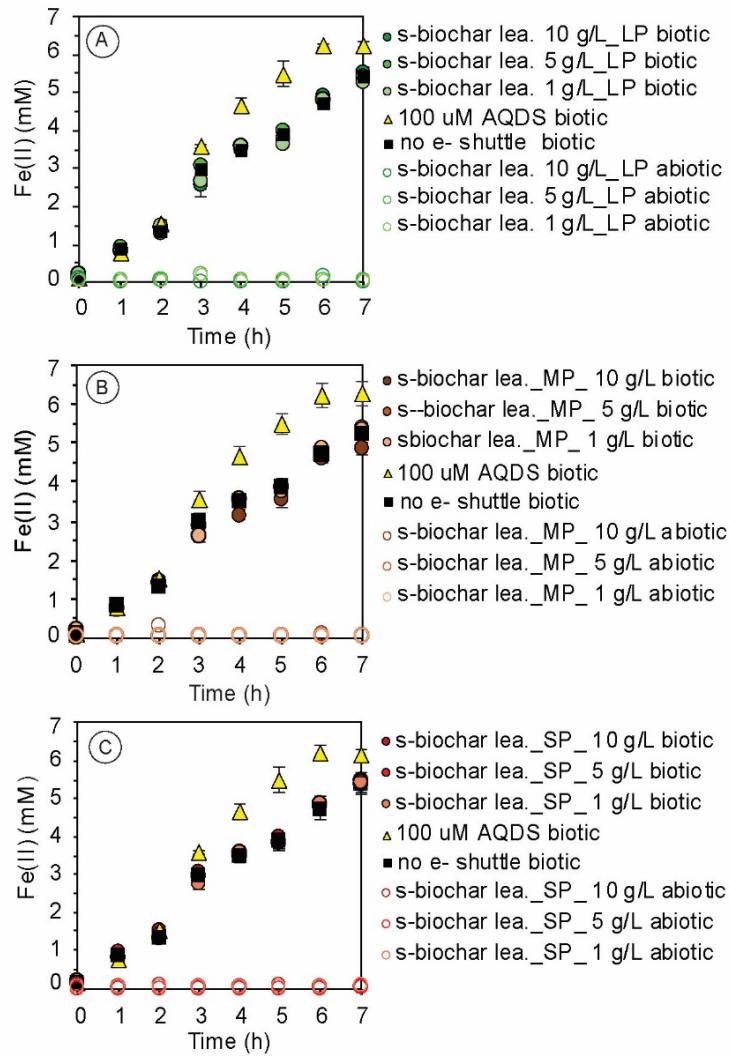


**Figure S10.** Microbial ferrihydrite (Fh, 15 mM) reduction by *S. oneidensis* MR-1 in the presence of (A) large-sized particles (LP) Swiss biochar (s-biochar) leachates from 1, 5 and 10 g/L of s-biochar suspensions, (B) Intermediate-sized particles (MP) s-biochar leachates from 1, 5 and 10 g/L of biochar suspensions, (C) Small-sized particles (SP) s-biochar leachates from 1, 5 and 10 g/L of biochar suspensions. Error bars represent standard deviations of triplicate experimental setups.



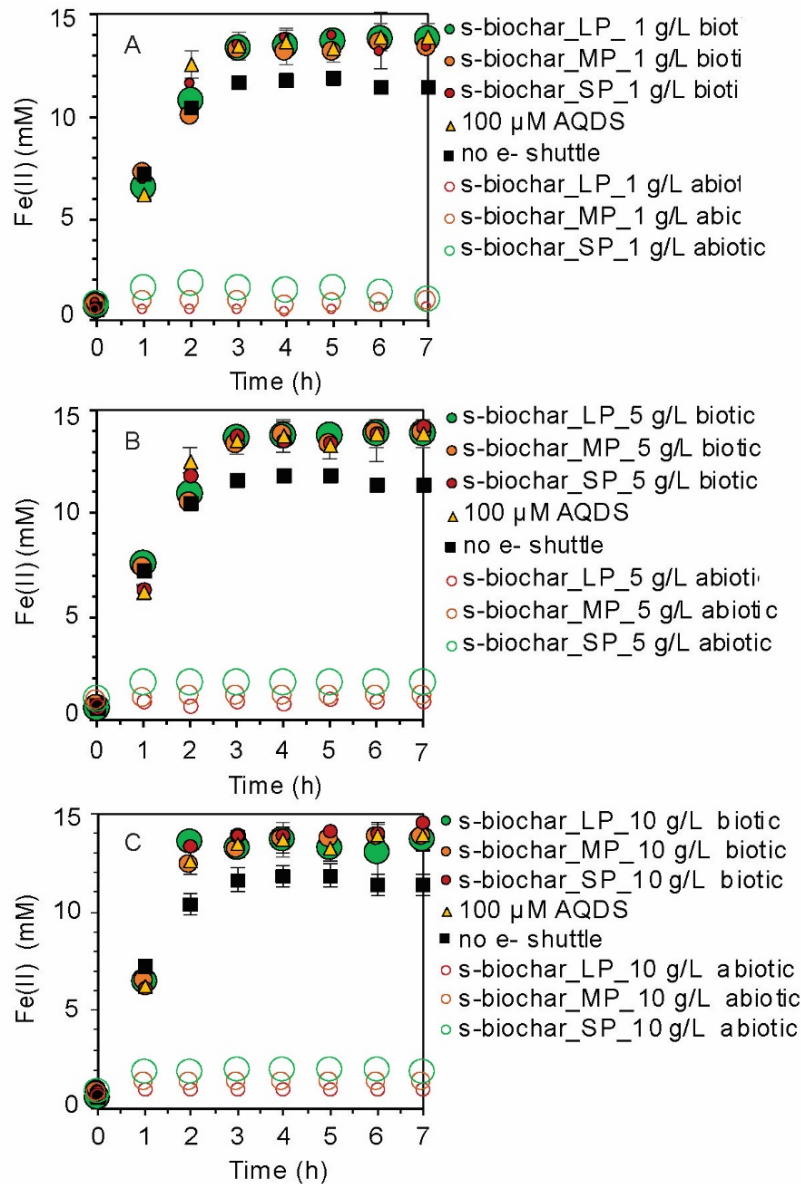


**Figure S11.** Microbial ferric citrate reduction by *S. oneidensis* MR-1 at different Swiss biochar (s-biochar):ferric citrate ratios. (A) Ratio 0.2 g/mmol Fe with 5 mM ferric citrate and 1 g/L of small-sized particles (SP), intermediate-sized particles (MP) and large-sized particles (LP) s-biochar; (B) Ratio 1.0 g/mmol Fe with 5 mM ferric citrate and 5 g/L of SP, MP and LP s-biochar; (C) Ratio 2.0 g/mmol Fe with 5 mM ferric citrate and 10 g/L of SP, MP and LP s-biochar. Error bars represent standard deviations of triplicate experimental setup.

**Iron Mineralogy during ferrihydrite (Fh) Reduction in the Absence and Presence of Biochar.** The high rates and extent of Fe(II) formation with more than 50% of Fh reduced within 10 hours are due to the high cell numbers used and prevented any Fe mineral phase transformation (e.g. goethite formation from Fh). We found that biochar addition altered the formation of secondary minerals during microbial Fh reduction compared to setups without electron shuttles. Previous studies showed magnetite and/or goethite formation during microbial Fh reduction without electron shuttle (i.e. without biochar) while siderite was formed in the presence of electron shuttles at high Fe(II) formation rates.<sup>1-4</sup> In our study, in the biotic setup with 10 g/L small-particle Swiss biochar (s-biochar) and 15 mM Fh, siderite was formed during microbial Fh reduction as revealed by Mössbauer spectroscopy (Figure S12). These results support previous studies that reported siderite formation in biochar-amended microbial Fh reduction experiments with *S. oneidensis* MR-1 cells MR-1.<sup>2,5</sup> Interestingly, in abiotic setups with 5 g/L small-particle-sized s-biochar and 5 mM Fh but without *S. oneidensis* MR-1 cells, 10% of the total Fe(III) present in Fh was already reduced to Fe(II) (Figure 3B) and Mössbauer spectroscopy identified the formed Fe(II) mineral as siderite (Figure S12C). Overall, ca. 0.5 mM Fe(II) was produced suggesting that even in the absence of microorganisms s-biochar donated almost 0.5 mM of electrons to Fe(III) minerals, reflecting its electron donating capacity (EDC) of  $0.23 \pm 0.02$  meq e<sup>-</sup>/g biochar.

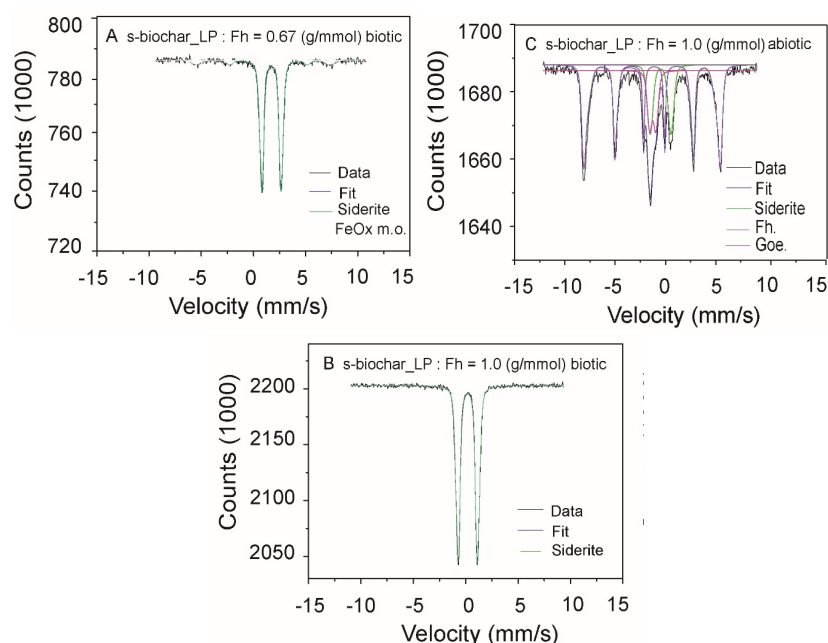


**Figure S12.** Mössbauer spectra of minerals formed during biogenic and abiogenic ferrihydrite (Fh) reduction in the presence of Swiss biochar (s-biochar). (A) 10 g/L small s-biochar:15 mM Fh ratio with *S. oneidensis* MR-1 cells; spectrum collected at 77K; (B) 5 g/L large s-biochar: 5 mM Fh ratio with *S. oneidensis* MR-1 cells; spectrum collected at 77K; (C) 5 g/L small s-biochar: 15 mM Fh without MR-1 cells; spectrum collected at 77K.

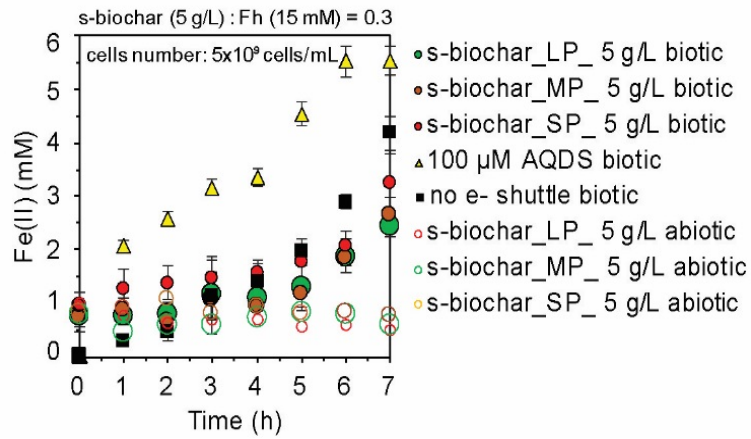


**Figure S13.** Fe(II) formation in cell suspension experiments conducted with 5 g/L of Swiss biochar (s-biochar) (different particle sizes), 15 mM ferrihydrite (Fh) and *S. oneidensis* MR-1 cells ( $5 \times 10^9$  cells/mL). The results showed that increasing cell numbers have no influence on microbial ferrihydrite reduction, i.e. increasing cell numbers did not overcome the inhibitory effect of biochar on Fh reduction.

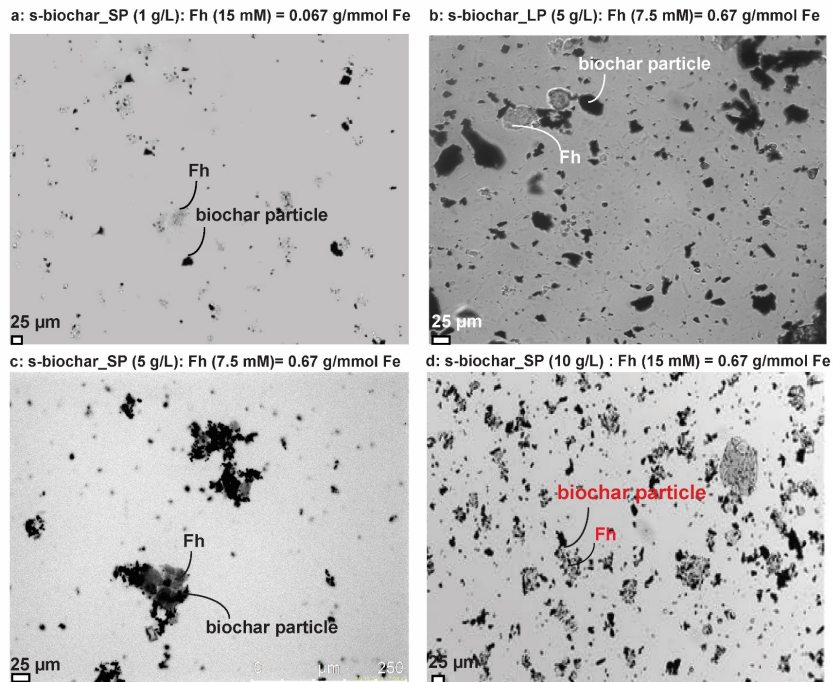


**Figure S14.** Light microscopy images at (a) ratio of Swiss biochar (s-biochar, 1 g/L) to ferrihydrite (Fh) (15 mM) with small-sized particles (SP) biochar, (b) ratio of s-biochar (5 g/L) to Fh (7.5 mM) with large-sized particles (LP) biochar, (c) ratio of s-biochar (5 g/L) to Fh (7.5 mM) with SP, and (d) ratio of s-biochar (10 g/L) to Fh (15 mM) with SP.

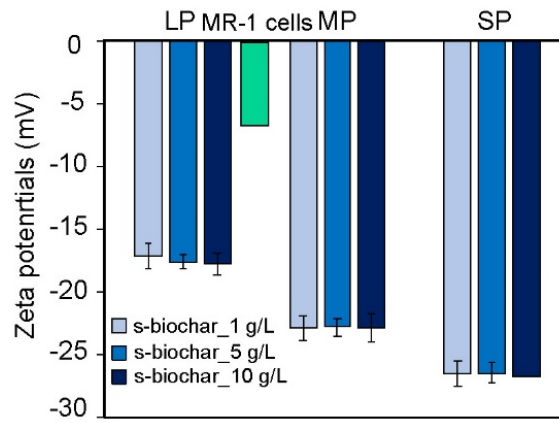


**Figure S15.** Zeta potentials of suspensions of different Swiss biochar (s-biochar) particle sizes and *S. oneidensis* MR-1 cells (pH 7, 20 mM NaHCO<sub>3</sub> buffer). The green bar indicates the zeta potential of *S. oneidensis* MR-1 cells grown on lysogeny broth (LB) liquid medium, harvested by centrifugation, washed with NaHCO<sub>3</sub> buffer and resuspended in NaHCO<sub>3</sub> buffer (pH 7, 20 mM).

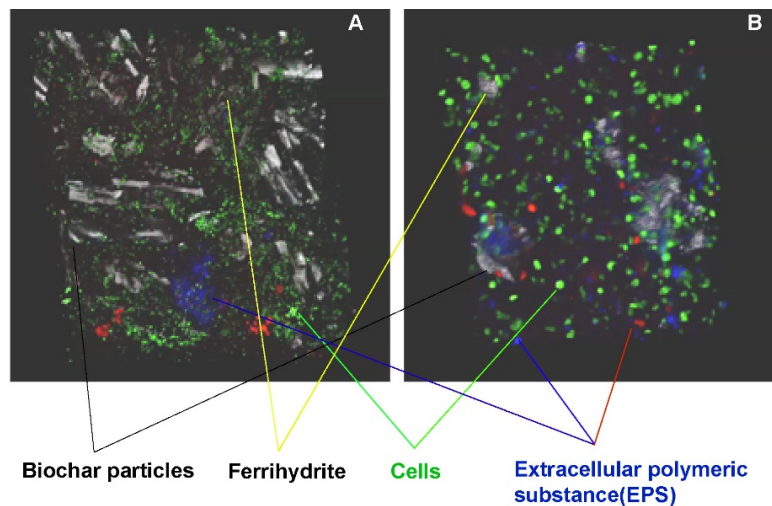


**Figure S16.** Three-dimensional aggregates of *S. oneidensis* MR-1, ferrihydrite (Fh) and Swiss biochar (s-biochar) visualized by Confocal Laser Scanning Microscopy (CLSM, Leica TCS SPE, Leica). Aggregates of *S. oneidensis* MR-1, 5 mM Fh and 5 g/L large particle size Swiss biochar (s-biochar). We used the lectin-dye conjugates WGA-Alexa555 (excited at 561 nm, shown in red) and SBA-Alexa647 (excited at 635 nm, shown in blue) to identify extracellular polymeric substances (EPS). These dyes also contained DNA dye Syto9 (excited at 488 nm, shown in green) to show the *S. oneidensis* MR-1 cells. The grey bar-like structures show the reflection signal at 488 nm and represent biochar particles. Fh is attached to biochar particles and results in blurry structures. Importantly, these two three-dimensional images are representative, but they cannot be used for quantification of certain aggregates/associations.

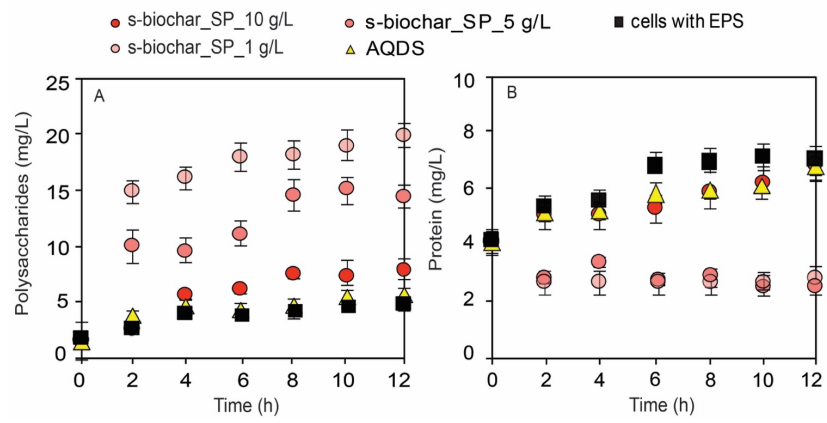


**Figure S17.** Effect of Swiss biochar (s-biochar) on extracellular polymeric substance (EPS) secretion from *S. oneidensis* MR-1 cells. Polysaccharides and protein contents are the main components of EPS over 12 hours of incubation. (A) Polysaccharide and (B) protein content after addition of small-sized particles s-biochar at different concentrations (1, 5 and 10 g/L). All setups contained  $2 \times 10^9$  *S. oneidensis* MR-1 cells/mL and 15 mM of ferrihydrite.

**Table S1.** Properties of Swiss biochar (s-biochar) and KonTiki biochar (k-biochar) used in experiments with large-sized particles (LP), intermediate-sized particles (MP) and small-sized particles (SP) biochar.

<b>Biochar samples</b>	<b>Particle type</b>	<b>SSA<sup>1</sup> (m<sup>2</sup>/g)</b>	<b>Pore size<sup>2</sup> (nm)</b>	<b>TPV<sup>3</sup> (cm<sup>3</sup>/g)</b>	<b>TOC (mg C/g)</b>	<b>Conductivity<sup>4</sup> (μS/cm)</b>
s-biochar	LP	201	2.05	4.3 x 10 <sup>-2</sup>	705±21	4.0x10 <sup>3</sup>
s-biochar	MP	N.D.	N.D.	N.D.	706±13	5.1x10 <sup>3</sup>
s-biochar	SP	258	2.01	3.7 x 10 <sup>-2</sup>	718±25	6.6x10 <sup>3</sup>
k-biochar	LP	107	2.02	1.9 x 10 <sup>-2</sup>	770±18	1.6x10 <sup>3</sup>
k-biochar	MP	N.D.	N.D.	N.D.	767±15	2.0x10 <sup>3</sup>
k-biochar	SP	118	2.04	1.8 x 10 <sup>-2</sup>	741±21	2.5x10 <sup>3</sup>

<sup>1</sup>Specific surface area (SSA) of biochar samples determined by BET at 77K.

<sup>2</sup>Pore size of biochar samples is presented as Barret-Joyner-Halenda (BJH) adsorption average pore width (4V/A).

<sup>3</sup>Total pore volume (TPV) of biochar samples is presented as BJH adsorption cumulative volume of pores between 1.7 nm and 3.0 nm width.

<sup>4</sup>Measured in powder phase under identical pressure.

<sup>5</sup>N.D. means not determined

**Table S2.** The fate of electrons stemming from oxidation of lactate (30 mM) to acetate that were recovered as Fe(II), theoretically be accepted by functional groups of Swiss biochar (s-biochar) and remaining electrons in the setups with s-biochar:ferrihydrate (Fh) ratios of 0.067, 0.3, 0.67 and 1.0 g/mmol Fe with large-sized particles (LP), intermediate-sized particles (MP) and small-sized particles (SP).

Biochar concentration in experiment	Biochar:Fh ratio	Particle size	EAC of biochar <sup>1</sup>	Acetate formed	Electrons released from lactate oxidation	Fe(II) formation in experiment	Fe(II) formation in experiment <sup>2</sup>	Electrons recovered as Fe(II) <sup>3</sup>	Electrons theoretically accepted by functional groups of biochar <sup>4</sup>	Remaining electrons <sup>5</sup>
(g/L)	(g/mmol Fe)		(meq e <sup>-</sup> )	(mmol)	(meq e <sup>-</sup> )	(mM)	(mmol)	(%)	(%)	(%)
1	0.067	LP	0.008	0.023	0.092	1.050	0.011	11	9	80
		MP	0.008	0.023	0.092	0.880	0.009	10	8	82
		SP	0.008	0.024	0.096	0.942	0.009	10	8	82
5	0.3	LP	0.040	0.029	0.116	1.530	0.015	13	34	53
		MP	0.038	0.026	0.104	2.280	0.023	22	36	42
		SP	0.039	0.027	0.108	2.340	0.023	22	36	42
5	0.67	LP	0.040	0.028	0.112	2.930	0.029	26	35	39
		MP	0.038	0.029	0.116	3.720	0.037	32	32	36
		SP	0.039	0.029	0.116	5.550	0.056	48	34	19
5	1.0	LP	0.040	0.023	0.092	3.750	0.038	41	43	16
		MP	0.038	0.023	0.092	4.110	0.041	45	41	15
		SP	0.039	0.023	0.092	4.600	0.046	50	42	8
10	0.67	LP	0.079	0.029	0.116	6.530	0.065	56	68	-24
		MP	0.075	0.029	0.116	8.010	0.080	69	65	-34
		SP	0.078	0.029	0.116	9.880	0.099	85	67	-52

<sup>1</sup>Calculation of the number of electrons acceptable by s-biochar (meq e<sup>-</sup> in our 10 mL experiments) using the EAC values (meq e<sup>-</sup>/g biochar) determined by electrochemical analysis multiplied by the biochar concentration (1, 5 and 10 g/L, respectively) and the volume of experiments (10<sup>-2</sup> L).

<sup>2</sup>Fe(II) formed (mmol) is calculated from Fe(II) formation during the microbial Fh reduction experiment (Fe(II) in mM) multiplied by the volume of the experiment (10<sup>-2</sup> L).

<sup>3</sup>Electrons recovered as Fe(II) (%) in our 10 mL experiments, in the presence or absence of biochar, are calculated as a ratio of the experimentally determined Fe(II) formation (mmol) from the microbial Fh reduction experiment to the theoretically (maximum) formed Fe(II) based on the number of electrons released from microbial lactate oxidation.

<sup>4</sup>Electrons theoretically accepted by biochar present in % of all electrons released from lactate oxidation calculated as ratio of “EAC of biochar” to the “electrons released from lactate oxidation”.

<sup>5</sup>Remaining electrons, Electron gap between total electrons released from lactate oxidation exclude electrons either recovered as Fe(II) and electrons accepted by functional groups. The remaining electrons were probably stored in the polyaromatic carbon matrices due to the double-layer capacitance in biochar and/or cells.

## References:

1. Klüpfel, L.; Keiluweit, M.; Kleber, M.; Sander, M., Redox properties of plant biomass-derived black carbon (biochar). *Environ. Sci. & Technol.* 2014, 48 (10), 5601-5611; DOI: 10.1021/es500906d.
2. Kappler, A.; Wuestner, M. L.; Ruecker, A.; Harter, J.; Halama, M.; Behrens, S., Biochar as an electron shuttle between bacteria and Fe(III) minerals. *Environ. Sci. & Technol. Lett.* 2014, 1 (8), 339-344; DOI: 10.1021/ez5002209.
3. Jiang, J.; Kappler, A., Kinetics of microbial and chemical reduction of humic substances: implications for electron shuttling. *Environ. Sci. & Technol.* 2008, 42 (10), 3563-3569; DOI:10.1021/es7023803.
4. Scott, D. T.; McKnight, D. M.; Blunt-Harris, E. L.; Kolesar, S. E.; Lovley, D. R., Quinone moieties act as electron acceptors in the reduction of humic substances by humics-reducing microorganisms. *Environ. Sci. & Technol.* 1998, 32 (19), 2984-2989; DOI: 10.1021/es982014z.
5. Wu, S.; Fang, G.; Wang, Y.; Zheng, Y.; Wang, C.; Zhao, F.; Jaisi, D. P.; Zhou, D. M, Redox-active oxygen-containing functional groups in activated carbon facilitate microbial reduction of ferrihydrite. *Environ. Sci. & Technol.* 2017, 51 (17), 9709-9717; DOI: 10.1021/acs.est7bb01854



#### Chapter 4 - Personal contribution

Experiments were conceptualized by myself and Prof. Andreas Kappler. The soil microcosm experiments and data collection were carried out by myself. Dr. Daniel Straub helped 16S rRNA sequencing analysis. The discussion and analysis of the obtained results were done by myself, Dr. Tianran Sun, Prof. Andreas Kappler, Prof. Sara Kleindienst, Prof. Ruben Kretzschmar, and Prof. LARGUS Angement. The manuscript was written by myself. All co-authors read and revised the manuscript.



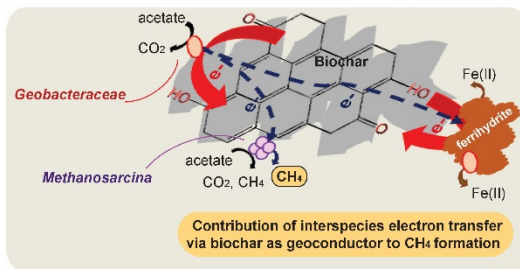
# 4

## Coupled Function of Biochar as Geobattery and Geoconductor Alters Soil Microbial Community Composition and Electron Transfer Pathways in a Paddy Soil

Submitted to Soil Biology and Biochemistry

### TOC art

Addition of biochar stimulated syntrophic activity of *Geobacteraceae* and *Methanosarcina* thus simultaneously contributing to **microbial Fe(III) reduction** and **methanogenesis** in a paddy soil



Biochar carbon matrix and redox-active functional groups    Shuttling of electrons via biochar as geobattery    Transfer of electrons via biochar as geoconductor

## **Coupled Function of Biochar as Geobattery and Geoconductor Alters Soil Microbial Community Composition and Electron Transfer Pathways in a Paddy Soil**

Zhen Yang<sup>1</sup>, Tianran Sun<sup>2</sup>, Sara Kleindienst<sup>3</sup>, Daniel Straub<sup>3,4</sup>, Ruben Kretzschmar<sup>4</sup>, Largus T. Angenent<sup>2</sup>, Andreas Kappler<sup>1\*</sup>

<sup>1</sup>*Geomicrobiology, Center for Applied Geoscience, Tuebingen, 72076, Germany*

<sup>2</sup>*Environmental Technology, Center for Applied Geoscience, Tuebingen, 72076, Germany*

<sup>3</sup>*Microbial Ecology, Center for Applied Geoscience, Tuebingen, 72076, Germany*

<sup>4</sup>*Quantitative Biology Center (QBiC), Tuebingen, 72076, Germany*

<sup>5</sup> *Soil Chemistry Group, Institute of Biogeochemistry and Pollutant Dynamics, CHN, ETH, Zurich, 8092, Switzerland*

\*To whom correspondence should be sent:

Andreas Kappler, Geomicrobiology, Center for Applied Geosciences

University of Tuebingen, Sigwartstrasse 10, D-72076 Tuebingen, Germany

Phone: +49-7071-2974992, Fax: +49-7071-29-295059

Email: [andreas.kappler@uni-tuebingen.de](mailto:andreas.kappler@uni-tuebingen.de)

Submitted to Soil Biology and Biochemistry

#### 4.1 Abstract

Biochar can participate in biogeochemical electron transfer processes due to its redox activity (*i.e.* electron accepting and donating processes via redox-active functional groups, functioning as a geobattery) and its conductivity (*i.e.* electron flow through conductive carbon matrices, functioning as a geoconductor). Each of these two functions has been separately demonstrated to play a role in biogeochemical iron cycling and formation of methane. Yet, little is known about the coupled effects of both electron transfer mechanisms, despite the fact that naturally occurring electron transfer through biochar is expected to rely on both geobattery and geoconductor mechanisms simultaneously. Here, we conducted anoxic microcosm incubations to investigate how the coupled electron transfer mechanisms in biochar influence the electron transfer pathways in a paddy soil and how this impacts the soil microbial community. We found that biochar, functioning as geobattery and geoconductor, simultaneously stimulated microbial Fe(III) reduction and methanogenesis by 2.6 and 2.3 fold, respectively, compared to microcosms without biochar. Smaller biochar particles caused higher rates of Fe(III) reduction and methanogenesis than larger particles. In contrast, the redox-active model compound anthraquinone-2,6-disulfonate (AQDS), which functions solely as a geobattery, only stimulated Fe(III) mineral reduction. Microbial community analysis showed that addition of biochar enriched syntrophic acetate-oxidizing *Geobacteraceae* taxa and methane-producing *Methanosarcina* taxa, as well as increased the copy numbers of 16S rRNA genes specific for *Geobacter* spp. and of *mcrA* genes. This suggests that while the biochar geobattery function dominated microbial Fe(III) mineral reduction, the observed methanogenesis was likely a result of conductive-material interspecies electron transfer caused by biochar functioning as geoconductor. In summary, our results demonstrated a coupled effect of biochar functioning both as geobattery and geoconductor influencing soil microbial metabolisms and leading to electron transfer between either cells and minerals or cells and cells, thus, mitigating methane emission in a paddy soil.

**Keywords:** biochar, dissimilatory iron reduction, methanogenesis, electron transfer pathways, conductive-particle interspecies electron transfer

## 4.2 Introduction

Biochar is a carbon-rich organic material that contains redox-active functional groups (mainly quinone and phenol groups) (Keiluweit et al., 2010) and conductive polyaromatic carbon ring structures in the carbon matrices (Xu et al., 2013). Electron transfer pathways via biochar include i) electron accepting and donating cycles via the redox-active functional groups, which means biochar can function as a geobattery (Klöpffel et al., 2014; Wu et al., 2017, Sun et al., 2018) and ii) direct electron transfer via the conductive carbon matrices, which means biochar functions as a geoconductor (Yu et al., 2015; Sun et al., 2017; Sun et al., 2018). These pathways are responsible for biochar participating in multiple electron transfer processes in many biogeochemical processes. On the one hand, biochar-mediated microbial extracellular electron transfer (with biochar acting as a geobattery) was shown to participate in organic contaminant degradation (Oh et al. 2011; Yu et al., 2016), redox-active element cycling (e.g. microbial Fe(III) oxyhydroxide or nitrate reduction) (Kappler et al., 2014; Xu et al., 2016; Saquing et al., 2016; Prevotau et al., 2016) and greenhouse gas emissions (Zhou et al., 2017; Yuan et al., 2017). On the other hand, biochar functioning as a geoconductor can transfer electrons between cells and Fe(III) minerals promoting Fe(II) formation (Tan et al., 2018, Yang et al., 2019). In addition, biochar functioning as a geoconductor has been suggested to allow electron transfer between microbial cells with biochar serving as a cell to cell conduit for electrons flowing from electron-donating microorganisms to electron-accepting microorganisms (Liu et al., 2012; Chen et al., 2016), so-called conductive-material interspecies electron transfer (CIET). Biochar participating in CIET was shown for a co-culture of Fe(III)-reducing bacteria (*Geobacteraceae*) and methanogens (*Methanosarcina*), leading to methane production (Chen et al., 2016, Tremblay et al., 2017; Yang et al., 2018, Yuan et al., 2019).

Biochar, as a soil amendment, can stimulate microbial activity and alter microbial community composition in soils (Mukherjee et al., 2013; Zhu et al., 2017; Harter et al., 2016; Krause et al., 2018). Absorption of organic metabolic compounds (*i.e.* acetate) on biochar has been suggested to promote microbial growth on the biochar surface (Hill et al., 2019). In turn, the shifted microbial abundance and activity influence iron cycling and greenhouse gas (*i.e.* N<sub>2</sub>O, CH<sub>4</sub>) emissions (Woolf et al., 2010; Cayuela et al. 2013, Harter et al. 2014, Gul and Whalen 2016; Hagemann et al., 2017a; Hagemann et al., 2017b). ). In flooded rice paddies, most of the electrons stemming from the degradation of organic matter enter methanogenesis (Yang et al., 1998; Hori et al., 2009; Kögel-Knabner et al., 2010). However, microbial Fe(III) reduction represents an alternative electron-accepting process in anoxic paddy soils, leading to competition for electron donors between methanogens and dissimilatory Fe(III)-reducing

bacteria, thermodynamically suppressing methanogenesis (Lovley et al., 1987; Achtnich et al., 1995; Teh et al., 2008; Friedman et al., 2016; Miller et al., 2015).

The literature on how biochar influences soil CH<sub>4</sub> emission showed partially contradictory results. While some studies reported that biochar addition reduces methane emission from waterlogged paddy soil (Feng et al. 2012; Liu et al., 2011; Jeffery et al., 2016; Brassard et al., 2016), biochar amendment has also been shown to simultaneously increase the rates of both microbial Fe(III) reduction and methanogenesis compared to soils without biochar application (Zhou et al., 2017). The function of biochar as geobattery or geoconductor has been addressed separately in biogeochemical iron cycling and greenhouse gas emission studies. However, little is known about the coupling effect of both functions on Fe(III) reduction and methanogenesis. A synergistic effect of biochar as geobattery and geoconductor for boosting electron transfer has been demonstrated by electrochemical analysis (Sun et al., 2018, but its relevance in microbial activity is unknown. In general, small biochar particles (micro- and nano-sized) possess higher affinities than large particles (milli- to centimeter) for microorganisms and minerals, which leads to an aggregation of all phases (Zhang et al., 2010; Guggenberger et al., 2008, Yang et al., 2019) and potentially alters the fraction of electrons that end up in microbial Fe(III) reduction or methanogenesis. Here, we set up anoxic paddy soil microcosm experiments with different particle sizes of two different wood-derived biochars to investigate the coupling effect of biochar functioning as both geoconductor and geobattery functions and its impact on soil microbial community composition as well as on the kinetics and composition of microbial Fe(III) reduction and methanogenesis.

### **4.3 Materials and Methods**

#### *4.3.1 Preparation of Biochar Suspensions*

Two kinds of biochars, Swiss-biochar (s-biochar, Belmont-sur-Lausanne, VB, Switzerland) from mixed waste wood chips and KonTiki biochar (k-biochar) from pine wood chips, were used in microcosm incubations. Both biochars were produced by pyrolyzing biomass at 700°C. The different particle-sized biochar was prepared by milling (Pulverisette, zirconium oxide balls, Fritsch, Idar-Oberstein, Germany) as described in the supporting information. Small-sized (SP) biochar particles have a minor fraction (5-10% of volume distribution) of 0.1-0.3 µm and a main fraction (90-95% of volume distribution) of 5-20 µm and the large-sized (LP) biochar particles are in the size range of 50-100 µm. The anoxic biochar suspensions were prepared as reported previously (Kappler et al., 2014 and Yang et al., 2019).

#### *4.3.2 Microcosm Setups*

Paddy soil was collected from Vercelli, Italy. Detailed information on soil and biochar properties are shown in Tables S1 and S2. In the laboratory, wet paddy soil samples (100 g) were transferred into Schott bottles (1000 mL) with 500 mL anoxic doubly-deionized (DDI) water ( $>18.2 \text{ } \Omega\text{M}\cdot\text{cm}$ ; Milli-Q, Millipore Corporation) and over-head shaken at 120 rpm for 2 days at 25°C. Aliquots (5 mL) of the well-mixed slurry were added to serum vials (50 mL) containing 20 mL sterilized and anoxic medium. The basal medium (pH 6.8-7.2) contained  $\text{MgCl}_2 \cdot 6\text{H}_2\text{O}$  (0.4 g/L),  $\text{CaCl}_2 \cdot \text{H}_2\text{O}$  (0.1 g/L),  $\text{NH}_4\text{Cl}$  (0.027 g/L), and  $\text{KH}_2\text{PO}_4$  (0.6 g/L), 1 mL/L vitamin solution, 1 mL/L trace element solutions, and 30 mM bicarbonate buffer ( $\text{NaHCO}_3$ ). Acetate (Ace.) (1 mM) Fe(III) (5 mM as Fh) and Fe(III) (5 mM as Fh) were added as electron donor and electron acceptor, respectively. The medium pH was adjusted to 7.0-7.1 using NaOH or HCl (1 M). In total, four microcosm treatments (in triplicates each) were prepared: 1) “No amendment” containing soil slurry only; 2) “No biochar” with soil slurry amended with acetate (1 mM) and Fh (5 mM); 3) “s-(k-)biochar” with soil slurry amended with acetate, Fh, and s-biochar or k-biochar with two different particle sizes (SP and LP) final biochar/Fh ratio of 1.0 g/mmol Fe; 4) “s-(k-)biochar-abiotic” with gamma-sterilized soil slurry amended with acetate, Fh and s-biochar or k-biochar. Additional setups with soil slurry amended with acetate (1 mM) and soil slurry amended with Fh (5 mM) were analyzed for their microbial community composition. The bottles were incubated at 28°C without shaking in the dark. Detailed information on experimental setups is provided in Table S3. All experiments were done at environmentally relevant biochar particle sizes and Fe concentrations (Jones et al., 2011; Zimmerman et al., 2011 and Zhou et al., 2017). A application biochar rate and Fh content were used in soil microcosm with 125t/ha and 0.013g, respectively, which is relevant with the general biochar application rate of 0.5-135t/ha (Glaser et al., 2002; Bista et al., 2019; Zimmerman et al., 2011 and Zhou et al., 2017). All microcosms were subsampled every two days until day 18. Extractable Fe(II) and Fe(tot),  $\text{CH}_4$  and acetate were quantified over time. The pH values were determined and showed ranges of  $7.01 \pm 0.01$  on day 0 and  $7.04 \pm 0.02$  on day 18.

#### 4.3.3 Analytical Techniques

Total Fe(II) (soluble in 1M HCl) and Fe(tot) (soluble in 1M hydroxylamine hydrochloride, HAHC) were determined using the ferrozine assay as described by Amstaetter et al. (2012) and Stookey (1970).  $\text{CH}_4$  in the headspace was quantified using a SRI 8610C gas chromatograph (SRI Instruments Europe GMBH, Germany) equipped with a flame ionization detector (detection limit 2 ppmv). Liquid samples (ca. 200  $\mu\text{L}$ ) for acetate analyses were taken in an anoxic glovebox (100%  $\text{N}_2$ ) and filtered through 0.22  $\mu\text{m}$  filters before high-performance liquid chromatography (HPLC, LC-10AT, SHIMADZU) analysis equipped with a DAD and a RID detector.



#### 4.3.4 Bacterial and archaeal 16S rRNA Gene Amplification, Illumina Sequencing and Data Analysis

After 18-days of incubation, samples (approximately 3-4 g each) were collected by centrifugation (14,000 g, 30 min). DNA in all treatments was extracted using the Power-Soil™ DNA isolation kit (Mo Bio Laboratories, Carlsbad, CA) according to the manufacturer's protocol. The DNA of triplicate samples (i.e. biological replicated) was pooled equally, to yield a final concentration of 2 ng/μl for all biotic treatments. To investigate the bacterial and archaeal communities' structure and composition, the V4 regions of universal 16S rRNA genes were amplified by Polymerase Chain reaction (PCR) with the primer set 515f (5'-GTGCCAGCMGCCGCGTAA-3') and 806r (5'-GGACTACHVGGGTWTCTAAT-3') (Caporaso et al., 2011) using the pooled DNA samples as template. Amplicons were sequenced by Microsynth AG (Switzerland) with the Miseq platform (Illumina, San Diego, CA, USA) using the v2 chemistry (PE 250). Sequencing data were analyzed with nf-core/ampliseq v1.1.0 that wraps all analysis steps and software and is publicly available at <https://github.com/nf-core/ampliseq> (Straub et al. 2019). Briefly, primers were trimmed and untrimmed sequences were discarded (<6%) with Cutadapt v1.16 (Martin Marcel, 2011). Adapter and primer-free sequences were imported into QIIME2 v2018.06 (Bolyen, et al 2018) quality checked with demux (<https://github.com/qiime2/q2-demux>), and processed with DADA2 v 1.6.0 (Callahan et al., 2016 ) to remove PhiX contamination, trim reads before median quality falls below 35 (forward 181, reverse 107), correct errors, merge read pairs and remove PCR chimeras and, ultimately, produce amplicon sequencing variants (ASVs). Alpha rarefaction curves were produced with the QIIME2 diversity alpha-rarefaction plugin, which indicated that the richness of the samples has been fully observed. A Naive Bayes classifier was fitted with 16S rRNA gene sequences extracted with the PCR primer sequences from SILVA v132 QIIME compatible database clustered at 99% identity (Pruesse et al., 2007) . ASVs were classified by taxon using the fitted classifier (<https://github.com/qiime2/q2-feature-classifier>). ASVs classified as chloroplast or mitochondria were removed, totaling to <1% relative abundance per sample and the remaining ASVs had their abundances extracted by feature-table (Bolyen, et al 2018).

#### 4.3.5 Real-time Quantitative PCR

The abundances of bacterial 16S rRNA genes, archaeal 16S rRNA genes, *Geobacter* spp. specific 16S rRNA genes and methyl-coenzyme M reductase subunit alpha (*mcrA*) genes were analyzed using a IQ™5 Multicolor Real-time PCR Detection system (BIO-RAD Laboratories GmbH, München). The reaction mixture contained 3.15 μL DNA (2-3 ng/μL) as template for

each triplicate, 5  $\mu\text{L}$  of SYBR 2 Premix Ex *Taq*, 0.5  $\mu\text{L}$  of each primer, and 3  $\mu\text{L}$  of sterilized deionized water. Negative treatment control was carried out using sterilized deionized water instead of DNA template for each qPCR assay. Detailed information regarding the primers and thermal cycling conditions used is shown in the Supporting Information (Table S4).

#### 4.3.6 Statistical Analysis

Statistical analysis was performed by the statistics software package SPSS 22.0. Statistical significance was determined by Duncan's multiple range test and ANOVA was used to compare  $\text{CH}_4$  emission, Fe(II) production and acetate consumption among different microcosms. \*\*\*  $P < 0.001$ ; \*\* $P < 0.01$ , \* $P < 0.05$ , and n.s., not significant.

#### 4.3.7 Data availability

Raw sequencing data have been deposited at the National Center for biotechnology Information (NCBI) Sequence Read Archives (SRA) database under bioproject number (PRJNA597449).

### 4.4 Results and Discussion

#### 4.4.1 Stimulated Rates of Fe(III) Reduction and Methanogenesis in the Presence of Biochar

To investigate the effect of different biochar/Fh ratios on microbial Fe(III) reduction and methane emission in the paddy soil, Fe(II) concentrations, Fe(II)/Fe(tot) ratios and  $\text{CH}_4$  concentrations were monitored over 18 days (Fig. 1A and 1B). Compared to microcosms with soil only (no amendments), addition of both Fh and acetate (no biochar) led to faster Fe(II) formation but lower  $\text{CH}_4$  production (Fig. 1A and B). These results are in agreement with previous studies (Teh et al., 2008; Roden and Wedel, 2013), suggesting that Fh addition suppressed methane production, successfully competing for acetate, as was anticipated thermodynamically (Table S6), favoring direct microbial Fe(III) reduction. In contrast, we found that amendment of acetate, Fh, and biochar simultaneously stimulated both Fe(II) and  $\text{CH}_4$  production compared to microcosms without biochar (Fig. 1A and B,  $p < 0.001$ ). These results indicated that the addition of biochar stimulated Fe(II) production via facilitated electron transfer to Fh by biochar, probably as geobattery and geoconductor, which is in agreement with previous studies (Kappler et al., 2014; Yang et al., 2019). In addition, the stimulation of methanogenesis could have been caused by biochar functioning as geoconductor (Chen et al., 2014). The immobilization of cells on the biochar surface (Youngwilai et al., 2020) and adsorption of organic metabolites (e.g. acetate) by biochar can promote microbial growth (Hill

et al., 2019), thus, contributing to the stimulation of both methanogenesis and microbial Fe(III) reduction.

#### *4.4.2 Suppressed Methanogenesis by Microbial Fe(III) Reduction in the Presence of Biochar*

To clarify how methanogenesis competes with microbial Fe(III) reduction in the presence of biochar, we compared CH<sub>4</sub> production between microcosms amended with or without Fh in the presence of acetate and biochar. We found that in the presence of biochar, addition of Fh stimulated Fe(II) formation but lowered CH<sub>4</sub> production (Fig. 1A) compared to microcosms not amended with Fh (Fig. 1C and Fig. S4). This suggests that microbial Fe(III) reduction still outcompeted methanogenesis even in the presence of biochar, consistent with methanogenesis being thermodynamically more favorable than Fe(III) reduction (Table S6). Without addition of Fh (Fig. 1C) in the presence of biochar, microbial Fe(III) reduction did not outcompete methanogenesis probably due to a lack of terminal electron acceptor (Fe(III)). In this case, CH<sub>4</sub> was probably produced as a result of biochar-facilitated electron transfer to the methanogens with biochar as geoconductor as well as by direct acetoclastic methanogenesis. After addition of Fh and biochar, we observed lower CH<sub>4</sub> formation and an increase Fe(II) production, which is also in agreement with some previous studies (Liu et al., 2011; Jeffery et al., 2016). In summary, our results showed that it is important to consider the available Fe(III) content in the environment to evaluate the impact of biochar application on methanogenesis.

#### *4.4.3 Impact of Biochar Type and Particle Size on Rates of Microbial Fe(III) Reduction and Methanogenesis*

When comparing the two types of biochar, we generally observed faster Fe(II) and CH<sub>4</sub> production in microcosms amended with s-biochar (0.28-0.37 mM Fe(II)/d, 12.22-12.80 μM CH<sub>4</sub>/d, Fig 1D) than with k-biochar (0.25-0.35 mM Fe(II)/d, 10.13-11.65 μM CH<sub>4</sub>/d, Fig 1D), which could be due to the higher electron exchange capacity (EEC) and higher conductance of s-biochar compared to k-biochar (Table S2). In case of the same type of biochar (i.e., either s-biochar or k-biochar), we found that small biochar particles showed more than 1.5 times higher rates of Fe(II) (0.35-0.37 mM Fe(II)/d, Fig 1D) and CH<sub>4</sub> production (11.65-12.80 μM CH<sub>4</sub>/d, Fig 1D) than large biochar particles (0.25-0.28 mM Fe(II)/d and 10.13-12.22 μM CH<sub>4</sub>/d, respectively, Fig, 1D). These increased production rates were probably a result of a faster electron transfer rate induced by the increased surface area of small biochar particles (1.08% and 1.28% of surface area for s-biochar and k-biochar, respectively, Table S2) in comparison to large biochar particles. The higher electron transfer rates induced by smaller biochar particles also make sense because of the measured higher conductance of small biochar particles (Table S2), strengthening the importance of biochar as geoconductor. Additionally, the increased surface area in small biochar particles can promote adhesion of microorganisms

to the biochar surface (Jaafar et al., 2015; Afrooz et al., 2018; Yang et al., 2019). Promoting the growth and immobilization of microbial cells on biochar (Youngwilai et al., 2020, Hill et al., 2019) possibly led to faster Fe(II) and CH<sub>4</sub> formations in the presence of small biochar particles than large particles.

#### *4.4.4 Influence of Biochar in comparison to AQDS on Rates of Fe(III) Reduction and Methanogenesis*

Based on changes in Fe(II) and CH<sub>4</sub> production rates around day 9, we separated the incubation duration (18 days) into two periods (i.e. period 1 (days 1-9) and period 2 (days 10-18)). We found that after addition of biochar, up to 60% of Fe(II) production was accomplished in period 1 with a high rate of Fe(II) production ( $0.25 \pm 0.01$ - $0.37 \pm 0.01$  mM Fe(II)/d, Fig 1A, 1B and 1D) compared to microcosms without biochar ( $0.08 \pm 0.01$  mM Fe(II)/d, Fig 1A, 1B and 1D). Compared to period 1, the rates of Fe(II) production were much lower ( $0.02 \pm 0.002$ - $0.07 \pm 0.001$  mM Fe(II)/d, Fig. 1D) in period 2 in all microcosms with biochar amendment. In the absence of biochar, the CH<sub>4</sub> production rate was  $1.08 \pm 0.01$   $\mu$ M CH<sub>4</sub>/d in period 1 and increased to  $2.27 \pm 0.02$   $\mu$ M CH<sub>4</sub>/d in period 2. We used anthraquinone-2,6-disulfonate (AQDS), which is a well-known electron shuttle for stimulating microbial Fe(III) mineral reduction (Lovley et al., 1997, Chen et al., 2017), to investigate its effect on the competition between microbial Fe(III) reduction and methanogenesis in comparison to biochar. During period 1, the CH<sub>4</sub> production rates in microcosms amended with AQDS ( $1.75 \pm 0.30$   $\mu$ M CH<sub>4</sub>/d) were slower than in the biochar-amended setups ( $10.13 \pm 0.2$ - $12.22 \pm 0.3$   $\mu$ M CH<sub>4</sub>/d for large particle biochars and  $11.65 \pm 0.3$ - $12.80 \pm 0.3$   $\mu$ M CH<sub>4</sub>/d for small particle biochars), but similar to the “no biochar” setups ( $1.08 \pm 0.1$   $\mu$ M CH<sub>4</sub>/d, Fig. 1C). In contrast, addition of AQDS showed a significant stimulation of indirect microbial Fe(III) reduction mediated by AQDS as an electron shuttle in period 1 (days 1-9) ( $0.44$  mM Fe(II)/d) compared to setups that did not contain AQDS or biochar (‘no biochar’ setup with  $0.08$  mM Fe(II)/d). These results indicated that AQDS functioned as a geobattery and only favored microbial Fe(III) mineral reduction but not methanogenesis, which was consistent with an earlier study showing that adding AQDS did not stimulate methanogenesis (Liu et al., 2012).

In contrast, the higher rates and extent of CH<sub>4</sub> production in the presence of biochar were probably a result of the biochar functioning as geoconductor, in addition to its function as geobattery, which contributed to methanogenesis activity. Additionally, biochar can serve as an attachment matrix leading to a close aggregation of biochar with Fe(III)-reducers and methanogens. The surface areas of both s- and k-biochar (25-30 m<sup>2</sup> per setup) are 5-6 larger than that of ferrihydrite (5 m<sup>2</sup> per setup, Table S2). A larger surface area of the biochar is expected to promote the attachment of cells to biochar (Jaafar et al., 2015, Amonette et al, 2009), causing a closer aggregation of cells with biochar compared to cells with Fh (Yang et

al., 2019). This can then facilitate the direct electron transfer from electron-donating microorganisms to electron-accepting microorganisms through biochar carbon matrices functioning as geoconductor. This function as geoconductor between cells can partly bypass the electron flow from cells to Fh, even though Fh is more favorable in accepting electrons (Table S6), thus, leading to sustained CH<sub>4</sub> production.

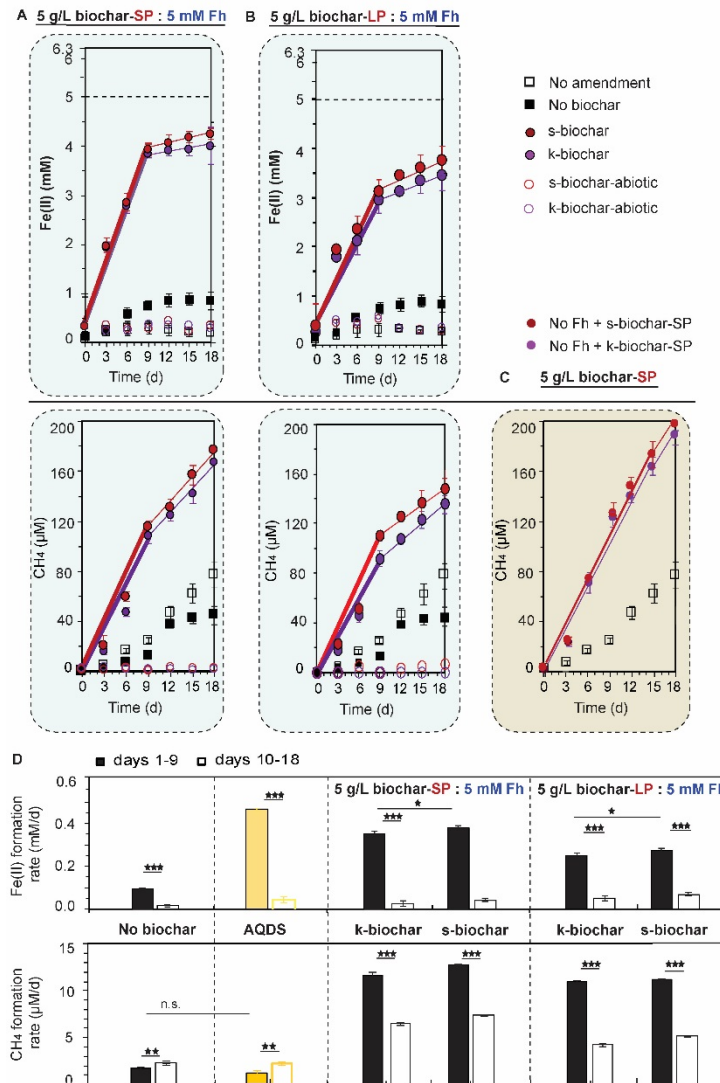


**Fig. 1.** Microbial Fe(III) reduction (upper panel) and methane emission (bottom panel) in anoxic paddy soil microcosms amendment with (A) small-particle size (SP) biochar including Swiss biochar (s-biochar, 5 g/L) and KonTiki biochar (k-biochar, 5g/L), acetate and ferrihydrite (Fh, 5 mM), (B) large-particle size (LP) biochar including s-biochar and k-biochar (5 g/L), acetate and Fh (5 mM). The “no amendment” setups contained only soil slurry (no biochar, no acetate, no Fh). The “no biochar” setups were amended with soil slurry, acetate and Fh. s-/k-biochar setups were amended with soil slurry, acetate, Fh, s-biochar or k-biochar (SP or LP), respectively. s-/k-biochar-abiotic setups were amended with sterilized soil slurry, acetate, Fh, s-biochar or k-biochar, respectively. (C) Influence of SP biochars on methanogenesis in microcosm amended without Fh. The ‘No Fh + s- (k-)biochar’ setups were amended with acetate, s-biochar-SP or k-biochar-SP, respectively. (D) Rates of microbial Fe(III) reduction (mM Fe(II)/d) and

methanogenesis ( $\mu\text{M CH}_4/\text{d}$ ) with biochar-SP/LP and Fh during two incubation periods (period 1: days 1-9 and period 2: days 10-18). The AQDS microcosm was amended with 100  $\mu\text{M}$  AQDS, 1 mM acetate and 5 mM Fh. Statistical significance was analyzed by a two-way analysis of variance (ANOVA) with Tukey's multiple-comparisons test. \*\*\*  $P < 0.001$ ; \*\* $P < 0.01$ , \* $P < 0.05$ , and n.s., not significant.

#### 4.4.5 Abundance of *Geobacteraceae*, *Methanosarcina* and Functional Genes Related to Methane production after addition of Biochar

To identify microorganisms that potentially contribute to Fe(III) reduction and methanogenesis depending on biochar addition, we analyzed the microbial community composition and the copy numbers of 16S rRNA genes specific for *Geobacter* spp. and *mcrA* genes (Fig. 2A, S1 and S2). *Geobacteraceae* became the predominant bacterial taxa by accounting for at least 42% of total 16S rRNA gene sequences in the setup without biochar amendment. Two known methanogens, *Methanosarcina* and *Methanobacterium*, were detected in all treatments with and without biochar amendment, one of them, *Methanosarcina*, is capable of metabolizing acetate to methane (Jetten et al., 1990) and also catalyzing hydrogenotrophic methanogenesis (Aglar et al., 2011). Particularly, it has been reported that biochar can modulate methanogenesis through electron syntrophy of *Geobacteraceae* and *Methanosarcina* (Yuan et al., 2018). Compared to microcosms with only soil (no amendments), in microcosms amended with 5 mM Fh and 1 mM acetate (no biochar) the relative abundance of *Geobacteraceae* and *Methanosarcina* both slightly increased from 42% to 46% ( $p < 0.05$ ) and from 0.2% to 0.4% (not significant) of the total 16S rRNA gene sequences, respectively (Fig. 2A). This suggests that Fh and acetate addition lead to a slight increase in the relative abundance of well-known Fe(III)-reducers affiliating with *Geobacteraceae* which is in agreement with a previous study (Zhou et al., 2017). However, no obvious change in the relative abundance of *Methanosarcina* was observed with Fh and acetate amendment. In microcosms amended with biochar, the relative abundance of *Geobacteraceae* slightly decreased from 42% to 39% ( $p < 0.05$ ) of total 16S rRNA gene sequences (Fig. 2A). However, *Methanosarcina* became the predominant archaeal taxa accounting for up to 7-13% ( $p < 0.001$ ) of total 16S rRNA gene sequences (Fig. 2A). Relative abundance of *Methanosarcina* of total 16S rRNA gene sequences increased 32-fold in the microcosm amended with biochar compared to the microcosm without biochar amendment. These results suggest that addition of biochar led to an increase in the relative abundance of *Methanosarcina* taxa compared to that of *Geobacteraceae*. Addition of biochar altered the relative abundance of several other bacterial taxa, including *Rhodocyclaceae*, which decreased in its relative abundance (10% to 5%), while *Desulfurmonadaceae* and *Syntrophobacterales* increased in relative abundance 3- and 8-fold, respectively, in biochar-amended microcosms compared to non-biochar-amended microcosms.

When comparing setups with small particle biochar to setups amended with large particle biochar, we found that the smaller biochar particles led to higher relative abundances of *Geobacteraceae* and *Methanosarcina*, probably resulting from the greater surface area of the small particles, supporting attachment of these microorganisms (Jaafar et al., 2015). To further support and quantitatively assess the role biochar plays in modifying soil microbial communities, we used qPCR specific for 16S rRNA genes of *Geobacter* spp. and for *mcrA* genes after the biochar application. Both genes were detected in all treatments and the abundance of *Geobacter* spp. genes and *mcrA* genes showed a similar trend, compared to the microbial community patterns based on 16S rRNA gene sequencing (Fig. 2B, 2C and Fig. S2). In biochar-amended setups, the copy numbers of 16S rRNA genes of *Geobacter* spp. and *mcrA* genes increased by 4-, and 7-fold, respectively, compared to setups without biochar (Fig. S2B and 2C). This further highlights the role of *Geobacter*-related Fe(III)-reducers and *mcrA*-carrying methanogenic archaea for the observed Fe(III) reduction and methanogenesis, respectively. Small particle-sized biochar and s-biochar led to higher gene copy numbers of *Geobacter* spp. and *mcrA* genes compared to large particle-sized biochar and k-biochar. These results suggest that s-biochar and small particle-sized biochar supported microbial growth of these populations more than k-biochar and large-sized biochar. We found a positive correlation between the copy numbers of 16S rRNA genes specific for *Geobacter* spp and *mcrA* gene (Fig. S2) for both s-biochar and k-biochar, suggesting that biochar/Fh application simultaneously stimulated growth of *Geobacter*-related Fe(III)-reducers and *mcrA*-carrying methanogenic archaea. Syntrophy between *Geobacteraceae* and *Methanosarcina* might have been facilitated in our microcosms by electron transfer from *Geobacteraceae* to *Methanosarcina* for CH<sub>4</sub> production through biochar, which is consistent with previous studies have been shown that biochar can stimulate methanogenesis by facilitating interspecies electron transfer between *Geobacteraceae* and *Methanosarcina* (Chen et al., 2014, Yuan et al., 2018).

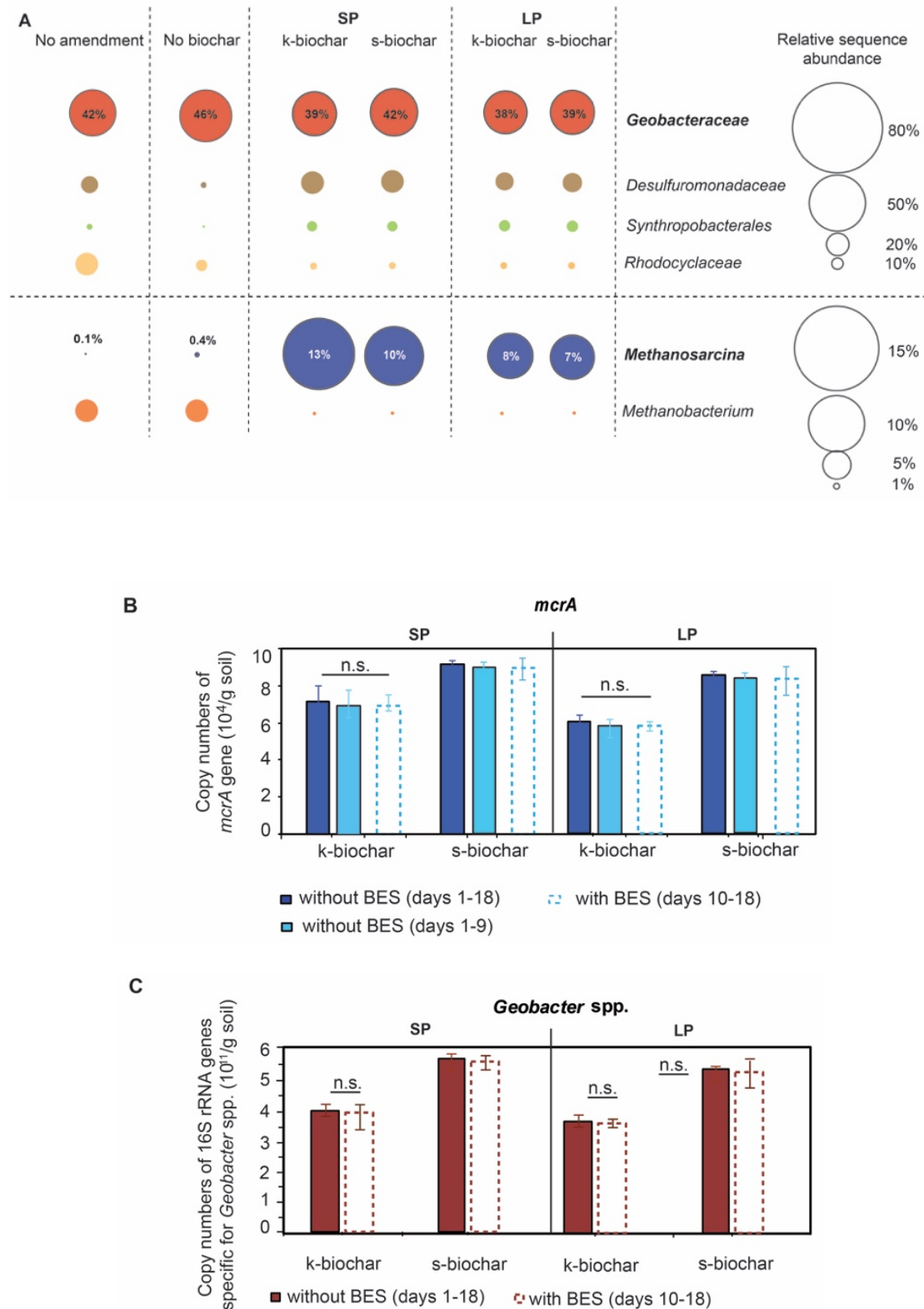


**Fig. 2.** (A) Relative abundance of *Geobacteraceae* and *Methanosarcina* based on 16S rRNA gene sequencing, respectively, after an 18-day incubation, in microcosms containing only soil slurry (no amendments), soil slurry amended with 1 mM acetate and 5 mM Fh (no biochar) and biochar setups with soil slurry amended with acetate, Fh and small and large-particle size (SP, LP) Swiss biochar (s-biochar) and KonTiki biochar (k-biochar); (B) Copy numbers of *mcrA* genes and (C) Copy numbers of 16S rRNA genes specific for *Geobacter* spp. per gram soil with BES (during days 10-18) and without



BES amendment (during days 1-18 and 1-9) in the presence of s- and k-biochar with SP and LP. The BES was added at day 9. Gene copy numbers were quantified at day 9 and 18 respectively. P values were determined by Paired Student's t test. \*\*\* P < 0.001; \*\*P < 0.01, \*P < 0.05, and n.s., not significant.

#### 4.4.6 Effect of BES as Methanogenic Inhibitor on the Contribution of Acetate as Electron Donor to Methanogenesis

To evaluate the fate of electrons from acetate oxidation via syntrophy of *Geobacteraceae* and *Methanosarcina* in the presence of biochar, methanogenesis was selectively inhibited by addition of 2-bromoethanesulfonate (BES). BES was added at day 9 to the microcosms that were amended with small particle biochars and Fh. We observed that BES addition immediately stopped methane production (Fig. 3A) while Fe(II) production (Fig. 3B) and the copy numbers of *Geobacter* spp. gene were not influenced (days 10-18) (Fig. 2C and 1A). This suggests that in period 2 (days 10-18), the electron flow from acetate oxidation was controlled by the metabolism of the Fe(III)-reducers (i.e. *Geobacteraceae*). The rates and extents of acetate oxidation were significantly higher ( $p < 0.001$ ) both in small and large particles biochar-amended setups or in setups with AQDS than in non-amended setups. We compared copy numbers of the *mcrA* gene in period 1 (days 1-9) and period 2 (days 10-18). No obvious increase ( $p > 0.05$ ) in gene copy numbers of *mcrA* was detected (Fig. 2B), implying that no significant growth of methanogens occurred in period 2 (days 10-18).

The remaining acetate concentration of 0.2 mM observed around day 9 in biochar-amended setups (Fig. 4B) suggests that after this time, CH<sub>4</sub> production by acetoclastic methanogens (*Methanosarcina*) stopped due to reaching this threshold concentration of acetate (0.20±0.01 mM) that has been described before for acetoclastic methanogenic bacteria (such as *Methanosarcina*) (Jetten et al., 1990). These results suggest that in biochar-amended setups, the CH<sub>4</sub> produced after day 9 when acetoclastic methanogenesis stopped (Fig. 3B), which was likely a result of CIET from the *Geobacteraceae* to the methanogen via biochar as geoconductor. Decreased acetate concentration (after day 9, from 0.20±0.01 to 0.08±0.01 mM) supported this hypothesis in biochar-amended microcosms. Similar CH<sub>4</sub> production with conductive materials (magnetite, activated carbon, or biochar) leading to methane production has been reported in electronic syntrophy of *Geobacteraceae* and *Methanosarcina* (Chen et al., 2014, Yuan et al., 2018).

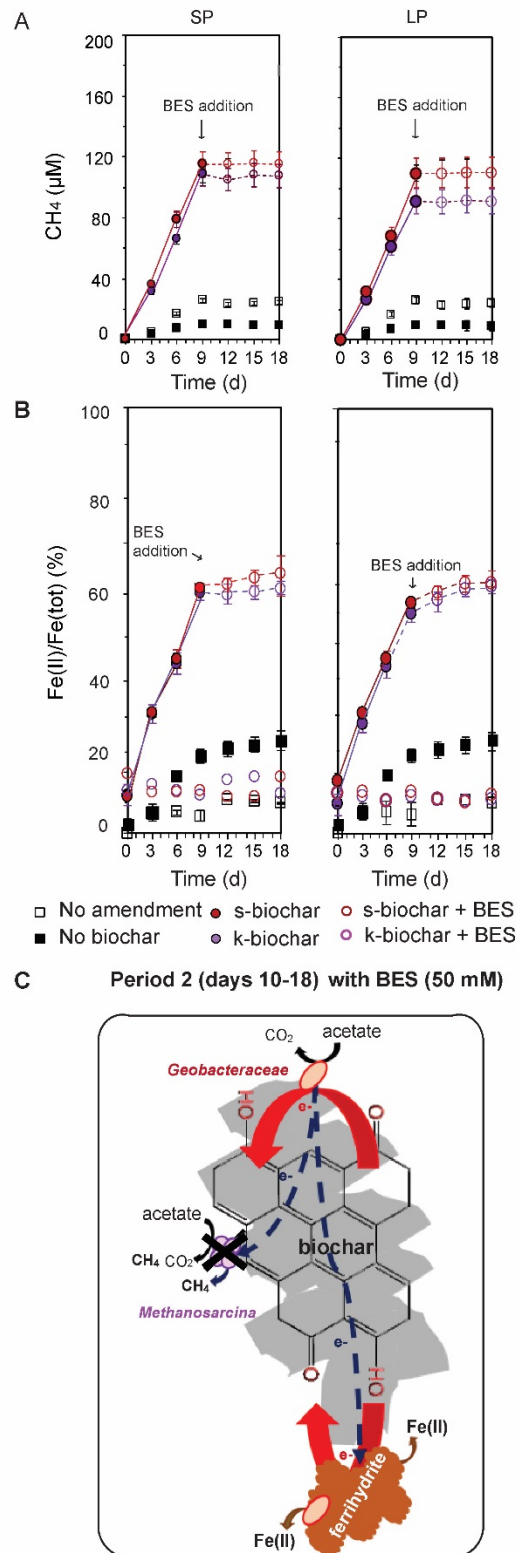


**Fig. 3.** CH<sub>4</sub> production (A) and microbial Fe(III) reduction (B) in paddy soil before and after adding a methanogenesis inhibitor (bromoethanesulfonate, BES, 50 mM). BES was added at day 9 in treatments with acetate/ferrihydrate containing either KonTiki biochar (k-biochar) or Swiss biochar (s-biochar) with large- (LP) and small-sized particles (SP) compared to microcosms containing only soil slurry (no amendments) and soil slurry amended with 1 mM acetate and 5 mM Fh (no biochar). Panel (C) shows a schematic of electron transfer pathways of biochar during the later periods of incubation (period 2;

days 10-18). After BES addition at day 9, electrons stemming from acetate metabolism by *Geobacteraceae* were still transported via biochar functioning as geobattery and geoconductor to form Fe(II). Therefore, Fe(II) production was not impacted but both CH<sub>4</sub> production by direct electron transfer via the carbon matrix of biochar and CH<sub>4</sub> production by acetoclastic methanogenesis by *Methanosarcina* were blocked (Panel A).

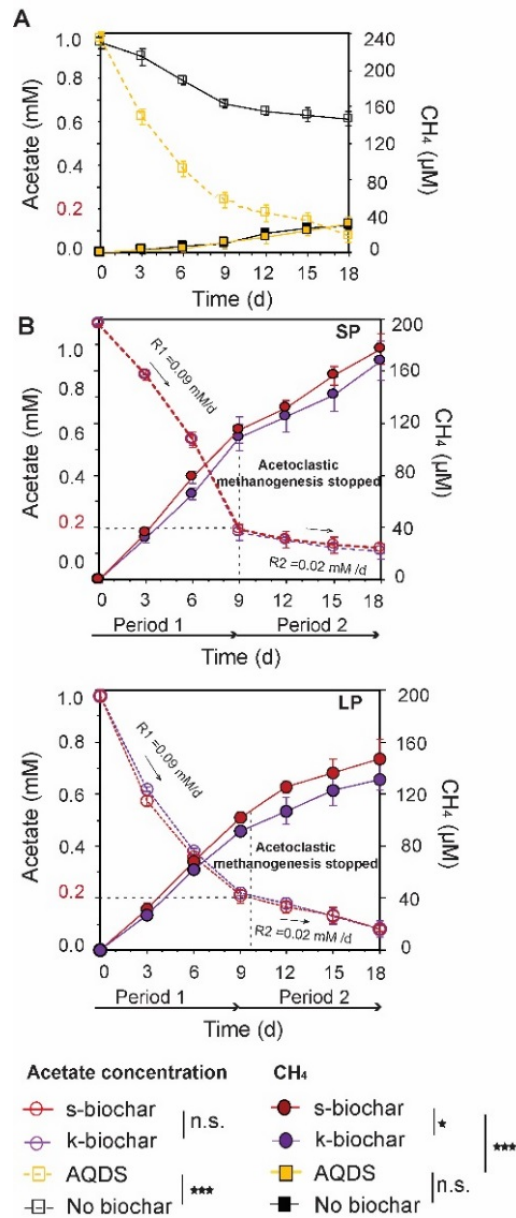


**Fig. 4.** Relationship of acetate and CH<sub>4</sub> production in different paddy soil microcosms. (A) No biochar setups were amended with soil slurry, 1 mM acetate and 5 mM Fh. AQDS setup was amended with soil slurry, 1 mM acetate, 5 mM Fh and 100 μM AQDS. (B) s-/k-biochar setups were amended with soil slurry, 1 mM acetate, and s-biochar or k-biochar with small and large-sized particles (SP and LP). The dashed lines indicate when acetoclastic methanogenesis stopped because it reached the thermodynamic acetate threshold concentration of 0.2 mM that was shown for acetoclastic methanogens such as *Methanosarcina* (Jetten et al, 1990 and 1992). P values were determined by Paired Student's t test. \*\*\* P < 0.001; \*\*P < 0.01, \*P < 0.05, and n.s., not significant.

#### 4.4.7 Implications for Altering Environmental Electron Transfer Pathways

In summary, our data has shown that without addition of biochar, microbial Fe(III) reduction is thermodynamically favored compared to methanogenesis (Fig. 5A). When Fh is depleted as terminal electron acceptor, biochar can function as geoconductor contributing to methanogenesis (Fig. 5B). Lower methanogenesis in the presence of biochar occurred when microbial Fe(III) reduction became the predominated electron accepting process (in the presence of sufficient Fe(III)) with biochar functioning as geobattery and geoconductor. With addition of Fh as Fe(III) source, the coupled function of biochar as a geobattery and geoconductor can offer a multiply electron transfer pathways for microbial Fe(III) reduction and methanogenesis. Biochar then promoted microbial Fe(III) mineral reduction through accepting and donating electrons (i.e. functioning as geobattery), and simultaneously contributed to CH<sub>4</sub> production possibly through CIET (between *Geobacteraceae* and *Methanosarcina*), functioning as geoconductor (Fig. 5D, 5E and 5G). In contrast, amendment of AQDS, which functions only as a geobattery, stimulated exclusively microbial Fe(III) reduction but did not affect CH<sub>4</sub> emissions (Fig. 4A and 5C). We estimated that 5.0-6.0% and 6.0-6.3% of the electrons from acetate oxidation were recovered as CH<sub>4</sub> in the first 9 days of incubation, in the presence of k-biochar and s-biochar, respectively (Fig. 5D, 5F, and Table S5). Afterward, when acetoclastic methanogenesis stopped, 2.0-3.2% and 2.2-3.4% of the acetate-derived electrons were transferred from *Geobacteraceae* to *Methanosarcina* through k-biochar and s-biochar, respectively, recovered as CH<sub>4</sub> (Fig. 5E 5F, Table S5). The stimulated Fe(III) reduction and CH<sub>4</sub> production were related to changes of the soil microbial community and probably its activity such as syntrophic acetate oxidation by Fe(III)-reducers and acetoclastic methanogens. The coupled function of biochar as geobattery and geoconductor may lead to long-distance electron transport either between cells and minerals or between cells and cells, both potentially relevant for CH<sub>4</sub> emission. Additionally, small biochar particles can easily aggregate with microorganisms in soil causing a fast soil microbial response. In this context, greenhouse gas mitigation by applying biochar in anoxic soil environments needs to consider the coupled electron transfer functions of biochar as well as its induced microbial responses.

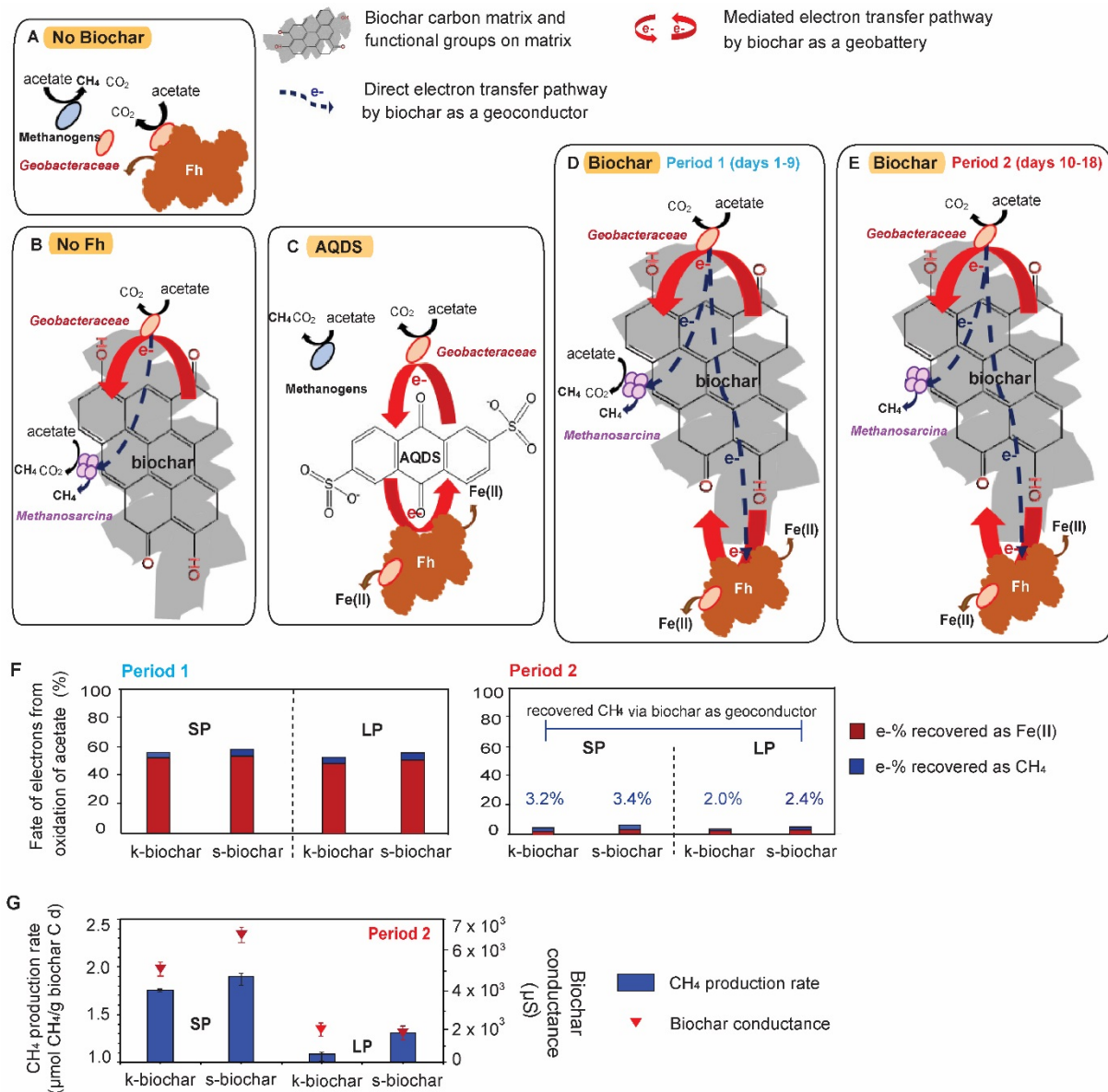


**Fig. 5.** Schematic of electron transfer pathways between Fe(III)-reducers (*Geobacteraceae*) and methanogens (acetoclastic methanogens or *Methanosarcina*) in anoxic paddy soil microcosm only amended with (A) acetate and ferrihydrite (Fh) (No biochar), (B) acetate and biochar (No Fh), (C) acetate and AQDS (AQDS), (D) acetate, Fh and biochar during period 1 (day 1-9) (biochar setup), and (E) acetate, Fh and biochar during period 2 (day 10-18) (biochar setup). Without biochar, microbial Fe(III) reduction outcompetes methanogenesis. Without Fh, biochar contributed to methanogenesis. AQDS as an electron shuttle facilitates electrons transfer between the Fe(III)-reducer and Fh suppressing methanogenesis. Biochar either mediated electron transfer between the Fe(III)-reducer and Fh or directly transferred electrons from the Fe(III)-reducer to the methanogen thus stimulating methane production. (F) Fate of electrons stemming from oxidation of acetate recovered as Fe(II) and  $\text{CH}_4$  in period 1 and 2, respectively, in the presence of Swiss biochar (s-biochar) and KonTiki biochar (k-biochar) with small and large particles (SP and LP). (G) Relationship between methane formation rates (in  $\mu\text{mol CH}_4/\text{g (biochar C}\cdot\text{d)}$ ) in period 2 and conductance of biochar (in  $\mu\text{S}$ ) in the presence of s-biochar and k-biochar with small and large particles (SP and LP).  $\text{CH}_4$  produced in period 2 (when acetoclastic

methanogenesis halted) by means of direct electron transfer via biochar as geoconductor between the Fe(III)-reducer and the methanogen.

#### 4.5 Supporting Information

The supporting information provides microbial communities' composition based on 16S rRNA gene sequencing (Fig. S1) as well as the quantification of bacterial and archaeal 16S rRNA genes, *Geobacter* spp. specific 16S rRNA genes, and *mcrA* genes based on real-time PCR (Fig. S2). Complete microbial Fe(III) reduction and methanogenesis data for microcosms amended with biochar/Fh with LP and SP biochar is shown in Fig. S3. The SI furthermore contains data on basic physical properties of the soil and biochars used (Table S1 and S2). Detailed information on experimental setups are shown in Table S3, primers and PCR conditions used for real-time PCR in Table S4. The recovery of electrons as CH<sub>4</sub> and Fe(II) in different microcosms shown in Table S5 and thermodynamic calculations shown in Table S6.

#### Acknowledgements

We gratefully acknowledge support by the China Scholarship Council Foundation (No. 201606510018) for Zhen Yang, Sara Kleindienst is funded by an Emmy-Noether fellowship (grant# 326028733) from the German Research Foundation (Deutsche Forschungsgemeinschaft; DFG). Daniel Straub is funded by the Institutional Strategy of the University of Tübingen (German Research Foundation; DFG, ZUK 63) and further supported by the Collaborative Research Center 1253 CAMPOS (German Research Foundation; DFG, Grant Agreement SFB 1253/1 2017). Largus Angenent acknowledges support by the state of Baden-Württemberg through bwHPC and the German Research Foundation (DFG) through grant no INST 37/935-1 FUGG (bwForCluster BinAC). We also thank Ellen Röhm for particle size, TOC/DOC, HPLC analysis, and Joseph G. Usack for methane analysis.

#### 4.6 References

- Achnich, C., Bak, F., Conrad, R., 1995. Competition for electron donors among nitrate reducers, ferric iron reducers, sulfate reducers, and methanogens in anoxic paddy soil. *Biology and Fertility of Soils* 19, 65-72.
- Amonette, J.E., Joseph, S., 2009. Biochar for environmental management: Characteristics of Biochar: Microchemical Properties. In: Lehmann, J., Joseph, S., (Eds.) *Biochar for environmental management: an introduction*. In *Biochar for environmental management*. Earthscan, London, 33-46.
- Amstatter, K., Borch, T., Kappler, A., 2012. Influence of humic acid imposed changes of ferrihydrite aggregation on microbial Fe(III) reduction. *Geochimica et Cosmochimica Acta* 85, 326-341.
- Bolyen, E., Rideout, J.R., Dillon, M.R., Bokulich, N.A., Abnet, C., Al-Ghalith, G.A., Alexander, H., Alm, E.J., Arumugam, M., Asnicar, F. Bai, Y., 2018. QIIME 2: Reproducible, interactive, scalable, and extensible microbiome data science (No. e27295v1). *PeerJ Preprints*.

- Bista, P., Ghimire, R., Machado, S. and Pritchett, L., 2019. Biochar Effects on Soil Properties and Wheat Biomass vary with Fertility Management. *Agronomy* 9, 623.
- Brassard, P., Godbout, S., Raghavan, V., 2016. Soil biochar amendment as a climate change mitigation tool: key parameters and mechanisms involved. *Journal of Environmental Management* 181, 484-497.
- Cayuela, M. L., Sánchez-Monedero, M. A., Roig, A., Hanley, K., Enders, A., Lehmann, J., 2013. Biochar and denitrification in soils: when, how much and why does biochar reduce N<sub>2</sub>O emissions? *Scientific Reports* 3, 1732.
- Chen, Z., Wang, Y., Jiang, X., Fu, D., Xia, D., Wang, H., Li, Q., 2017. Dual roles of AQDS as electron shuttles for microbes and dissolved organic matter involved in arsenic and iron mobilization in the arsenic-rich sediment. *Science of the Total Environment* 574, 1684-1694.
- Chen, S., Rotaru, A.E., Shrestha, P. M., Malvankar, N.S., Liu, F., Fan, W., Lovley, D. R., 2014. Promoting interspecies electron transfer with biochar. *Scientific Reports*, 4, 5019.
- Chen, S., Rotaru, A.E., Liu, F., Philips, J., Woodard, T.L., Nevin, K.P. Lovley, D.R., 2014. Carbon cloth stimulates direct interspecies electron transfer in syntrophic co-cultures. *Bioresource Technology* 173, 82-86.
- Cruz Viggì, C., Rossetti, S., Fazi, S., Paiano, P., Majone, M., Aulenta, F., 2014. Magnetite particles triggering a faster and more robust syntrophic pathway of methanogenic propionate degradation. *Environmental Science and Technology* 48, 7536-7543.
- DeLuca, T.H., Gundale, M.J., MacKenzie, M.D., Jones, D.L., 2015. Biochar effects on soil nutrient transformations. *Biochar for environmental management: science, technology and implementation* 2, 421-454.
- EBC (2012) 'European Biochar Certificate - Guidelines for a Sustainable Production of Biochar.' European Biochar Foundation (EBC), Arbaz, Switzerland. <http://www.europeanbiochar.org/en/download>. Version 8.2E of 19th April 2019, DOI: 10.13140/RG.2.1.4658.7043
- Feng, Y., Xu, Y., Yu, Y., Xie, Z., Lin, X., 2012. Mechanisms of biochar decreasing methane emission from Chinese paddy soils. *Soil Biology and Biochemistry* 46, 80-88.
- Friedman, E.S., McPhillips, L.E., Werner, J.J., Poole, A.C., Ley, R.E., Walter, M.T. Angenent, L.T., 2016. Methane emission in a specific riparian-zone sediment decreased with bioelectrochemical manipulation and corresponded to the microbial community dynamics. *Frontiers in Microbiology* 6, 1523.
- Glaser, B., Lehmann, J. and Zech, W., 2002. Ameliorating physical and chemical properties of highly weathered soils in the tropics with charcoal—a review. *Biology and fertility of soils* 35, 219-230.
- Gul, S., Whalen, J.K., 2016. Biochemical cycling of nitrogen and phosphorus in biochar-amended soils. *Soil Biology and Biochemistry* 103, 1-15.
- Hagemann, N., Kammann, C.I., Schmidt, H.P., Kappler, A., Behrens, S., 2017a. Nitrate capture and slow release in biochar amended compost and soil. *PLoS One* 12, e0171214.
- Hagemann, N., Joseph, S., Schmidt, H.P., Kammann, C.I., Harter, J., Borch, T., Kappler, A., 2017b. Organic coating on biochar explains its nutrient retention and stimulation of soil fertility. *Nature Communications* 8, 1089.
- Hansel, C.M., Benner, S.G., Fendorf, S., 2005. Competing Fe(II)-induced mineralization pathways of ferrihydrite. *Environmental Science and Technology* 39, 7147-7153.

- Harter, J., Weigold, P., El-Hadidi, M., Huson, D.H., Kappler, A., Behrens, S., 2016. Soil biochar amendment shapes the composition of N<sub>2</sub>O-reducing microbial communities. *Science of the Total Environment* 562, 379-390.
- Harter, J., Krause, H. M., Schuettler, S., Ruser, R., Fromme, M., Scholten, T., Behrens, S., 2014. Linking N<sub>2</sub>O emissions from biochar-amended soil to the structure and function of the N-cycling microbial community. *The ISME Journal* 8, 660.
- Hori, T., Müller, A., Igarashi, Y., Conrad, R., Friedrich, M.W., 2010. Identification of iron-reducing microorganisms in anoxic rice paddy soil by <sup>13</sup>C-acetate probing. *The ISME journal* 4, 267.
- Jaafar, N.M., Clode, P.L., Abbott, L.K., 2015. Soil microbial responses to biochars varying in particle size, surface and pore properties. *Pedosphere* 25, 770-780.
- Jeffery, S., Verheijen, F. G., Kammann, C., Abalos, D., 2016. Biochar effects on methane emissions from soils: a meta-analysis. *Soil Biology and Biochemistry* 101, 251-258.
- Jetten, M.S., Stams, A.J., Zehnder, A.J., 1990. Acetate threshold values and acetate activating enzymes in methanogenic bacteria. *FEMS Microbiology Ecology* 6, 339-344.
- Kappler, A., Wuestner, M. L., Ruecker, A., Harter, J., Halama, M., Behrens, S., 2014. Biochar as an electron shuttle between bacteria and Fe (III) minerals. *Environmental Science and Technology Letters* 1, 339-344.
- Kato, S., Hashimoto, K., Watanabe, K., 2012. Methanogenesis facilitated by electric syntrophy via (semi) conductive iron-oxide minerals. *Environmental microbiology* 14, 1646-1654.
- Keiluweit, M., Nico, P.S., Johnson, M.G. Kleber, M., 2010. Dynamic molecular structure of plant biomass-derived black carbon (biochar). *Environmental Science and Technology* 44, 1247-1253.
- Krause, H.M., Hueppi, R., Leifeld, J., El-Hadidi, M., Harter, J., Kappler, A., Hartmann, M., Behrens, S., Maeder, P., Hattinger, A., 2018. Biochar affects community composition of nitrous oxide reducers in a field experiment. *Soil Biology and Biochemistry* 119, 143-151.
- Klüpfel, L., Keiluweit, M., Kleber, M., Sander, M., 2014. Redox properties of plant biomass-derived black carbon (biochar). *Environmental Science and Technology* 48, 5601-5611.
- Kögel-Knabner, I., Amelung, W., Cao, Z., Fiedler, S., Frenzel, P., Jahn, R., Schloter, M., 2010. Biogeochemistry of paddy soils. *Geoderma* 157, 1-14.
- Lehmann, J., Rillig, M. C., Thies, J., Masiello, C.A., Hockaday, W.C., Crowley, D., 2011. Biochar effects on soil biota—a review. *Soil biology and biochemistry* 43, 1812-1836.
- Li, H., Chang, J., Liu, P., Fu, L., Ding, D., Lu, Y., 2015. Direct interspecies electron transfer accelerates syntrophic oxidation of butyrate in paddy soil enrichments. *Environmental Microbiology* 17, 1533-1547.
- Liu, Y., Yang, M., Wu, Y., Wang, H., Chen, Y., Wu, W., 2011. Reducing CH<sub>4</sub> and CO<sub>2</sub> emissions from waterlogged paddy soil with biochar. *Journal of Soils and Sediments* 11, 930-939.
- Liu, F., Rotaru, A.E., Shrestha, P.M., Malvankar, N.S., Nevin, K.P., Lovley, D.R., 2012. Promoting direct interspecies electron transfer with activated carbon. *Energy and Environmental Science* 5, 8982-8989.
- Lin, R., Cheng, J., Ding, L. and Murphy, J.D., 2018. Improved efficiency of anaerobic digestion through direct interspecies electron transfer at mesophilic and thermophilic temperature ranges. *Chemical Engineering Journal*, 350, 681-691.



- Lovley, D.R., Phillips, E.J., 1987. Competitive mechanisms for inhibition of sulfate reduction and methane production in the zone of ferric iron reduction in sediments. *Applied Environmental Microbiology* 53, 2636-2641.
- Miller, K.E., Lai, C.T., Friedman, E.S., Angenent, L.T. Lipson, D.A., 2015. Methane suppression by iron and humic acids in soils of the Arctic Coastal Plain. *Soil Biology and Biochemistry* 83, 176-183.
- Minami, K., Neue, H.U., 1994. Rice paddies as a methane source. *Climatic Change* 27, 13-26.
- Mukherjee, A., Lal, R., 2013. Biochar impacts on soil physical properties and greenhouse gas emissions. *Agronomy* 3, 313-339.
- Martin, M., 2011. Cutadapt removes adapter sequences from high-throughput sequencing reads. *EMBnet. Journal* 17, 10-12.
- Neue, H.U., 1997. Fluxes of methane from rice fields and potential for mitigation. *Soil Use and Management* 13, 258-267.
- Oh, S.Y., Son, J.G., Lim, O.T., Chiu, P.C., 2012. The role of black carbon as a catalyst for environmental redox transformation. *Environmental Geochemistry and Health* 34, 105-113.
- PrévotEAU, A., Ronsse, F., Cid, I., Boeckx, P., Rabaey, K., 2016. The electron donating capacity of biochar is dramatically underestimated. *Scientific Reports* 6, 32870.
- Pruesse, E., Quast, C., Knittel, K., Fuchs, B.M., Ludwig, W., Peplies, J. Glöckner, F.O., 2007. SILVA: a comprehensive online resource for quality checked and aligned ribosomal RNA sequence data compatible with ARB. *Nucleic Acids Research* 35, 7188-7196.
- Roden, E.E., Wetzel, R.G., 2003. Competition between Fe(III)-reducing and methanogenic bacteria for acetate in iron-rich freshwater sediments. *Microbial Ecology*, 45, 252-258.
- Rotaru, A.E., Shrestha, P.M., Liu, F., Markovaitė, B., Chen, S., Nevin, K.P., Lovley, D.R., 2014. Direct interspecies electron transfer between *Geobacter metallireducens* and *Methanosarcina barkeri*. *Applied Environmental Microbiology* 80, 4599-4605.
- Schulze, E.D., Luysaert, S., Ciais, P., Freibauer, A., Janssens, I.A., Soussana, J.F., Heimann, M., 2009. Importance of methane and nitrous oxide for Europe's terrestrial greenhouse-gas balance. *Nature Geoscience* 2, 842.
- Schwietzke, S., Sherwood, O. A., Bruhwiler, L. M., Miller, J. B., Etiope, G., Dlugokencky, E. J., Tans, P. P., 2016. Upward revision of global fossil fuel methane emissions based on isotope database. *Nature* 538, 88.
- Sun, T., Levin, B.D., Guzman, J.J., Enders, A., Muller, D.A., Angenent, L.T., Lehmann, J., 2017. Rapid electron transfer by the carbon matrix in natural pyrogenic carbon. *Nature communications*, 8,14873.
- Sun, T., Levin, B. D., Schmidt, M. P., Guzman, J. J., Enders, A., Martínez, C. E., Muller, D.A., Angenent, L.T., Lehmann, J., 2018. Simultaneous quantification of electron transfer by carbon matrices and functional groups in pyrogenic carbon. *Environmental Science and Technology* 52, 8538-8547.
- Singh, B.K., Bardgett, R.D., Smith, P., Reay, D.S., 2010. Microorganisms and climate change: terrestrial feedbacks and mitigation options. *Nature Reviews Microbiology* 8, 779.
- Stookey, L.L., 1970. Ferrozine---a new spectrophotometric reagent for iron. *Analytical Chemistry* 42, 779-781.

- Straub, D., Blackwell, N., Fuentes, A.L., Peltzer, A., Nahnsen, S., Kleindienst, S., 2019. Interpretations of microbial community studies are biased by the selected 16S rRNA gene amplicon sequencing pipeline. *bioRxiv*.
- Tan, W., Li, R., Yu, H., Zhao, X., Dang, Q., Jiang, J., Xi, B., 2018. Prominent Conductor Mechanism-Induced Electron Transfer of Biochar Produced by Pyrolysis of Nickel-Enriched Biomass. *Catalysts* 8, 573.
- Tremblay, P.L., Angenent, L.T., Zhang, T., 2017. Extracellular electron uptake: among autotrophs and mediated by surfaces. *Trends in biotechnology*, 35, 360-371.
- Teh, Y.A., Dubinsky, E.A., Silver, W.L., Carlson, C.M., 2008. Suppression of methanogenesis by dissimilatory Fe (III)-reducing bacteria in tropical rain forest soils: Implications for ecosystem methane flux. *Global Change Biology* 14, 413-422.
- Van Groenigen, K. J., Osenberg, C.W., Hungate, B. A., 2011. Increased soil emissions of potent greenhouse gases under increased atmospheric CO<sub>2</sub>. *Nature* 475, 214.
- Walter, K.M., Zimov, S.A., Chanton, J.P., Verbyla, D., Chapin, F. S., 2006. Methane bubbling from Siberian thaw lakes as a positive feedback to climate warming. *Nature* 443, 71.
- Wu, S., Fang, G., Wang, Y., Zheng, Y., Wang, C., Zhao, F., Zhou, D., 2017. Redox-active oxygen-containing functional groups in activated carbon facilitate microbial reduction of ferrihydrite. *Environmental Science and Technology* 51, 9709-9717.
- Woolf, D., Amonette, J.E., Street-Perrott, F.A., Lehmann, J., Joseph, S., 2010. Sustainable biochar to mitigate global climate change. *Nature Communications* 1, 56.
- Xiao, L., Liu, F., Liu, J., Li, J., Zhang, Y., Yu, J., Wang, O., 2018. Nano-Fe<sub>3</sub>O<sub>4</sub> particles accelerating electromethanogenesis on an hour-long timescale in wetland soil. *Environmental Science: Nano* 5, 436-445.
- Xu, W., Pignatello, J.J., Mitch, W.A., 2013. Role of black carbon electrical conductivity in mediating hexahydro-1,3,5-trinitro-1,3,5-triazine (RDX) transformation on carbon surfaces by sulfides. *Environmental Science and Technology* 47, 7129-7136.
- Yang, S.S., Chang, H.L., 1998. Effect of environmental conditions on methane production and emission from paddy soil. *Agriculture, Ecosystems and Environment* 69, 69-80.
- Yang, Z., Sun, T., Subdiaga, E., Obst, M., Haderlein, S.B., Maisch, M., Kretzschmar, R., Angenent, L.T., Kappler, A., 2019. Aggregation-dependent electron transfer via redox-active biochar particles stimulate microbial ferrihydrite reduction. *Science of The Total Environment*, 135515.
- Yu, L., Yuan, Y., Tang, J., Wang, Y., Zhou, S., 2015. Biochar as an electron shuttle for reductive dechlorination of pentachlorophenol by *Geobacter sulfurreducens*. *Scientific Reports* 5, 16221.
- Yu, L., Tang, J., Zhang, R., Wu, Q., Gong, M., 2013. Effects of biochar application on soil methane emission at different soil moisture levels. *Biology and Fertility of Soils* 49, 119-128.
- Yuan, Y., Bolan, N., PrévotEAU, A., Vithanage, M., Biswas, J. K., Ok, Y.S., Wang, H., 2017. Applications of biochar in redox-mediated reactions. *Bioresource Technology* 246, 271-281.
- Yuan, H.Y., Ding, L.J., Zama, E.F., Liu, P.P., Hozzein, W.N., Zhu, Y.G., 2018. Biochar modulates methanogenesis through electron syntrophy of microorganisms with ethanol as a substrate. *Environmental Science and Technology* 52, 12198-12207.

Zhu, X., Chen, B., Zhu, L., Xing, B., 2017. Effects and mechanisms of biochar-microbe interactions in soil improvement and pollution remediation: a review. *Environmental Pollution* 227, 98-115.

Zhou, G.W., Yang, X.R., Marshall, C.W., Li, H., Zheng, B.X., Yan, Y., Zhu, Y.G., 2017. Biochar addition increases the rates of dissimilatory iron reduction and methanogenesis in ferrihydrite enrichments. *Frontiers in Microbiology* 8, 589.

Zhang, C., Zhang, N., Xiao, Z., Li, Z., Zhang, D., 2019. Characterization of biochars derived from different materials and their effects on microbial dechlorination of pentachlorophenol in a consortium. *RSC Advances* 9, 917-923.

## SUPPORTING INFORMATION

---

### **Coupled Function of Biochar as Geobattery and Geoconductor Alters Microbial Community Composition and Electron Transfer Pathways in a Paddy Soil**

Zhen Yang<sup>1</sup>, Tianran Sun<sup>2</sup>, Sara Kleindienst<sup>3</sup>, Daniel Straub<sup>3,4</sup>, Ruben Kretzschmar<sup>5</sup>, Lergus T. Angenent<sup>2</sup>, Andreas Kappler<sup>1\*</sup>

<sup>1</sup>*Geomicrobiology, Center for Applied Geoscience, Tuebingen, 72076, Germany*

<sup>2</sup>*Environmental Biotechnology, Center for Applied Geoscience, Tuebingen, 72076, Germany*

<sup>3</sup>*Microbial Ecology, Center for Applied Geoscience, Tuebingen, 72076, Germany*

<sup>4</sup>*Quantitative Biology Center (QBiC), Tuebingen, 72076, Germany*

<sup>5</sup>*Soil Chemistry Group, Institute of Biogeochemistry and Pollutant Dynamics, CHN, ETH Zurich, 8092 Zurich, Switzerland*

Number of figures in supporting information: 4

Number of tables in supporting information: 6

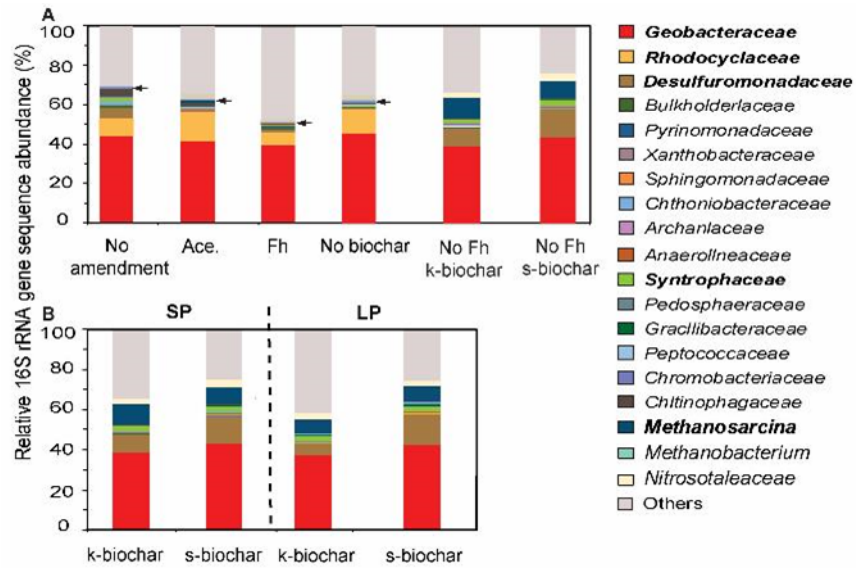


**Fig. S1.** Microbial community composition based on 16S rRNA gene sequence abundance (%) in anoxic paddy soil after an 18-day incubation in different setups (A) with either only paddy soil incubated without amendments (no amendment), amended with 1 mM acetate (Ace.), amended with 5 mM ferrihydrite (Fh), amended with 1 mM acetate and 5 mM Fh without biochar (no biochar), and amended with 1 mM Ace, Swiss biochar (s-biochar, 5 g/L) and KonTiki biochar (k-biochar, 5 g/L) without Fh or (B) with Ace. , Fh and two different types of biochar. For the biochar setups we used s-biochar and k-biochar to achieve final biochar/Fh ratios of 1.0 g biochar/mmol Fe with different particle sizes of biochar (SP = small particle biochar; LP = large particle biochar). Arrows in Fig. S1A point towards *Methanosarcina* in incubation setups without biochar.

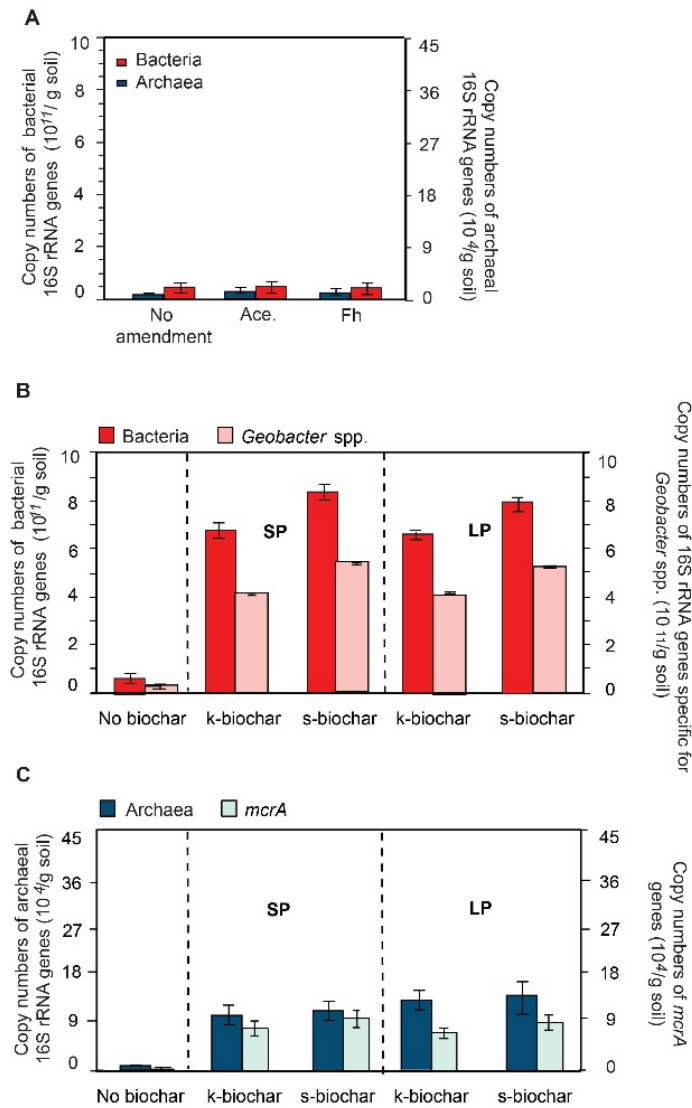


**Fig. S2.** (A) Copy numbers of bacterial and archaeal 16S rRNA genes and (B) Copy numbers of 16S rRNA genes specific for *Geobacter* spp. and copy numbers of *mcrA* genes after 18 days of incubation from setups with 1 mM acetate and 5 mM ferrihydrite (no biochar) soil microcosms and microcosms with large-sized particles (LP) and small-sized particles (SP) biochar. For the biochar setups, we used Swiss biochar (s-biochar) and KonTiki biochar (k-biochar) at biochar/ Fh ratios of 1.0 g/mmol Fe.

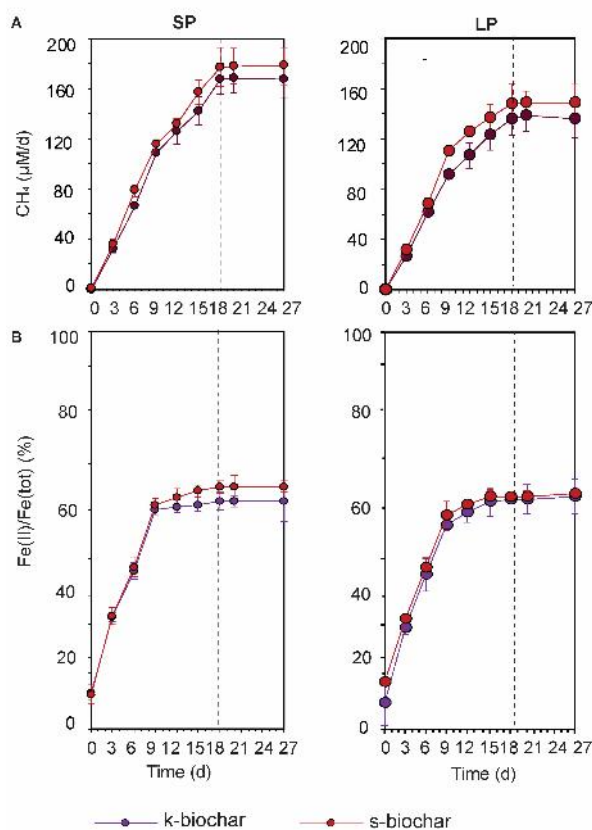


**Fig. S3.** Microbial Fe(III) reduction (A) and CH<sub>4</sub> production (B) in paddy soil over 27 days of incubation. Small and large particle biochar (SP and LP) are shown in the left and right panel, respectively.

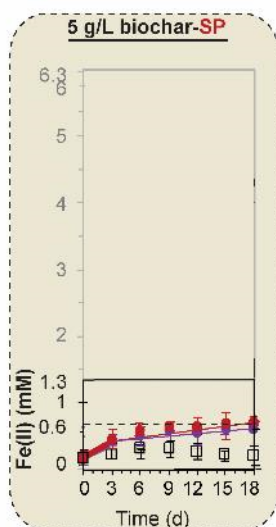


**Fig. S4.** Influence of small-particle size (SP) biochar on Fe(III) reduction in microcosm amended without Fh. The 'No Fh + s- (k-)biochar' setups were amended with acetate, s-biochar or k-biochar with SP, respectively. Calculated approximately 1.3 mM Fe(III) in initial soil per setup.

**Table S1.** Main elemental composition and properties of the paddy soil used for the microcosm experiments.

Soil pH <sup>1</sup>	TOC g/kg	C <sup>2</sup> g/kg	N g/kg	Fe g/kg	Fe(II) <sup>3</sup> mmol
6.9 ± 0.1	14.0 ± 0.1	15.7	0.80	2.01	0.002

<sup>1</sup>Soil pH was measured in deionized water.

<sup>2</sup>'C' content refers to total carbon element content including inorganic and organic carbon in soil.

<sup>3</sup>Fe(II) was measured using 1 M HCl.

**Table S2.** Properties of small particle-sized (SP) and large particle-sized (LP) of Swiss biochar (s-biochar) and KonTiki biochar (k-biochar).

Biochar samples	Particle size distribution	SSA <sup>1</sup>	Surface area of amendment in exp. <sup>2</sup> (m <sup>2</sup> )	TOC (%)	EEC <sup>3</sup> (meq e <sup>-</sup> /g C)	Conductance <sup>4</sup> (μS)
s-biochar	LP, 50-100 μm	201	25	71	1.02	2.0 × 10 <sup>3</sup>
	SP, minor fraction 0.1-0.3 μm <sup>5</sup>	258	32	72	1.01	6.6 × 10 <sup>3</sup>
	Main fraction 5-20 μm <sup>5</sup>					
k-biochar	LP, 50-100 μm	107	25	77	0.71	1.5 × 10 <sup>3</sup>
	SP, minor fraction 0.1-0.5 μm <sup>5</sup>	118	27	74	0.71	2.5 × 10 <sup>3</sup>
	Main fraction 5-20 μm <sup>5</sup>					
Ferrihydrite <sup>6</sup>			5			

<sup>1</sup>Specific surface area (SSA) of biochar determined by BET at 77K.

<sup>2</sup>Surface area of biochar in experiments calculated from specific surface area of biochar multiply 1.25 × 10<sup>-1</sup> g biochar used in 5 g/L biochar in 2.5 × 10<sup>-2</sup> L solution.

<sup>2</sup>EEC of biochar is electron exchange capacity of biochar, which is sum of measured electron accepting capacity and electron donating capacity of biochar by electrochemical analysis.

<sup>4</sup>Conductivity was measured a dried powder. Conductance calculation took 1 cm length of the dried powder put into a plastic syringe tube into consideration. Conductivity (i.e., the number of transferred electrons per unit area) was unchanged between large and small particle sizes from the same type of biochar. The conductance changed because it depends on the surface area of biochar between small and large particle sizes.

<sup>5</sup>Minor faction refers to 5%-10% of volume distribution and main fraction refers to 90-95% of volume number.

<sup>6</sup>Surface area of ferrihydrite (Fh, Fe(OH)<sub>3</sub>) in experiments calculated from specific area of Fh (363 m<sup>2</sup>/g) multiply 0.013 g Fh used in 5 mM Fh in 2.5 × 10<sup>-2</sup> L solution.



**Table S3.** Detailed information on microcosm setups amended with acetate (Ace.), ferrihydrite (Fh) in the presence and absence of Swiss biochar (s-biochar) and KonTiki biochar (k-biochar) with small-sized particles (SP) and large-sized particles (LP).

	Soil slurry	Acetate (mM)	Ferrihydrite (mM)	Biochar concentration <sup>1</sup> (g/L)	Biochar Particle size
No amendment	Non-sterilized	-	-	-	-
No biochar	Non-sterilized	1	5	-	-
No Fh	Non-sterilized	1	-	5	SP
k-biochar	Non-sterilized	1	5	5	SP
s-biochar	Non-sterilized	1	5	5	SP
k-biochar	Non-sterilized	1	5	5	LP
s-biochar	Non-sterilized	1	5	5	LP
k-biochar	Gamma-sterilized	1	5	5	SP
s-biochar	Gamma-sterilized	1	5	5	SP
k-biochar	Gamma-sterilized	1	5	5	LP
s-biochar	Gamma-sterilized	1	5	5	LP
Acetate control	Non-sterilized	1	-	-	-
Ferrihydrite control	Non-sterilized	-	5	-	-

<sup>1</sup>Since biochar is chemically recalcitrant and mostly resistant to microbial degradation (Lehmann et al., 2011; Deluca et al., 2015), biochar is not expected to serve to a large extent as organic carbon and electron source for microbial Fe(III) reduction and methanogenesis in our setups.

**Table S4.** List of primers, primers sequences and thermal programs used for quantification of bacterial and archaeal 16S rRNA gene, *Geobacter* spp. specific genes and methyl-coenzyme M reductase subunit alpha (*mcrA*) gene copy numbers.

	<b>bacterial 16S rRNA genes</b>	<b>archaeal 16S rRNA genes</b>	<b><i>Geobacter</i> spp. specific genes</b>	<b><i>mcrA</i> genes</b>
Primers	341F (CCTACGGGAGGCAGCAG) 797R (GGACTACCAGGGTATCTAATCCTGTT)	ar109F (ACKGCTCAGTAACACGT) ar915R (GTGCTCCCCGCCAATTCCT)	577F (GCGTGTAGGCGGTTTSTTAA) 822R (TACCCGCRACACCTAGTACT)	mcr-ME1F (GCMATGCARATHGGWATGTC) mcr-ME2R (TCATKGCRTAGTTDGGRTAGT)
Thermal cycling conditions	98°C 2 min 98°C 5s 60°C 12s } 40 cycles 95°C 1 min 60°C 1 min 50°C 10s	98°C 3 min 98°C 5 s 52°C 10 s 72°C 15 s } 40 cycles 98°C 1 min 52°C 1 min 52 – 95°C 10s	95°C 3 min 95°C 30s 55°C 20s 72°C 30s } 40 cycles 55°C 30s 81 cycles	94°C 2 min 94°C 30 s 50°C 1 min 94°C 1 min 50°C 1 min 50°C 10 s } 30 cycles

**Table S5.** Fate of electrons stemming from microbial acetate oxidation (1 mM) that were recovered as Fe(II) and CH<sub>4</sub>, during different periods of incubation (period 1 between days 1-9 and period 2 between days 10-18), in different microcosms with soil slurry amended with 1 mM acetate, 5 mM Fh, and 100 μM AQDS (AQDS setups), and with 1 M acetate, 5 mM Fh and 5 g/L Swiss biochar (s-biochar) or KonTiki biochar (k-biochar). For the biochar setups we used small particle size (SP) and large particle size (LP) biochar at biochar:Fh ratio of 1.0 g/mmol Fe (k-biochar and s-biochar setups). The acetate concentration was determined at day 9 and day 18, respectively.

Samples	Acetate addition	Acetate remaining	Acetate consumed	Acetate consumed in exp. <sup>1</sup>	Fe <sup>2+</sup> formation in exp. <sup>2*</sup>	CH <sub>4</sub> production in exp. <sup>3</sup>	Electrons from acetate oxidation <sup>4</sup>	Electrons used for Fe <sup>2+</sup> production	Electrons used for CH <sub>4</sub> production	Electron recovery as Fe <sup>2+</sup> during days 1-9 based on total number of electrons <sup>5</sup>	Electron recovery as CH <sub>4</sub> during days 1-9 <sup>6</sup>	Electron recovery as Fe <sup>2+</sup> during days 10-18 <sup>7</sup>	Electron recovery as CH <sub>4</sub> during days 10-18 <sup>8</sup>
	(mM)	(mM)	(mM)	(mmol)	(mmol)	(μmol)	(meq e <sup>-</sup> )	(meq e <sup>-</sup> )	(meq e <sup>-</sup> )	(%)	(%)	(%)	(%)
AQDS (day 9)	1.00	0.21	0.79	0.020	0.10	0.40	0.158	0.102	0.002	55.16	0.9		
k-biochar-SP (day 9)	1.00	0.18	0.82	0.021	0.09	2.72	0.164	0.099	0.011	53.5	6.8		
s-biochar-SP (day 9)	1.00	0.19	0.81	0.020	0.10	2.88	0.162	0.101	0.012	54.8	6.3		
k-biochar-LP (day 9)	1.00	0.22	0.78	0.020	0.09	2.29	0.156	0.092	0.009	49.9	5.0		
s-biochar-LP (day 9)	1.00	0.21	0.79	0.020	0.10	2.65	0.158	0.095	0.011	51.2	6.0		
AQDS (day 18)	1.00	0.08	0.92	0.023	0.11	0.96	0.184	0.114	0.005			6.5	1.8
k-biochar-SP (day 18)	1.00	0.08	0.92	0.023	0.10	4.18	0.184	0.100	0.017			2.3	3.2
s-biochar-SP (day 18)	1.00	0.08	0.92	0.023	0.11	4.43	0.184	0.106	0.018			4.4	3.4
k-biochar-LP (day 18)	1.00	0.08	0.92	0.023	0.10	3.39	0.184	0.099	0.013			2.9	2.0
s-biochar-LP (day 18)	1.00	0.08	0.92	0.023	0.10	3.69	0.184	0.101	0.015			3.8	2.2

<sup>1</sup>Acetate consumed (mmol) was calculated from the concentrations of acetate consumed (mM) that is the difference between acetate addition and remaining acetate at day 9 or day 18 multiplied by the solution volume of the experiment ( $2.5 \times 10^{-2}$  L).

<sup>2</sup>Fe(II) formed (mmol) was calculated from Fe(II) formation during the microbial Fh reduction experiment (Fe(II) in mM) multiplied by the solution volume of the experiment ( $2.5 \times 10^{-2}$  L).

<sup>3</sup>CH<sub>4</sub> production (μmol) was calculated from CH<sub>4</sub> quantified in the headspace (CH<sub>4</sub> in ppm) by GC according to the Ideal Gas Law multiplied by the headspace volume of the bottle ( $2.5 \times 10^{-2}$  L).

\*Dissolved methane has not been taken into consideration in the current study due to an extremely low Ostwald coefficient (L is a common measure of gas solubility) of CH<sub>4</sub> with 0.03607 (T=298.15 K, partial gas pressure is 1 atm) reported by Wilhelm et al. (1977). This means that only 3.6% of the dissolved methane is in solution vs 96.4% of the methane is in the headspace. Considering the maximum methane detected in the headspace (177 μM converted from 4.3 ppb CH<sub>4</sub> detected by GC according to The Ideal Gas Law in biochar-amended setups), the calculated dissolved methane would be 6 μM which is even far less than the 70 μM that we measured in the microcosms without amendment. Additionally, several previous studies of methane emission in the presence of biochar demonstrated that dissolved methane concentrations are low and can be ignored.

<sup>4</sup>The numbers of electrons stemming from oxidation of acetate are based on the following equation:  $\text{CH}_3\text{COO}^- + 8\text{Fe}^{3+} + 4\text{H}_2\text{O} = 8\text{Fe}^{2+} + 2\text{HCO}_3^- + 9\text{H}^+$

<sup>5,7</sup>Electrons recovered as Fe(II) (%) in our experiments ( $2.5 \times 10^{-2}$  L) during the days 1-9 and days 10-18 in the presence or absence of biochar, are calculated as a ratio of the experimentally determined Fe(II) formation (mmol) from the microbial Fh reduction experiment to the theoretically (maximum) formed Fe(II) based on the total number of electrons released from microbial acetate oxidation (day 18).

<sup>6,8</sup>Electrons recovered as CH<sub>4</sub> in the headspace of the bottle ( $2.5 \times 10^{-2}$  L) during the days 1-9 and days 10-18 in the presence or absence of biochar, are calculated as a ratio of the calculated CH<sub>4</sub> formation (mmol) from methanogenesis to the theoretically (maximum) formed CH<sub>4</sub> based on the total number of electrons released from microbial acetate oxidation (day 18).

**Table S6.** Gibbs free energy of reactions regarding Fe(III) reduction and methanogenesis in the presence and absence of AQDS or biochar.

Table A	Half Reaction	n	F (col/mol)	E <sub>H</sub> <sup>0'</sup> (V) <sup>2</sup>	Reference
1	$\text{Fe}(\text{OH})_3^1 + \text{e}^- + 3\text{H}^+ \rightarrow \text{Fe}^{2+}(\text{aq}) + 3\text{H}_2\text{O}$	1	96.485	0	Thamdrup, 2000
2	$2\text{CO}_2 + 8\text{H}^+ + 8\text{e}^- \rightarrow \text{CH}_3\text{COOH} + 2\text{H}_2\text{O}$	8	96.485	-0.29	
3	$\text{CO}_2 + 8\text{e}^- + 8\text{H}^+ \rightarrow \text{CH}_4 + 2\text{H}_2\text{O}$	8	96.485	-0.24	

Table B	Reaction	ΔG <sup>0'</sup> (kJ/mol <sub>CH<sub>3</sub>COOH</sub> )	ΔG <sup>0'</sup> (kJ/mol <sub>Fe(OH)<sub>3</sub></sub> )	ΔG <sup>0'</sup> (kJ/mol <sub>CH<sub>4</sub></sub> )
4	$8\text{Fe}(\text{OH})_3 + 16\text{H}^+ + \text{CH}_3\text{COOH} = 8\text{Fe}^{2+}(\text{aq}) + 2\text{CO}_2 + 22\text{H}_2\text{O}$	-224	-28	-
5	$\text{CH}_3\text{COOH} = \text{CO}_2 + \text{CH}_4$	-38.6	-	-38.6
6	$4\text{H}_2 + \text{CO}_2 = \text{CH}_4 + 2\text{H}_2\text{O}$	-	-	-131.0

<sup>1</sup>Fe(OH)<sub>3</sub> formula refers to ferrihydrite.

<sup>2</sup>E<sub>h</sub><sup>0'</sup> is reduction potentials at pH 7 and vs SHE (E<sub>h</sub><sup>0'</sup>).

**References:**

Ma, Y., Xu, J., Wei, Q., Yang, S., Liao, L., Chen, S., Liao, Q. 2017. Organic carbon content and its liable components in paddy soil under water-saving irrigation. *Plant, Soil and Environment*, 63(3), 125-130.

Wilhelm, E., Battino, R., Wilcock, R. J. 1977. Low-pressure solubility of gases in liquid water. *Chemical reviews*, 77(2), 219-262.

Zeng, F., Ali, S., Zhang, H., Ouyang, Y., Qiu, B., Wu, F., Zhang, G. 2011. The influence of pH and organic matter content in paddy soil on heavy metal availability and their uptake by rice plants. *Environmental pollution*, 159(1), 84-86.

Thamdrup, B., 2000. Bacterial manganese and iron reduction in aquatic sediments. In: Schink, B. (Ed.), *Advances in Microbial Ecology*. Kluwer Academic/Plenum Publishers, New York.

## Discussion and outlook

Biochar, carbon-rich material, is made intentionally by biomass pyrolysis. Biochar contains redox-active functional groups (mainly quinone and phenol groups) (Keiluweit et al., 2010) and conductive polyaromatic carbon ring structures in the carbon matrices (Xu et al., 2013). Charge and discharge cycles of biochar surface functional groups, such as quinone/hydroquinone pairs, been shown to serve as a 'geobattery' that can reversibly accept and donate electrons (Lovely et al., 1998; Kappler et al., 2014). In contrast to the known geobattery mechanism of surface functional groups, interface electron transfer by biochar carbon matrices as 'geoconductor' is proposed by a recent study (Sun et al., 2017; Sun et al., 2018), which directly transfers electrons that are generated or consumed by surface electrochemical reaction elsewhere. It has been demonstrated that a transition from a mediated electron transfer exclusively by quinone groups to a direct electron transfer dominated by carbon matrices is a result of greater graphite structures caused by an increase of pyrolysis temperature (Sun et al., 2018). In the temperature range of 600-700°C, similar kinetic performance is demonstrated between the geoconductor and geobattery mechanisms. More ordered carbon structures in high-temperature pyrogenic carbons created a rapid pathway that conducted electron transfer more than three times faster than the redox cycles of the geobattery mechanism. However, little is known about whether electron transfer mechanisms of biochar impact electron transfer between microorganisms and Fe(III) minerals, especially in iron-rich paddy soil environment.

Additionally, biochar is a favorable habitat for many microorganisms and changes of microbial community and activity are more pronounced by addition of high temperature ( $\geq 700^\circ\text{C}$ ) biochar. Before microbial colonization, the access or attachment to biochar is probably the rate-limiting step for electron transfer considering its a competition between microbes and Fe(III) minerals. To this end, this thesis discusses aggregation-dependence of electron transfer via biochar, its impact on microbial Fe(III) reduction and its effects on greenhouse gas emission (e.g.  $\text{CH}_4$ ) and iron mineral biogeochemistry once applied this biochar to a paddy soil.

### **Coupled functions of biochar as geobattery and geoconductive between Fe(III)-reducing bacteria and Fe(III) minerals**

The results of the studies presented herein provided detailed information about the important role of biochar as geobattery and geoconductor between Fe(III)-reducing bacteria (e.g. *Shewanella oneidensis* MR-1) and a poorly soluble Fe(III) mineral (e.g. ferrihydrite). Wood-derived biochars produced by pyrolysis at 700°C used in this study have a capacity of either transferring electrons by charge and discharging cycles via surface functional groups

(geobattery) or by directly transferring electrons via polyaromatic carbon matrices (geoconductor). Although biochar has been suggested to function as an electron shuttle to facilitate electron transfer and stimulate microbial ferrihydrite (Fh) reduction. Lower concentrations of biochar result in a lower rate and extent of microbial Fe(III) reduction compared to direct microbial Fe(III) reduction (Kappler et al., 2014). Chapter 3 in this study prove that stimulation of microbial Fe(III) reduction is dependent on a high ratio of biochar:Fh and small particle size of biochar. This stimulation of microbial Fe(III) reduction is related to a close aggregation of cells, biochar and Fh (a high extent of aggregation) (Chapter 3).

Overall, at small biochar particle size and high biochar:Fh ratios, the biochar, MR-1 cells and Fh closely aggregated, therefore addition of biochar stimulated electron transfer and microbial Fh reduction. In contrast, large biochar particles and low biochar/Fh ratios inhibited the electron transfer and Fe(III) reduction due to the lack of effective aggregation. These results suggest that for stimulating Fh reduction, a certain biochar particle size and biochar/Fh ratio are needed to form a close aggregation of all phases. The reason behind this observation is that a close aggregation of cells, biochar and Fh favors electron transfer from cells to Fh via redox cycling of the electron donating and accepting functional groups of biochar and via direct electron transfer through conductive biochar carbon matrices (Fig. 1). The results shown in this thesis improve our understanding of electron transfer between microorganisms and Fe(III) minerals via redox-active biochar and help to evaluate the impact of biochar on electron transfer processes in the environment.

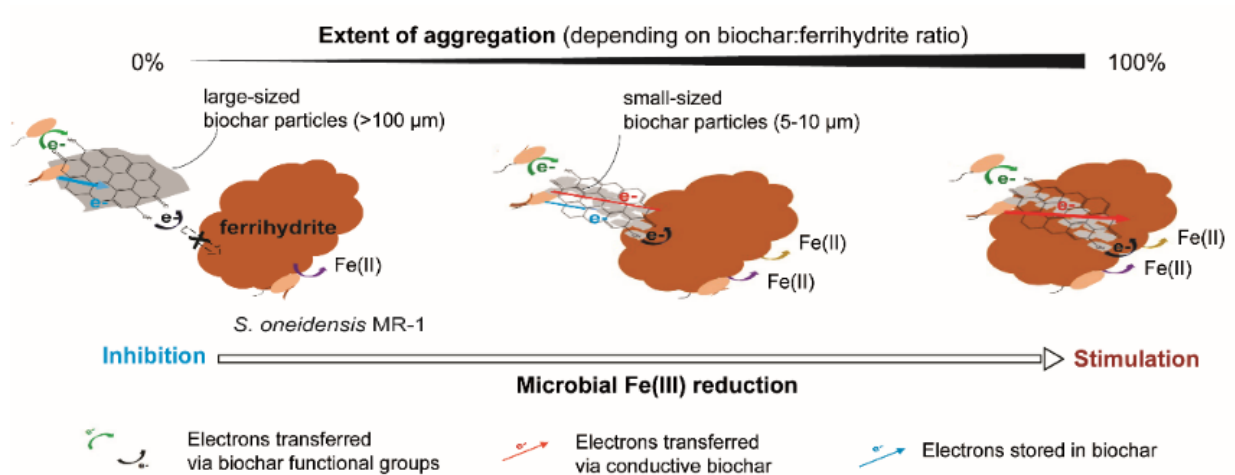


**Fig. 1.** Electron transfer pathways between *S. oneidensis* MR-1 cells and ferrihydrite (Fh) in the presence of biochar particles depending on the extent of aggregation of biochar and Fh. When Fh as electron acceptor is not close to the biochar (i.e. the extent of aggregation of biochar to Fh is close to 0%), electrons released from microbial lactate oxidation can be accepted by functional groups (quinones) of biochar or can be stored in biochar by the capacitance of carbon matrices. In this case, Fh reduction is only possible by cells directly associated with the Fh. With increasing extent of aggregation of biochar with Fh, the electrons start to be transferred to Fh by both electron donation of the hydroquinone groups and direct electron transfer by the carbon matrices, so that more and more Fe(II) will be produced.



### **Potential factors influencing the aggregation of cells, biochar and Fh**

The results in this thesis (Chapter 3) showed that although biochar and cells both have a negative charge and Fh has a positive charge, MR-1 cells can bind efficiently to the biochar surface using hydrophobic interactions thus overcoming the repulsion by negative surface charges in our study. A previous study has reported that with increasing Fh concentrations, the mineral particles can aggregate forming large minerals assemblages with a lower weight-based surface area and less binding sites for biochar and cells (Villacis-Garcia et al., 2015).

Three-dimensional analysis of the samples using confocal laser scanning microscopy confirmed the close aggregation of cells, biochar and Fh and also revealed the section of extracellular polymeric substances (EPS). Biochar addition promoted EPS secretion from *Shewanella oneidensis* MR-1. EPS was shown to store redox-active flavins and cytochromes, enabling EPS-bound cells to transport electron extracellularly to electron acceptor via extracellular electron transport (EET), *i.e.* electron hopping across the EPS. High concentrations of biochar increased protein secretion from MR-1 cells compared to no addition setups. This high protein content detected in the presence of biochar helps microorganisms attach to biochar surface, which is consistent with previous results that surface proteins contribute the adhesion of the dissimilatory Fe(III)-reducing bacterium *S.alga* BrY to poorly crystalline ferric hydroxide (Caccavo, 1999).

However, although contribution of EPS to electron transfer between Fe(III)-reducing bacteria and biochar particles has been proved, little is understood on whether biochar impact protein and polysaccharide composition in EPS, whether electrons could be lost during pathway of electrons transport from outer membrane and biochar via EPS as transient media. To further understand it, future study on investigating morphological and chemical analysis of both EPS bound cells and EPS-depleted cells in the presence and absence of biochar are needed.

### **Biochar impacts microbial community composition shifting in a paddy soil microcosm**

Biochar was reported to be responsible for high soil organic matter contents and soil fertility of anthropogenic soils (Terra Preta) found in central Amazonia. Biochar is relatively recalcitrant at high pyrolysis temperature (above 600°C) therefore it cannot serve as a food for microorganisms. However, biochars are able to provide habitat matrix due to high pyrolysis temperature generally improved surface area of biochar (Glaser et al., 2002). In addition, biochar as conductive material participates in conductive-material interspecies electron transfer (CIET) process (Martins et al., 2018). During CIET process, biochar can act as a cell

conduit between electron-donating microorganisms (e.g. *Geobacter* spp.) and electron-accepting microorganisms (e.g. *Methanosarcina*). *Geobacteraceae* and *Methanosarcina* is known to be a syntrophic acetate-oxidizing consortia in anaerobic environments where Fe(III) minerals can be used as alternative electron acceptor and acetate as electron donor. (i.e. paddy soil and sediment) (Yuan et al., 2017; Rotaru et al., 2018). The results in the thesis (Chapter 4) showed that biochar (700°C) addition alters microbial community composition with increased abundances of *Geobacteraceae* and *Methanosarcina* of 16S bacterial and archaeal rRNA, respectively, as well as the copy numbers of 16S rRNA gene specific for *Geobacter* spp. and *mcrA*. This increase in acceleration of abundance and copy numbers for syntrophic acetate-oxidizing consortia with increased surface area and conductance of biochar.

Thermodynamically, microbial Fe(III) reduction is more favorable than methanogenesis because of a significantly high reduction potential for  $\text{Fe}^{2+}/\text{Fe}(\text{OH})_3$  (-0.1 V - 0.1 V, Thamdrup, B., 2000) than  $\text{CO}_2/\text{acetate}$  (-0.29 V). However, methanogenesis is more kinetically favorable than microbial Fe(III) reduction, which could be related to a faster microbial colonization outcompeting a slow accessibility of Fh to biochar. Therefore, surface attachment of cells and conductive biochar plays a curial role in microbial colonization and this aggregation of cells and biochar provides an alternative electron transfer pathway between microorganisms via biochar. However, in this thesis, we could not exclude whether acetate adsorption on the surface of biochar contributed to high usability for microbial colonization. Future studies on estimating adsorption of organic compounds on biochar are needed.

### **Coupled functions of biochar as geobattery and geoconductor alters electron transfer pathways between microbial Fe(III) reduction and methanogenesis.**

The results presented in Chapter 4 showed simultaneous stimulation of microbial Fe(III) reduction and methanogenesis in microcosm with biochar compared to microcosm without biochar. In general, microbial Fe(III) reduction is more thermodynamically favorable than methanogenesis. Compared to addition of AQDS which only stimulated Fe(II) rate (Liu et al., 2018), biochar stimulates both rates of Fe(II) and  $\text{CH}_4$  formation. For microbial Fe(III) reduction, biochar as geobattery is able to stimulate microbial Fe(III) reduction by means of charging and discharging cycles via surface functional groups between *Geobacteraceae* and Fh. Conductive carbon matrix in biochar as geoconductor also facilitated electron transfer to microbial Fe(III) reduction. With regards to methanogenesis, after biochar was applied, an alternative electron transfer pathway from *Geobacteraceae* to *Methanosarcina* through the conductive carbon matrix in biochar (as geoconductor) was provided, which contributed to methanogenesis (Fig.

2). Small particles of biochar showed a higher CH<sub>4</sub> formation rate than large particles which is related to high conductance due to smaller particle biochar has larger surface area.

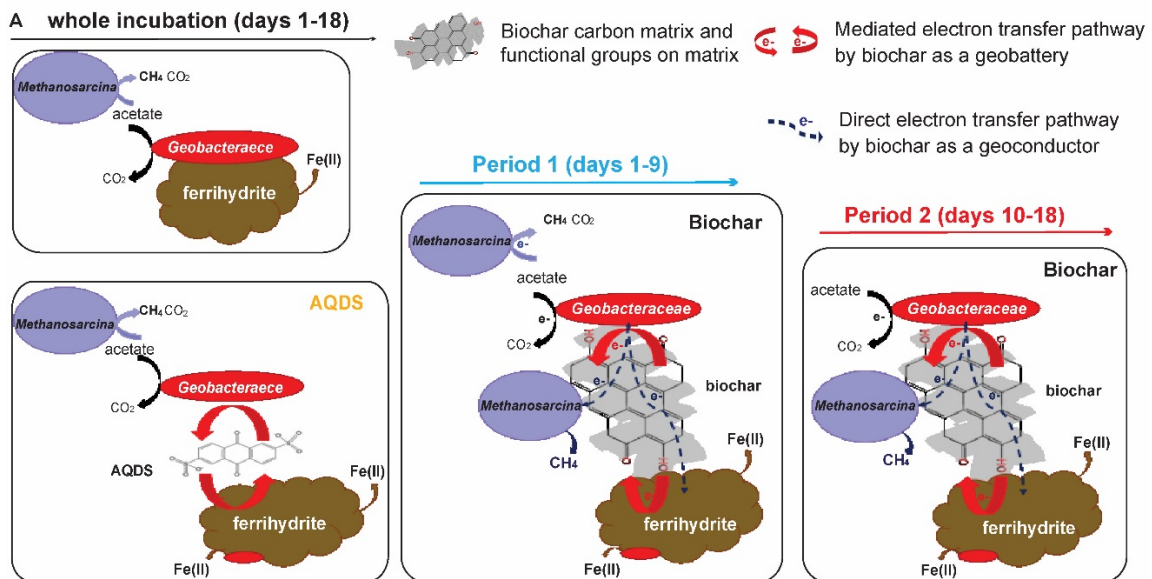


**Fig. 2.** Schematic of electron transfer pathways between Fe(III)-reducers (*Geobacteraceae*) and methanogens (acetoclastic methanogens or *Methanosarcina*) in anoxic paddy soil microcosm only amended with Fh and acetate (no biochar), with AQDS or biochar, respectively during the whole incubation. Without biochar, microbial Fe(III) reduction outcompetes methanogenesis. AQDS as an electron shuttle facilitates electrons transfer between the Fe(III)-reducer and ferrihydrite (Fh) suppressing methanogenesis. Biochar either mediated electron transfer between the Fe(III)-reducer and ferrihydrite (Fh) or directly transferred electrons from the Fe(III)-reducer to the methanogen thus stimulating methane production.

Taken all together, the goal of this thesis was to increase our understanding of the impact of biochar as geobattery and geoconductor on microbial Fe(III) reduction in pure Fe(III)-reducers cultures and its role in coupling to methanogenesis in a paddy soil. This is because biochar has been suggested as a powerful tool to mitigate climate change and shape biogeochemical process. However, biochars need to be selected with care. Electron transfer mechanisms of biochar coupled to microbial community compositions is a two-way effect in environments. Both research and users of biochar should first define a clear biogeochemical constraint that they want to address by the application of biochar in order to design successful application regimes.

## References

- Caccavo, F., 1999. Protein-mediated adhesion of the dissimilatory Fe (III)-reducing bacterium *Shewanella alga* BrY to hydrous ferric oxide. *App. Environ. Microbiol.*, 65 (11), 5017-5022.
- Lovley, D.R., 2017. Happy together: microbial communities that hook up to swap electrons. *The ISME journal*, 11(2), 327.
- Kappler, A., Wuestner, M. L., Ruecker, A., Harter, J., Halama, M., Behrens, S., 2014. Biochar as an electron shuttle between bacteria and Fe (III) minerals. *Environmental Science & Technology Letters*, 1(8), 339-344.
- Keiluweit, M., Nico, P.S., Johnson, M.G. Kleber, M., 2010. Dynamic molecular structure of plant biomass-derived black carbon (biochar). *Environmental Science and Technology* 44, 1247-1253.
- Glaser, B., Lehmann, J. and Zech, W., 2002. Ameliorating physical and chemical properties of highly weathered soils in the tropics with charcoal—a review. *Biology and fertility of soils*, 35(4), 219-230.
- Martins, G., Salvador, A.F., Pereira, L. and Alves, M.M., 2018. Methane production and conductive materials: a critical review. *Environmental science & technology*, 52(18), 10241-10253.
- Rotaru, A.E., Calabrese, F., Stryhanyuk, H., Musat, F., Shrestha, P.M., Weber, H.S., Snoeyenbos-West, O.L., Hall, P.O., Richnow, H.H., Musat, N. and Thamdrup, B., 2018. Conductive particles enable syntrophic acetate oxidation between *Geobacter* and *Methanosarcina* from coastal sediments. *MBio*, 9(3), e00226-18.
- Thamdrup, B., 2000. Bacterial manganese and iron reduction in aquatic sediments. In: Schink, B. (Ed.), *Advances in Microbial Ecology*. Kluwer Academic/Plenum Publishers, New York.
- Sun, T., Levin, B. D., Guzman, J. J., Enders, A., Muller, D. A., Angenent, L. T., Lehmann, J., 2017. Rapid electron transfer by the carbon matrix in natural pyrogenic carbon. *Nature communications*, 8, 14873.
- Sun, T., Levin, B. D., Schmidt, M. P., Guzman, J. J., Enders, A., Martínez, C. E., Lehmann, J., 2018. Simultaneous quantification of electron transfer by carbon matrices and functional groups in pyrogenic carbon. *Environmental science & technology*, 52(15), 8538-8547.
- Xu, W., Pignatello, J.J., Mitch, W.A., 2013. Role of black carbon electrical conductivity in mediating hexahydro-1,3,5-trinitro-1,3,5-triazine (RDX) transformation on carbon surfaces by sulfides. *Environmental Science and Technology* 47, 7129-7136.

-Curriculum vitae-

## Curriculum Vitae

### Personal Information

---

Given and Surname: Zhen Yang  
Date of birth: 14<sup>th</sup> Mar.1991  
Place of birth: Xian Yang, Shannxi, China  
Citizenship: Chinese

### Academic Education

---

**Ph.D** (Since 03/2017)

University/Institute Geomicrobiology,  
Eberhard Karls University of Tuebingen, Germany  
PhD-thesis: Effect of biochar as geobattery and geoconductor on  
microbial Fe(III) reduction and methanogenesis in a  
paddy soil  
Supervisors: Prof.Andreas Kappler and Prof.Ruben Kretzschmar

**M.Sc.** (10/2014-09/2016)

University/Institute Environmental Science and Engineering institute  
Beijing Forestry University, China  
Master-thesis Effect of different molecular weight fractions of  
humic substances on reducing capacity and  
distribution of redox functional groups  
Supervisors: Prof. Jie Jiang and Prof. Guoxin Sun

**B.Sc** (10/2010-09/2014)

University/Institute Environmental Science and Engineering institute  
Beijing Forestry University, China  
Bachelor-thesis Study on redox properties of humic substance by  
using spectroscopy methods

Supervisors

Prof. Jie Jiang and Prof. Guoxin Sun

## Work Experience

---

Undergraduate research assistant (10/2016-02/2017)

Environmental Science and Engineering institute  
Peking University, China

## Supervision

---

- ◆ Lead undergraduate student research team (5 students) in 2011 National Undergraduate Scientific and Technological Innovation Project, China.
- ◆ Supervise research team (3 students) in 2012 National Undergraduate Scientific and Technological Innovation Project, China.
- ◆ Supervise research team (3 students) in 2013 National Undergraduate Scientific and Technological Innovation Project, China.

## Publications

---

### Published:

**Yang, Z.**, Sun, T., Subdiaga, E., Obst, M., Haderlein, S.B., Maisch, M., Kretzschmar, R., Angenent, L.T. and Kappler, A., (2019). Aggregation-dependent electron transfer via redox-active biochar particles stimulate microbial ferrihydrite reduction. *Science of The Total Environment*, 23, p.135515.

**Yang, Z.**, Kappler, A. and Jiang, J., (2017). Reducing capacities and distribution of redox-active functional groups in low molecular weight fractions of humic acids. *Environmental Science & Technology*, 50, 12105-12113.

**Yang, Z.**, Du, M. and Jiang, J., (2016). Reducing capacities and redox potentials of humic substances extracted from sewage sludge. *Chemosphere*, 144, 902-908.

**Yang, Z.** and Jiang, J., (2015). Study on redox property and spectroscopic characterizations of commercial humic acids. [J]. *Environmental Chemistry*, 34:1134-1141.

Tian, W., **Yang, Z.**, Zhang, X., Ma, W. and Jiang, J., (2018). Redox properties of humic substances under different environmental conditions. *Environmental Science and Pollution Research*, 25, 25734-25743.

Contribution: Performed 3DEEM spectroscopy and evaluated data.

**Submitted:**

**Yang, Z.**, Sun, T.R., Kleindienst S., Straub D., Kretzschmar, R., Angenent, L. T., Kappler A., (2020) 'Coupled function of biochar as geobattery and geoconductor alters soil microbial community composition and electron transfer pathway in a paddy soil.' Submission to Soil Biology and Biochemistry

**In preparation:**

**Yang, Z.**, Jiang, J. Obst, M., Byrne, J.R., Kappler, A., (2020) 'Biochars impact extracellular polymeric substances secretion from *Shewanella oneidensis* MR-1 accelerating electron transfer during microbial Fe(III) reduction.'

**Presentations**

---

- ◆ Goldschmidt Conference, 2019, Barcelona, 2019. (Poster and Flask Talk)
- ◆ Goldschmidt Conference, 2018, Boston, 2018. (Poster)
- ◆ German Biochar PhD Workshop, Koblenz, 2018.
- ◆ The Asia Pacific Bioinformatics Conference (APBC), Korea, 2017. (Oral)
- ◆ ACS Spring National Meeting, San Diego, 2016. (Oral)
- ◆ 12<sup>th</sup> International Conference of the East and Southeast Asia Federation of Soil Science Societies (ESAFS), Nanjing, 2015. (Oral)

\*\*\*\*\*



### **Statement of personal contribution**

The work described herein was financially supported by a personal stipend provided to me by China Scholarship Council Foundation (No. 201606510018). The proposal was mainly written by me and the quality of the proposal was greatly improved by Prof. Andreas Kappler and Prof. Ruben Kretzschmar. Prof. Andreas Kappler was the main supervisor throughout the project and Prof. Ruben Kretzschmar was the second supervisor. Unless otherwise stated, experiments were either conceptualized by myself or together with Prof. Andreas Kappler and were carried out by me. The final analysis and discussion of the results, as well as all manuscript were completed in cooperation with Prof. Andreas Kappler.

In Chapter 3, electrochemical analysis of biochar and XAD-8 suspension were conducted by Edisson Subdiaga. The FTIR, three-dimensional CLSM and mössbauer analysis of biochar samples were carried out by Annette Flicker, Prof. Martin Obst and Markus Maisch, respectively. The manuscript was read and improved by all authors.

In Chapter 4, the 16S rRNA analysis were carried out by Daniel Straub. The manuscript was read and improved by all authors.

Other contributions of people in the laboratory were: TOC/DOC and particle size analysis in Chapter 3 were measured by Ellen Roehm. Dr. Franziska Schädler prepared the primers of 16S rRNA illumina amplicons and helped me doing qPCR in Chapter 4.

## **Acknowledgements**

The work presented within this thesis was performed from 03. 2017 to 02. 2020 within the Geomicrobiology research group of Prof. Andreas Kappler. My work was financially supported by China Scholarship Council Foundation (No. 201606510018).

As science is teamwork, there are many people who supported me and this thesis in many ways. It is my honor to mention them here and say 'Thank you', 'Dankeschön' and '谢谢'! A wonderful and unforgettable 3-year time in my lifetime in the Geomicrobiology group at University of Tuebingen.

First of all, I would like to thank my supervisor Prof. Andreas Kappler for introducing such an amazing biochar material and providing the opportunity to work in the inspiring group on a topic that we designed to my specific scientific interests. In early 2017, when Andreas mentioned that an interesting topic on biochar as an electron shuttle influence microbial Fe(III) reduction (the paper published in 2014), it extended my interests to biochar and also took my way to microbiology study. Although in some cases experiment results and observations brought us 'surprise', Andreas helped me figure out the science truth behind these observations during every discussion. Andreas also showed me a good model both how to work as a good scientist, quantified teacher, and father. The experience of studying under his supervision would benefit me for a lifetime.

Furthermore, I would like to thanks to Prof. Ruben Kretzschmar for being my second supervisor, his support in promoting my Ph.D project and his great suggestions in experiment design. I also would like to thank Prof. Martin Obst helped me look up aggregation and overcome three-dimensional aggregation challenging question by CLSM. Thank Edison Subdiaga-Rondon and Prof. Stefan Haderlein for assisting in electrochemical analysis. Thank Prof. Sara Kleindienst and Daniel Straub for helping analysis results of molecular microbiology. I would like to thank Prof. Lars T. Angenent and Tianran Sun for their useful guidance and assistance in manuscripts. I want to thank James Byrne for valuable advice and feedback on presentations and discussion. I would also thank Casey Bryce and Zhe Zhou for helping check and very helpful suggestions for my PhD thesis. My thanks also go to Ulf Lüder for helping me during application and finish PhD defense process.

I also would like to thank Ellen Röhm and Lars Grimm for their well organization in the lab. Thank Franziska Schäder for teaching me a lot in molecular microbiology experiments and preparation of qPCR amplicons in advance. Thanks to all lovely colleagues in Geomicrobiology group for your ever every help.

-Acknowledgements-

A special thanks goes to my all officemates in room S516, Markus Maisch, Yuge Bai, Natalia Jakus, and Jiangrong Huang. Thanks for a great time! Warm atmosphere and quick scientific discussion with you always inspired and helped me a lot. Thank to Markus and Natalia for their constant cooperativeness and scientific assistance by detecting XRD and mössbauer samples, providing Vercelli paddy soil, as well as translating the abstract section. Particularly thank all Chinese colleagues in Geomicrobiology group and Applied Geoscience department for their care and assistance in every moment we spent together. I would also never forget and enjoyed a great time during Goldschmidt conference 2018 in Boston and Goldschmidt conference 2019 in Barcelona together with my lovely colleagues.

Importantly, I would like to thank to my families and friends for supporting me and encouraging me to do whatever I want to do. Thanks for all my friends and Jie's care from China. 谢谢爸妈，谢谢在这里相遇的所有朋友们给予我的温暖和一起度过的那些阳光灿烂的日子！

02.02.2020

\*\*\*\*\*

